“Analysing the possible influence of transposon TCl4.7 insertion on the function of the genome of *Cydia pomonella* granulovirus”

Dissertation

Zur Erlangung des Grades

Doktor der Naturwissenschaften

am Fachbereich Biologie

der Johannes Gutenberg-Universität Mainz

Wael Hassan Ali Elmenofy

geb. in Kairo, Ägypten

Mainz, 2008

Tag der mündlichen Prüfung: 08. Dezember 2008

CONTENTS

ABBREVIATIONS

General

bp	base pair
bdH_2O	bidistilled water
BV	budded virus
Chl^R	chloramphenicol resistance gene
CM	codling moth
dpi	days post infection
h	hour
hpi	hours post infection
hrs	homologous regions
Kan^R	kanamycin resistance gene
kDa	kilo Dalton
L	liter
LC_{50}	median lethal concentration
LD_{50}	median lethal dose
mA	milli Ampere
min	minute
nt	nucleotide
OB	occlusion body
ODV	occlusion-derived virus
ori	origin of replication
pAB	polyclonal antibody
PCR	Polymerase Chain Reaction
pi	post infection
PM	peritrophic membrane
3' RACE	rapid amplification of 3' cDNA ends by PCR
5' RACE	rapid amplification of 5' cDNA ends by PCR
REN	restriction endonuclease
RT-PCR	reverse transcription PCR
s	second
ST_{50}	median survival time
Tet^R	tetracycline resistance gene
TEs	transposable elements
V	Volt
v/v	volume per volume
w/v	weight per volume
wt	wild-type

Viruses

AcMNPV	*Autographa californica* MNPV
AdorGV	*Adoxophyes orana* GV
AgseGV	*Agrotis segetum* GV
AgseNPV	*Agrotis segetum* NPV
BmNPV	*Bombyx mori* NPV
CfMNPV	*Choristoneura fumiferana* MNPV
ChchNPV	*Chrysodeixis chalcites* NPV
ChocGV	*Choristoneura occidentalis* GV
CpGV	*Cydia pomonella* GV
CrleGV	*Cryptophlebia leucotreta* GV
CuniNPV	*Culex nigripalpus* NPV
EcobNPV	*Ecotropis obliqua* NPV
EppoNPV	*Epiphyas postvittana* NPV
HearNPV-G4	*Helicoverpa armigera* NPV
HearGV	*Helicoverpa armigera* GV
LdMNPV	*Lymantria dispar* MNPV
MacoNPV-A	*Mamestra configurata* NPV
NeabNPV	*Neodiprion abietis* NPV
NeleNPV	*Neodiprion lecontii* NPV
NeseNPV	*Neodiprion sertifer* NPV
OpMNPV	*Orgyia pseudotsugata* MNPV
PhopGV	*Phthorimaea operculella* GV
PlxyGV	*Plutella xylostella* GV
PsunGV	*Pseudalatia unipuncta* GV
SeMNPV	*Spodoptera exigua* MNPV
SpliGV	*Spodoptera litura* GV
TnGV	*Trichoplusia ni* GV
TnSNPV	*Trichoplusia ni* SNPV
XecnGV	*Xestia c-nigrum* GV

I. SUMMARY

CpGV-MCp5 is a natural mutant of the *Cydia pomonella* granulovirus Mexican strain (CpGV-M) that harbors an insect host transposon termed TCl4.7 in its genome (Jehle et al., 1995). TCl4.7 is located between the open reading frames Cp15 and Cp16 and separates two homologous regions hr3 and hr4, which have been recently shown to be origins of replication of CpGV (ori) (Hilton and Winstanley, 2007). Previous competition experiments had demonstrated that MCp5 has a significant replication disadvantage compared to wild-type CpGV-M (Arends et al., 2005).

In order to better understand the consequences of the integration of TCl4.7 on the genome of CpGV, the effect of TCl4.7 insertion on transcription of Cp15, Cp16 and F protein (Cp31) as well as on replication of MCp5 were studied. Moreover, the CpGV-M bacmid (CpBAC) that can replicate in *E. coli* as a plasmid and can infect *C. pomonella* (CM) larvae was constructed in order to allow easy manipulation of the CpGV-M genome and facilitate knockout of Cp15 and Cp16 and thus determining their role in the context of CpGV-M life cycle. Knocking out of Cp15 and Cp16 was performed using the generated CpBAC and the Red/ET-Recombination system.

Temporal transcriptional analyses using RT-PCR and quantitative real-time PCR (qRT-PCR) revealed that Cp15 and Cp16 transcription was initiated as early as 6-12 hour post infection (hpi) in CpGV-M until 96 hpi and in MCp5 until 48 hpi in infected CM larvae. However, a significant delay or reduction of Cp15 and Cp16 transcripts was observed in MCp5. The F protein transcription was detected at 24 hpi until 96 hpi in CpGV-M and at 6 hpi until 24 hpi in MCp5 with a low transcriptional level of MCp5 transcripts. Similar to the RT-PCR observations, the qRT-PCR analysis showed a reduced cDNA levels for Cp15, Cp16 and F protein in MCp5 compared to CpGV-M. These observations suggested a general delay or reduction of MCp5 gene transcription compared to wt CpGV-M in all investigated time points based on RT-PCR and qRT-PCR. Temporal protein expression analysis for both Cp15 and Cp16 did not show any immuno-reactive signals using mono-specific polyclonal antibody generated against both proteins.

The generated CpBAC^{Cp15KO} (Cp15-null) was not able to produce virus infection after injection into the hemocoel of CM larvae. In contrast, the generated CpBAC^{Cp16KO} (Cp16-null) caused infection to CM larvae after larval hemocoelic injection and produced infectious virus OBs by oral feeding. These results suggest that Cp15 is an essential gene for virus

infection cycle, whereas Cp16 is non-essential for virus *in vivo* infection of *C. pomonella*. In order to investigate whether the deletion of Cp16 from CpGV-M had an influence on the virus biological fitness against CM larvae, the median lethal concentration (LC_{50}) was determined. No significant difference was observed between the LC_{50} value for $CpBAC^{Cp16KO}$ and the wt CpGV-M suggesting that the deletion of Cp16 from CpGV-M did not affect virus biological fitness based on LC_{50}.

Moreover, a mutant CpBAC with a deletion of palindromes hr3 and hr4 ($CpBAC^{hr3/hr4KO}$) and another with an insertion of a kanamycin resistance gene (Kan^R) between hr3 and hr4 ($CpBAC^{hr3\text{-}kan\text{-}hr4}$), were generated in order to examine whether the interruption of hrs will influence the virus infection cycle. $CpBAC^{hr3\text{-}kan\text{-}hr4}$ was generated to mimic the interruption of hr3 and hr4 as it was observed in MCp5 carrying the TCl4.7 transposon at the same locus between hr3 and hr4. Both mutant bacmids replicated and produced infectious virus OBs after hemocoelic injection of CM larvae, suggesting that the disruption of hr3 and hr4 or their complete deletion did not impair the viral infection cycle.

In order to investigate whether the interruption of hr3 and hr4 had influenced the biological fitness of the mutant viruses $CpBAC^{hr3/hr4KO}$ and $CpBAC^{hr3\text{-}kan\text{-}hr4}$, LC_{50} and the median survival time (ST_{50}) values were determined. The LC_{50} of $CpBAC^{hr3/hr4KO}$ (5044 OB/ml) and the $CpBAC^{hr3\text{-}kan\text{-}hr4}$ (2837 OB/ml) did not statistically differ from CpBAC (2439 OB/ml). Thus, deletion or interruption of hr3 and hr4 did not influence concentration mortality response of CM larvae. The ST_{50} value for CpBAC (150 hour), $CpBAC^{hr3/hr4KO}$ (150 hour) and $CpBAC^{hr3\text{-}kan\text{-}hr4}$ (142 hour) was not statistically different. From the LC_{50} and ST_{50} analyses it was concluded that neither the deletion nor the interruption of hr3 and hr4 of CpGV had affected the virus infectivity or the biological efficacy based on the LC_{50} and ST_{50} parameters.

Additionally, competition experiments between $CpBAC^{hr3\text{-}kan\text{-}hr4}$ and CpBAC on CM larvae were performed in order to analyse the potential selection constraints on $CpBAC^{hr3\text{-}kan\text{-}hr4}$ in the presence of CpBAC. Co-infection experiments were performed on CM larvae using $CpBAC^{hr3\text{-}kan\text{-}hr4}$ and CpBAC in order to investigate whether the $CpBAC^{hr3\text{-}kan\text{-}hr4}$ carrying Kan^R between hr3/hr4 has a replication disadvantage in the presence of the parental bacmid CpBAC. By comparing the CpBAC: mutant ratio in the virus inoculum's with the ratio in the virus progeny it was shown that $CpBAC^{hr3\text{-}kan\text{-}hr4}$ was efficiently out-competed by CpBAC in all co-infections experiments using different ratios of both viruses. Based on these results, a

functional co-operation between hr3 and hr4, which was interrupted by the Kan^R insertion in $CpBAC^{hr3\text{-}kan\text{-}hr4}$ and possibly by TCl4.7 insertion in MCp5 and thus affected the replication rate of the mutants MCp5 and $CpBAC^{hr3\text{-}kan\text{-}hr4}$ in the presence of the parental viruses CpGV-M and CpBAC, is predicted. This study demonstrates that genotype mutation which can not be measured in terms of virulence parameters may have a quantifiable effect on population level.

II. INTRODUCTION

Baculovirus form a unique group of insect-specific DNA viruses. Most of these viruses infect insects of the orders Lipedoptera, Hymenoptera and Diptera. Baculovirus infections have been reported in more than 600 insect species. Only a limited number of these baculoviruses have been studied and characterized in detail, mainly from insects that have agricultural importance.

Although baculovirus infections were originally discovered when silkworm cultures were decimated by a disease indicated as jaundice, baculoviruses are mainly considered 'beneficial from an arthropocentric point of view' (Miller, 1997). In nature, baculoviruses are thought to control the size of insect populations and this is the basis for their application as bio-control agents of insect pests in many agricultural crops (Hunter-Fujita et al., 1998; Moscardi, 1999). Increasing insight in baculovirus molecular biology enabled their exploitation as expression vectors for recombinant proteins in insect cells (Miller, 1988; Summers, 2006).

1. Baculovirus structure and taxonomy

The baculoviruses belong to the family *Baculoviridae* which forms a large family of rod-shaped, invertebrate infecting viruses with large double-stranded, covalently closed circular DNA genomes of 80-180 kbp. The family is taxonomically divided into two genera, Nucleopolyhedrovirus (NPV) and Granulovirus (GV) (Theilmann et al., 2005).

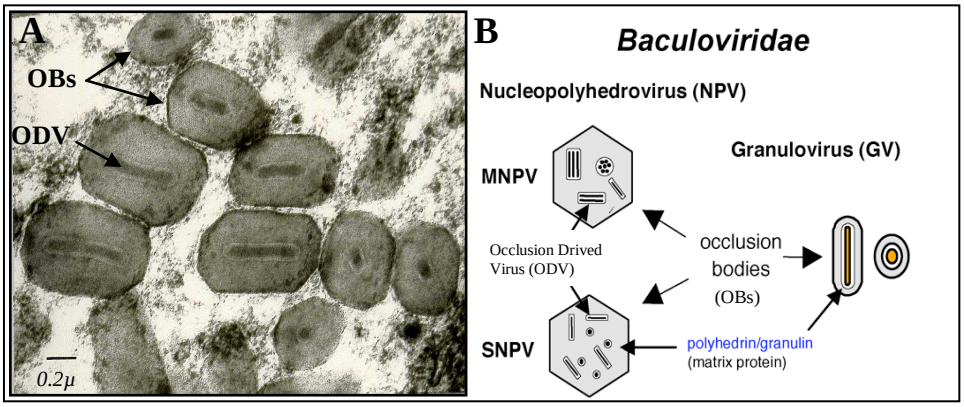

Fig. 1. (A) Electron microscopic dissection of CpGV occlusion bodies. Virus occlusion bodies (OBs) with occlusion-derived virus (ODV) are clearly visible. (Photo: Dr. A. Huger, BBA Darmstadt). **(B)** Comparison of OB morphology in multiple (M) and single (S) nucleocapsids NPVs, and GVs (modified from van Oers and Vlak, 2007).

The present classification into NPVs and GVs is primarily based on occlusion body (OB) morphology. NPVs have large polyhedra (polyhedrin matrix protein) with diameters between 0.5-3 (15) µm and occlude many Occlusion Derived Virus (ODV), whereas GVs have small granule-like OBs, which average size is approximately 0.13 x 0.50 µm occluding a single virion (Fig. 1A) (Theilmann et al., 2005). Phenotypically, GVs have a single nucleocapsid enveloped within each virion, whereas NPVs contain single or multiple nucleocapsids per virion (Fig. 1B) (Theilmann et al., 2005). Replication of baculoviruses occurs in the nucleus (NPV) or nucleo-cytoplasmic stroma after disintegration of the nuclear membrane (GV) (Theilmann et al., 2005).

The NPVs pathogenic to lepidopteran insects show a further phylogenetic subdivision into group I and group II NPVs (Bulach et al., 1999; Herniou et al., 2001). Group II NPVs show more variation than group I NPVs (Lange et al., 2004). NPVs are generally designated as either single (S) or multiple (M), depending on the number of nucleocapsids packaged within an ODV (Fig. 1B). This feature has no taxonomic value but is a convenient practical description and often maintained in the nomenclature. Molecular tools for phylogenetic analyses, based on the sequence of a few conserved genes, have been developed to facilitate the discrimination of virus species (Herniou et al., 2004; Jehle et al., 2006b; Lange et al., 2004).

For the lepidopteran baculoviruses the taxonomic division in NPVs and GVs was underpinned by genomic sequence data. When genome sequences from NPVs infecting sawflies (*Neodiprion*) and mosquito (*Culex*) species became available, it revealed that that lepidoteran NPVs and GVs were closer related to each other than to NPVs from dipteran (Afonso et al., 2001; Duffy et al., 2006; Moser et al., 2001) and hymenopteran hosts (Garcia-Maruniak et al., 2004; Lauzon et al., 2004). Thus the baculovirus phylogeny follows the evolution of the host more closely than the OB morphology (Jehle et al., 2006a). Based on this finding a new classification is proposed: Alphabaculovirus: lepidopteran NPVs; Betabaculovirus: lepidopteran GVs; Gammabaculovirus: hymenopteran NPVs and Deltabaculovirus: dipteran NPVs (Jehle et al., 2006a).

The best studied GV is the *Cydia pomonella* granulovirus (CpGV) (Crook, 1991). CpGV is highly pathogenic to the larvae of codling moth (CM) *C. pomonella* (*Cydia pomonella* L., Lep.: Tortricidae), which is an important economic pest of commercial apple orchards throughout the world (Fig. 2) (Cross et al., 1999). Formulated products of CpGV are

now available in many countries worldwide (Cross et al., 1999). The genome of CpGV-M (Mexican isolate) has a genome of 123,500 bp with 143 ORFs (Luque et al., 2001). Other characterized CpGV isolates, e.g. CpGV-E (English isolate) and CpGV-R (Russia isolate), show only small genotypic differences compared to CpGV-M (Crook et al., 1997; Crook et al., 1985; Harvey and Volkman, 1983).

Fig. 2. (A) Healthy fourth instar of codling moth *C. pomonella* larvae. **(B)** CpGV infected young larvae of the *C. pomonella*. **(C)** *C. pomonella* fourth instar larvae bores into an apple fruit. (Photos: DLR-Rheinpfalz, Germany & INRA, France).

2. Baculovirus infection cycle

As shown in Fig. 3, the life cycle of baculovirus occurs when susceptible larvae take up the OBs as contaminants on plant surfaces and in the soil. After ingestion by the host insect larvae, the crystalline OB (polyhedrin/granulin) matrix is solubilized in the alkaline midgut of the insects releasing the infectious ODVs and allowing for infection of the midgut epithelial cells. The ODVs released from the OBs enter midgut cells by fusion with the membrane of the midgut epithelial cells. After being recognized by a specific receptor they migrate through the cytoplasm to the nucleus, and are uncoated in the nucleus (Fig. 3) (Granados and Williams, 1986).

Viral replication in the nucleus produces progeny nucleocapsids which bud through the plasma membrane. Infection in the polarized midgut cells results in a second viral phenotype, the Budded Viruses (BVs), which are released from the basement membrane side of the cell (Keddie et al., 1989). The BVs continue to spread infection within the larval host.

Late in the replication cycle, progeny nucleocapsides become membrane bound within the nucleus. At that time, large amount of polyhedrin (NPVs) or granulin (GVs) protein are synthesized. The polyhedrin/granulin protein crystallizes around the membrane-bound particles, forming OBs.

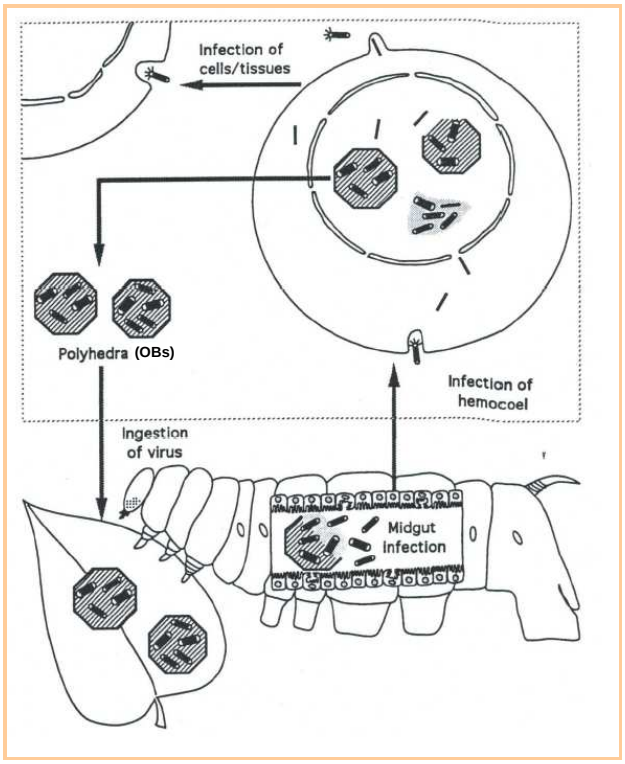

Fig. 3. The life cycle of the baculovirus is depicted. The occluded form of the virus (OBs) is ingested and results in a primary infection. The BVs are released into the hemocoel, resulting in secondry infection. At the late stages of infection the ODVs and OBs are again produced and released (Shuler et al., 1995).

During a typical baculovirus infection, the insect continues to feed during most of the infection process, which takes approximately five to seven days. The integument becomes swollen and changes in luster. Both BVs and OBs are produced in most of the tissues infected during the secondary phase of infection. Death occurs after approximately 10 rounds of viral replication. There may be 30 or more OB in infected cells, and late instar larvae may produce up to 10^{10} OB before death (Evans, 1986). OBs are relatively stable in the environment, although they exhibit significant sensitivity to UV light. They are naturally dispersed by a variety of routes, and may eventually be taken up by another permissive insect host, thereby ensuring horizontal transmission to other host individuals (Evans, 1986).

3. Host range, specificity and virulence of baculovirus

Studies on baculovirus host specificity have shown that these viruses possess relatively narrow host ranges both *in vivo* and *in vitro* (Granados and Williams, 1986). In some invertebrate viruses, the initial attachment of a virus to a host cell receptor is considered as an important process defining host specificity (Lenz et al., 1991). In the infection process of group I NPVs, an envelope glycoprotein (GP64) plays an important role in the attachment of BV to the host cell surface (Volkman et al., 1984). GP64 is involved in viral attachment and is required for low-pH-mediated membrane fusion during virus entry (Blissard and Wenz, 1992; Hefferon et al., 1999). GP64 is also required for efficient budding of the BV (Oomens et al., 1995). Although GP64 proteins have been identified in group I NPVs, recent data from the complete genomic sequences of a number of baculoviruses suggest that *gp64* genes are not present in group II NPVs or GVs. An envelope protein gene named F (fusion) protein that is unrelated to *gp64* was identified in *Lymantria dispar* MNPV (LdMNPV) (Pearson et al., 2000), *Spodoptera exigua* MNPV (SeMNPV) (Ijkel et al., 2000) and homologues of this gene have been identified in other group II NPVs and GVs. The full length F protein is involved in entry of BVs into cells and in budding of newly made BVs from the cell (a function taken over by GP64 in group I NPVs) (Lung et al., 2002; Monsma et al., 1996; Oomens and Blissard, 1999). The F protein is glycosylated, which appears to be important for virus infectivity (Long et al., 2006a; Long et al., 2006b). The F protein is found in all lepidopteran baculovirus genomes and is present only in BVs. However, it is also present in a truncated form in group I NPVs where it may have a different function (van Oers and Vlak, 2007). The truncated form of F protein in AcMNPV (ac23) present in group I NPVs, is not needed for infectivity but enhances viral pathogenicity (Lung et al., 2003). Recently, F Protein of *Plutella xylostella* GV (PlxyGV) was found to be a functional analogue of the GP64 envelope fusion protein of *Autographa californica* MNPV (AcMNPV) (Yin et al., 2008).

In some GVs, dissolution of the protective OBs releases a factor known as the viral enhancin protein which enhances the likelihood of efficient infection of the midgut cells (Corsaro, 1993; Derksen and Granados, 1988). Enhancins are baculovirus proteins capable of enhancing infections in insect larvae by other baculoviruses (Roelvink et al., 1995). It was reported that enhancin proteins can enhance the infectious activity of an NPV by increasing the NPV's efficiency of attachment to the host cell surface (Yamamoto and Tanada, 1978), or by disruption of a peritrophic membrane, the barrier organ inside the insect midgut (Derksen and Granados, 1988). Enhancin genes have been found in several GVs including *Helicoverpa*

armigera GV (HearGV) (Roelvink et al., 1995), *Pseudalatia unipuncta* GV (PsunGV) (Roelvink et al., 1995), *Trichoplusia ni* GV (TnGV) (Hashimoto et al., 1991) and *Xestia c-nigrum* GV (XecnGV) (Hayakawa et al., 1999). The first GV genome to be completely sequenced, that of XecnGV, was found to have four different enhancing genes (Hayakawa et al., 1999). In contrast, PlxyGV (Hashimoto et al., 2000), CpGV (Luque et al., 2001), *Cryptophlebia leucotreta* GV (CrleGV) (Lange and Jehle, 2003) genomes lack enhancin genes.

The mechanisms of host specificity may occur at the cellular level as observed in the sloughing off of infected midgut epithelial cells in the midgut lumen (Engelhard and Volkman, 1995), and in the encapsulation of the infected tissue by haemocytes and subsequent clearing of infected cells (Washburn et al., 1996). Another cellular defense reaction is apoptosis, a programmed cellular suicide process, by which damaged or harmful cells are eliminated from multicellular organisms (Wyllie et al., 1980). Apoptosis is a cellular self-destruction mechanism that is activated in response to diverse signals during normal development, tissue homeostasis, and disease pathogenesis. Apoptotic signals converge upon a highly conserved, central death pathway that leads to the activation of one or more members of the caspase family of cysteine proteases that are required for cell death (LaCount and Friesen, 1997). Cells undergoing apoptosis show distinct morphological changes including cell shrinkage, membrane blebbing, chromatin condensation, apoptotic body formation and DNA fragmentation (Wyllie et al., 1980). Apoptosis acts as a host defense mechanism, by which virus infected midgut epithelial cells are eliminated to limit the propagation of viruses (Clem, 2005; Clem and Miller, 1994). Numerous viruses not only induce programmed cell death but also encode apoptotic suppressors, suggesting that apoptosis plays a significant role in virus replication (Clem, 2005). As a consequence, baculoviruses have evolved distinct apoptotic suppressors that block this host response (Clem, 2001; Friesen, 2007). An elucidated mechanism preventing apoptosis is displayed by AcMNPV *p35* and Inhibitor of Apoptosis Proteins (IAPs), involving specific inhibition of caspases, a type of induced cellular protease involved in the apoptotic response (Bertin et al., 1996; LaCount et al., 2000; Lannan et al., 2007; Manji et al., 1997). The first iap gene, now referred to as *iap-3*, was identified in CpGV by complementation of AcMNPV *p35* mutants (Crook et al., 1993). In addition to *iap-3* (Cp17), sequence analysis of CpGV genome has revealed two additional CpGV *iap* genes (Cp94 and Cp116) (Luque et al., 2001). Indeed, apoptosis affects virus production, establishment of latent and persistent infections, and viral pathogenesis (Clem, 2005).

4. Baculoviruses as biocontrol agents

It is well known that the use of chemical insecticides has resulted in the appearance of harmful effects to humans, animals and the environment. The baculoviruses, as one of the microbial control agents, are specific, efficient and safe to non-target organisms (Bilimoria, 1991; Gröner, 1990). They provide an alternative to broad spectrum insecticidies without the disruption of natural enemy complexes that often occurs with conventional inseciticides (Lacey et al., 2002). The use of baculovirus in pest management can be historically traced back to 19th century. This was first observed in 1911 by Reiff, who suggested that the gypsy moth wilt disease, which was in fact a baculovirus infection, could be used as a control agent (Glaser, 1927). During the 1950s-1970s, efforts to develop viruses as microbial insecticides were intensified. This had significant influence on the development and worldwide use of other baculoviruses as insect control agent. This feature has been exploited and baculovirus have been registered and used as a natural pest control agent (Lacey et al., 2002).

CpGV is a specific and extremely virulent pathogen that has been developed as one of the most efficient and environmentally safe insecticides for control of CM (Huber, 1998). CpGV was first described in CM larvae collected from orchards of apple and pear in Mexico (Tanada, 1964). CpGV is highly pathogenic for CM but harmless for nontarget organisms. Because of this characteristic, CpGV-based microbial agents are used in biological control of CM in apple orchards (Baudry et al., 1996; Guillon and Biache, 1995; Jaques et al., 1994; Lacey, 2000). Several CpGV based products are commercialized and widely used in biological and in integrated apple production. It is estimated that these products are applied on more than 100,000 ha in Europe, with a steadily increasing market due to their superior efficacy, environmental safety, and the control failure of many chemical insecticides (Eberle and Jehle, 2006).

Since 2004, several local codling moth populations with a reduced susceptibility to CpGV have been reported from Germany and from France (Asser-Kaiser et al., 2007; Fritsch et al., 2005; Sauphanor et al., 2006). These populations were detected in organic apple plantations, where CM control failed despite intensive CpGV application. It was concluded that implementation of resistance monitoring and resistance management will be needed in order to sustain the ecological and economic benefits of CpGV and other baculoviruses (Asser-Kaiser et al., 2007).

5. Baculovirus replication and gene regulation

Baculovirus genes are expressed in a temporarily regulated cascade of transcriptional events revealing four classes of genes: immediate early genes (IE), delayed-early genes (DE), late (L) and very late (VL) genes. Baculovirus early genes are transcribed by the host RNA polymerase II and contain a conserved 5'-CAGT-3' motif, which encompasses the transcription start site and is proceeded by a TATA box (Friesen, 1997). The TATA box is the primary element that determines the transcription start site, while mutations in the CAGT motif affect the efficiency of transcription initiation (Blissard et al., 1992; Guarino and Smith, 1992; Kogan et al., 1995). Some of the early genes encode proteins needed for viral DNA replication and genes to reprogramme the host cells towards virus replication. The late phase of gene expression begins concomitant with or shortly after replication of the viral genome, and viral DNA replication appears to be a necessary prerequisite to late gene transcription. Inhibitors of viral DNA replication (such as aphidicolin) also block late gene expression in infected cells (Lu et al., 1997). Late and very late genes are transcribed by a viral RNA polymerase (Guarino et al., 1998) that recognizes distinct late promoters. Most if not all, late gene promoters contain the conserved sequence 5'-TAAG-3' (Rohrmann, 1986) at the transcription start site. The conserved core TAAG sequence plus non-conserved flanking sequence of at least 8 to 12 nucleotides (nt) appear to comprise the late promoter sequences that are necessary for wild-type levels of late transcription (Lin and Blissard, 2002). Except for the conserved core TAAG motif, little is known regarding the cis-acting regulatory sequence for late promoter recognition and activation. The late phase of gene expression is followed by the very late gene expression, which is characterized by the hyper-expression of two genes, *polyhedrin* (*or granulin*) and *p10* (Lu and Miller, 1997). Very late promoters appear to be similar to late promoters in that they also include the conserved core TAAG motif and flanking sequences, but differ in that they also require an additional sequence called a 'burst' sequence. The exceptionally high levels of transcription from the polyhedrin and p10 genes appear to be regulated or mediated by binding of viral protein VLF-1 to the 'burst' sequence which is located downstream of the transcription start site. The 'burst' sequence appears to regulate the burst of very late transcription (Lin and Blissard, 2002).

6. Open reading frames (ORFs) and gene conservation

Baculovirus genes in general do not contain introns, making it fairly easy to predict ORFs from primary sequence data. An exception is the AcMNPV *ie0 transcriptional unit*

which has an intron of 4,528 kb (Chisholm and Henner, 1988; Dai et al., 2004). All baculovirus ORFs start with an ATG, and alternative translational start codons have not been reported for these viruses. In baculovirus genome studies all ORFs with a size larger than 150 bp (50 aa) are considered as potential ORFs, unless they show considerable overlap with other ORFs. In that case comparison with other baculovirus genomes may help to define the real ORF or the presence of promoter sequences, otherwise the longest ORF is often chosen. This artificial limit of 50 amino acids, does not exclude the possibility that ORFs smaller than 50 amino acids play a role, for instance the minicistron identified in the AcMNPV *gp64* gene (van Oers and Vlak, 2007).

The sequence analysis of 43 baculovirus genomes to date has provided a thorough insight in the minimal collection of genes conserved in all baculoviruses, independent of the taxonomic position of their host (lepidopteran, hymenopteran or dipteran) or whether being an NPV or a GV. The number of genes conserved among all sequenced baculoviruses is 30 (McCarthy and Theilmann, 2008). Although homologues of some of these genes are present in other DNA viruses, the collective presence of these 30 genes seems to characterize a baculovirus and these genes are therefore, assigned as baculovirus core genes. Since they are conserved in all baculovirus genomes to date, the comparison of these genes is a highly suitable tool for phylogenetic studies (van Oers and Vlak, 2007).

7. Homologous repeated sequences (hrs)

Most baculovirus genomes contain regions of repeated sequences, which occur at multiple positions in the genome and are, therefore, called homologous regions (hrs). Hrs have been reported to function as enhancers for early gene expression (Guarino et al., 1986; Lu et al., 1997; Theilmann and Stewart, 1992), and as origins of DNA replication (ori) (Kool et al., 1993; Pearson et al., 1992; Pearson and Rohrmann, 1995), but the latter only in transfection assays. In general, hrs are AT rich regions, often containing reiterated palindromic motifs, which may be alternated with direct repeats (Broer et al., 1998; Crouch and Passarelli, 2002; Nakai et al., 2003). The hr palindromes may contain recognition sequences of DNA restriction endonucleases. AcMNPV hrs, for instance, contain multiple *Eco*RI-restriction sites, whereas SeMNPV hrs coincide with numerous *Bgl*II sites (Broer et al., 1998; Cochran et al., 1982). Thirteen imperfect palindromes hrs of 74-76 bp, with similarity to each other, have been recently identified in the CpGV genome (Luque et al., 2001). Each CpGV palindrome appears as singleton, not occurring as multiple tandem repeats

like a typical AcMNPV hr element. The entire genome of CpGV was systematically screened for origins of DNA replication, using infection-dependent DNA replication assay in the granulovirus-permissive *C. pomonella* cell line, Cp14R (Hilton and Winstanley, 2007). The results showed that the 13 imperfect palindromes within the CpGV genome replicated in an infection-dependent assay and therefore may function as oris. No other area of DNA in the CpGV genome was found to replicate, including a non-hr ori-like region. The entire 76 bp palindrome was needed for any replication, with flanking regions enhancing replication (Hilton and Winstanley, 2007). So far no evidence exists that the number of hrs is correlated with replication efficiency or pathogenicity of a baculovirus. However, decreasing the distance between two hrs by inserting an extra hr enhanced the genome stability of AcMNPV in cell culture (Pijlman et al., 2004). Within a genome, variation occurs in the number of repeats per hr, either palindromic or direct, and within an hr the sequence of a repeat unit is slightly variable. In general, the nucleotide sequence as well as the length of the repeat unit of hrs varies per virus species (van Oers and Vlak, 2007).

8. Transposable elements and baculoviruses

Transposable Elements (TEs) are segments of DNA that can move around to different positions in the genome of a single cell. By this process, they cause mutations in the genome. There are two distinct types of TEs: (i) DNA transposons consisting only of DNA that moves directly from place to place (Fig. 4a), (ii) Retrotransposons, which first transcribe the DNA into RNA and then use reverse transcriptase to make a DNA copy of the RNA to insert in a new location (Fig. 4b) (Lodish et al., 2000).

In the late 1970s, TEs were considered as "genomic parasites" or "selfish DNA" since the genomic information carried by TEs is primarily used for self-multiplication without direct benefit to the host (Doolittle and Sapienza, 1980; Orgel and Crick, 1980). At individual level, the mutations introduced by TEs can be deleterious to the organism which contains them. On the other hand, TEs may play an important role by lateral gene transfer and by rearranging existing sequences, which are important genetic mechanisms for the evolution of genomes (Britten, 1997; Capy et al., 2000; Miller, 1997). Insertion of a transposon within or near a gene can activate or alter the level, tissue specificity, or developmental timing of gene expression (Errede et al., 1980; McGinnis, 1983; Reynolds, 1981). Excision of TEs can also influence gene expression. Excision is often imprecise, and this leads to sequence alterations at the excision sites (Bender, 1983; Carbonare and Gehring, 1985; Tsubota and Schedl, 1986).

Such imprecise excision of TEs may result in proteins altered in size (Shure et al., 1983), enzymatic activities (Tsubota and Schedl, 1986), or developmental patterns of expression (Coen et al., 1986).

In baculoviruses, different studies suggest that TEs may play a major role in the variation observed in baculoviruses genomes. TEs are frequent drivers of recombination between the insect host genomes and baculoviruses (Fraser, 1986; Friesen, 1993; Jehle, 1996). Variation in baculovirus genomes through the action of mobile elements occurs spontaneously and frequently during propagation in lepidopteran cell cultures but has also been demonstrated *in vivo* (Jehle et al., 1995; Jehle et al., 1998). Few-polyhedra (FP) mutants of NPVs are one of the well-known phenomenons during serial passage of virus in cell culture. Under these circumstances such mutants produce low yields of OBs and poorly occlude virions, but they are selected for through advantageous rates of BV replication. Spontaneous insertion of TEs originating from host cell DNA into the viral FP25 gene has been shown to be a common cause of the FP25 phenotype (Bull et al., 2003).

Most transposons in baculoviruses cannot transpose themselves anymore to other DNA molecules as they do not encode an active transposase gene. This suggests that baculovirus genomes serve as a ‘sink’ for transposons (van Oers and Vlak, 2007). Baculoviruses are serious candidates to shuttle transposons between insect species (Blissard and Rohrmann, 1990; Friesen, 1993). Beside the fact that many baculoviruses have different hosts, several facets of their replication strategy and genome organization permit the spontaneous accommodation of transposons (Jehle et al., 1998). Firstly, replication of the double stranded viral DNA genome takes place within the host nucleus which allows the virus and insect DNA to come in close contact giving the transposon a potential chance for horizontal escape (Granados and Williams, 1986). Secondly, baculoviruses are flexible with regard to the size of genomic DNA packaged during virion assembly. Thirdly, baculoviruses contain non-essential genomic regions where foreign DNA can integrate (Friesen, 1993). Finally, baculoviruses do not necessarily kill their host, they can have abortive infections in non-permissive hosts without complete virus replication (Bilimoria, 1991). Sublethal infections are also reported (Sait et al., 1994). This may allow the transposon to move from a baculovirus genome back to an insect genome. Many transposon-derived insertions in baculovirus genomes originate from insertions of relative small elements that exhibit a remarkable specificity for TTAA target sites. Upon insertion, the TTAA is duplicated together

with short inverted repeats present on both ends of the inserted DNA. These elements normally do not have ORFs (Friesen, 1993).

Depending on the integration site, the effect of transposon insertion can vary from an advantageous to a silent event or a devastating mutation. Disruption of an essential ORF or its regulatory sequences can lead to a non-viable virus mutant. Furthermore, integration of such transposon within regulatory regions or introns of various genes may result in enhancement or inhibition of expression (Friesen, 1993). These alterations occur due to insertion of new promoters, termination signals, or both, located within the transposon. A good example was in AcMNPV, insertion of such transposons into the FP25k locus ORF61 resulted in the FP phenotype (Beames and Summers, 1988; Miller and Miller, 1982).

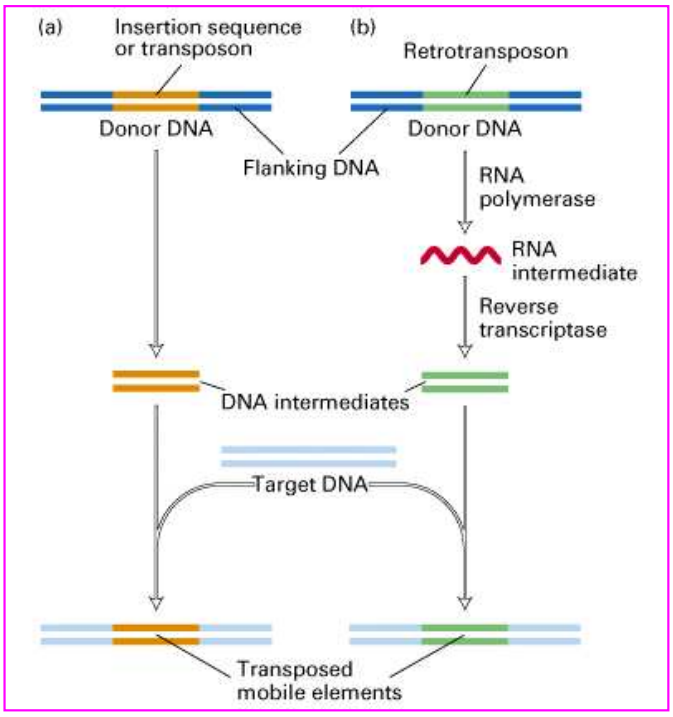

Fig. 4. Flowchart of the DNA transposon **(a)** and retrotransposon **(b)** as descriped by Lodish *et al.*, 2000.

A frequently observed event is the insertion into a baculovirus of a retrotransposable element, called TED (gypsy family), which is derived from the *T. ni* genome (Friesen and Nissen, 1990; Hajek and Friesen, 1998; Miller and Miller, 1982; Ozers and Friesen, 1996). TED is recognized by long terminal repeats (LTRs) in both ends that flanking three open reading frames analogous in size and position to the retroviral gag, pol, and env genes (Friesen, 1993; Friesen et al., 1986). Insertion of TED in AcMNPV and subsequent excision

(possibly via homologous recombination between the LTRs) leaves LTRs in the viral genome. This element showed promoter activity in both directions and hence may alter gene expression of flanking genes (Friesen et al., 1986). Insertion of a TED also results in an FP phenotype (Miller and Miller, 1982).

9. Transposons in CpGV

TEs have been found in genetic variants of CpGV after *in vivo* cloning experiments, which resulted in isolation of spontaneous mutants named MCp5 and MCp4 (Jehle et al., 1995; Jehle et al., 1998). The mutant MCp5 contains a 4.7 kb long insertion (TCl4.7) derived from *C. leucotreta*, an alternative host of CpGV. MCp4 mutant has a transposon of 3.2 kbp (TCp3.2) originating from *C. pomonella*, with 750 bp inverted terminal repeats (ITRs). This latter transposon caused inversions in the CpGV genome by homologous recombination between the ITRs (Arends and Jehle, 2002). By nucleotide sequencing of the TCl4.7 transposon located in MCp5, it was reported that the TCl4.7 transposon is 4726 bp in size, flanked by imperfect inverted terminal repeats of 29 bp, and integrated into the target dinucleotide TA that is duplicated during the transposon integration as it is typical for many *Tc1-like/mariner* transposon (Fig. 5). TCl4.7 encompasses a defective ORF sharing homologies to transposase genes of TC1-related transposable elements found in *Caenorhabditis* and *Drosophila* species (Jehle et al., 1995). The TA integration site of TCl4.7 is located in a non-protein-coding region between ORFs Cp15 and Cp16 at nt 11987-11988 of the CpGV-M genome and separates two palindromes hr3 and hr4, which have been recently shown to be CpGV origins of replication (Fig. 5) (Hilton and Winstanley, 2007; Jehle et al., 1995; Luque et al., 2001).

Cp15 is a conserved baculovirus gene which is located in all sequenced baculoviruses sequenced to date (van Oers and Vlak, 2007). Cp16 is moderately conserved among a number of GVs however the conservation of Cp16 ORF within NPVs group I and II is lower than GVs (Luque et al., 2001). The DNA sequences encoding for Cp15 and Cp16 genes were previously investigated for the presence of putative transcription start sites, such as TATA(A), the consensus early transcription initiation motif (ATCA(G/T)T(C/T) and the essential TAAG motif for late genes transcription, in the regions upstream of Cp15 and Cp16 genes (Arends, 2003). Consensus early and late transcription initiation motifs were found 118 bp and 20 bp upstream from the first ATG start codon of Cp15, respectively. CpGV Cp15 shows homology to AcMNPV *ac142* with 37% amino acid sequence identity (Luque et al., 2001).

Transcriptional analysis of AcMNPV ac142 suggested that it is a late gene and transcribed from the promoter region which contains a single late gene transcriptional start site (ATAAG) located 18 bp upstream from the translational start codon (McCarthy et al., 2008). Recently, proteomic analyses of three baculoviruses, AcMNPV, *Helicoverpa armigera* SNPV (HearSNPV), and *Culex nigripalpus* NPV(CuniNPV), identified *ac142* or its homologs (*Hear9*, *Cuni30*) as proteins associated with ODV structure (Braunagel et al., 2003; Deng et al., 2007; Huang et al., 2007). As it is a core gene and is associated with ODV, *ac142* plays a potentially vital structural function in the viral life cycle (Huang et al., 2007).

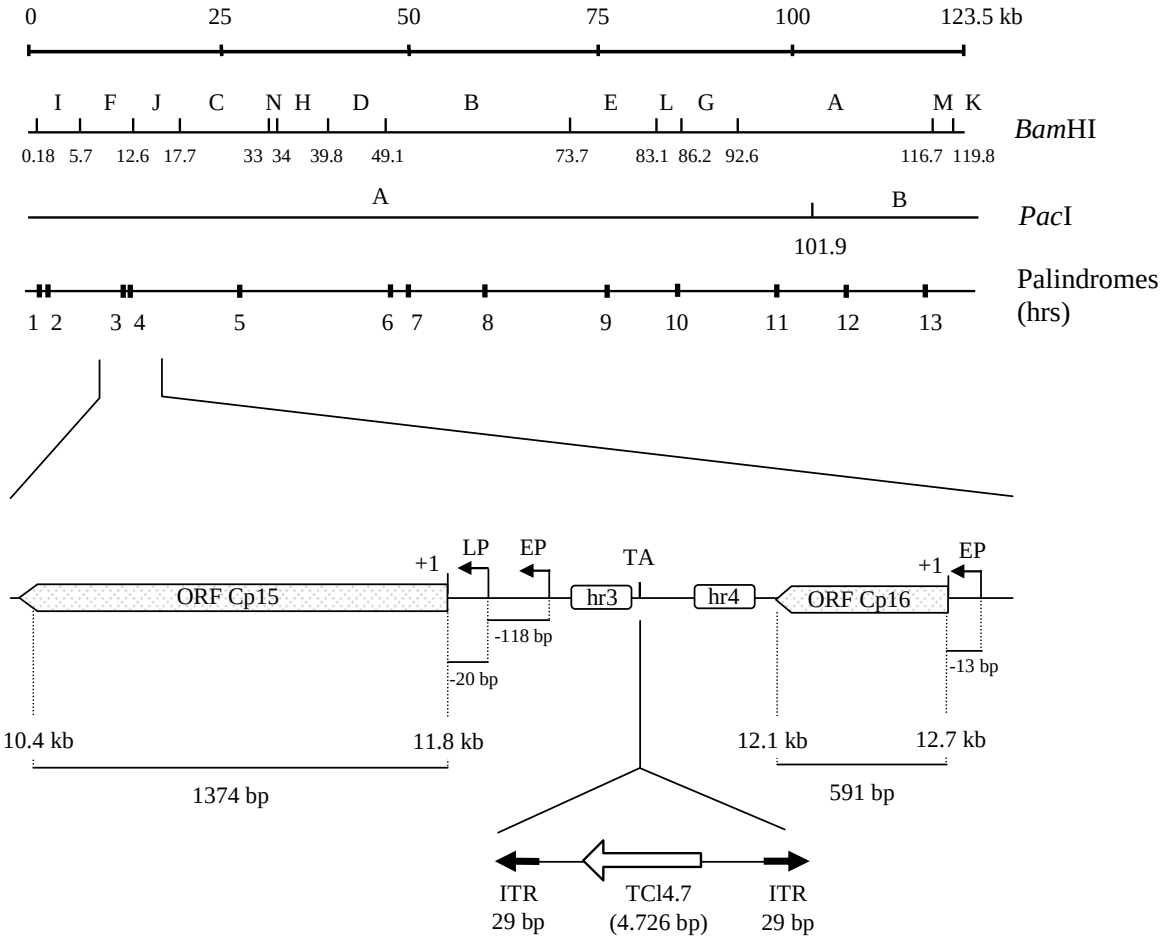

Fig. 5. Location and organization of the TA dinucleotide insertion site of the transposon TCl4.7 within the CpGV-M genome. On top, the restriction maps of *Bam*HI and *Pac*I endonucleases are indicated according to the CpGV complete genome sequence (Luque et al., 2001). The position in kb of each restriction site is shown. The zero point for the map is the start of the granulin gene. The CpGV 13 palindromes (hr*s*) are depicted by black bars. Below, the size and the orientation of open reading frames (ORFs) Cp15 and Cp16 flanking the transposon insertion site are indicated by shaded arrows. Location of the potential early promoter motifs (EP) or late promoter motifs (LP) are shown upstream of each ORF ATG start codon (Luque et al., 2001). The TA (11987-11988 nt) TCl4.7 insertion site and the relative position of hr3 and hr4 are also indicated.

On the other hand, Cp16 is possibly an early transcribed gene with unknown function since a consensus TATA box and a consensus transcription initiation sequence CAGT were located 24 bp and 13 bp upstream from the first putative ATG start codon of Cp16, respectively (Fig. 5) (Arends, 2003).

10. Influence of TCl4.7 transposon integration in CpGV-M

Infection parameter median lethal dose (LD_{50}), median survival time (ST_{50}) and virus offspring production revealed no difference between the analyzed viruses CpGV-M and the mutant MCp5 carrying TCL4.7 transposon. No evidence for decreased infectivity of mutant MCp5 was found (Arends et al., 2005; Jehle et al., 1995). Considering the ST_{50}, the mutant MCp5 appeared to kill fifth instar *C. pomonella* larvae slightly slower than CpGV-M. In addition, the progeny virus yields of the parental CpGV-M and the MCp5 did not reveal a statistically significant difference between the genotypes (Arends et al., 2005). Taken together, the bioassays demonstrated that the MCp5 retained their virulence and their ability to complete the replication cycle and produce infective OB in *C. pomonella* larvae. However, when the competitiveness of virus genotypes was determined in co-infection and passaging experiments, a rapid out-competition of the mutant MCp5 by CpGV-M was observed (Arends et al., 2005). This result indicated a tremendous selection disadvantage of MCp5 compared to CpGV-M.

The molecular mechanism causing the replication disadvantage of MCp5 is not clear yet and further experiments will be necessary to analyse whether the transposon insertion can alter the transcription regulation of the adjacent genes (Cp15 and Cp16). And thus, whether the insertion of TCl4.7 transposon into the non-coding genomic region between ORFs Cp15 and Cp16 is linked to the tremendous difference of competitiveness observed between CpGV-M and MCp5.

Aim of work and outline of thesis

This study was performed in order to obtain a better understanding of the effect of the TCl4.7 transposon insertion in the genome of CpGV-M on virus gene regulation including its potential to alter the expression profile of the ORFs Cp15 and Cp16 adjacent to the TCl4.7 transposon integration site.

The aim of this study was to find out answers for two main questions:

(1) What is the plausible reason for the unusual pathology (similar virulence, different competitiveness of MCp5 (mutant carrying TCl4.7 transposon) compared to the CpGV-M?

(2) Does TCl4.7 transposon integration affect gene regulation of adjacent ORFs Cp15 and Cp16?

To identify the molecular basis of the difference between both CpGV-M and MCp5, the following molecular studies were aimed:

(1) Studying the temporal transcription of the ORFs Cp15 and Cp16 using RT-PCR and quantitative Real-Time PCR in both CpGV-M and MCp5.

(2) Studying the temporal protein expression of Cp15 and Cp16 ORFs through Western blotting analysis in a time course experiment.

(3) Examining the ability of CpGV-M to replicate in the absence of Cp15 and Cp16 ORFs, by using bacmid technology to generate mutant viruses lacking Cp15 and Cp16.

(4) Moreover the deletion of palindromes hr3 and hr4 which are flanking the integration site of the TCl4.7 transposon will carried out in order to identify the ability of virus replication in the absence of both palindromes, which are identified recently as a part of CpGV-M origin of replication (ori).

(5) *In vitro* insertion of Kan^R resistance cassette between the palindromes hr3 and hr4, as a mimic construction for TCl4.7 transposon insertion, will be carried out in order to investigate whether the interruption of the region between hr3/hr4 can influence the viral infection cycle.

(6) Determination of virulence parameters LC_{50} and ST_{50} for the generated mutant bacmids will be performed in order to identify the absence effect of the target genes on virus's virulence and efficacy.

III. MATERIALS AND METHODS

1. MATERIALS

1.1. Insects

Codling moth (CM) (*Cydia pomonella* L., Lep.: *Tortricidae*) used for virus propagation and bioassay experiments were derived from the insect rearing facility of the Agricultural Service Centre Palatinate (DLR Rheinpfalz), Neustadt/Weinstr, Germany. The larvae were kept at 26°C, 60% relative humidity and a 16/8 h light/dark photoperiod. Larvae were reared on a semi-artificial diet (Appendix I) described by (Ivaldi-Sender, 1974). Briefly, the diet was prepared by dissolving corn flowers and agar–agar in a known amount of tap water; the mixture was autoclaved for 20 min at 120°C then mixed well with wheat germ and brewer‘s yeast and left to cool to 60-65°C. Then nipagin (methyl-4-hydroxybenzoate) dissolved in 5 ml ethanol and ascorbic acid dissolved in 10 ml water were added and mixed well with the medium. The medium was poured in rearing plates (Raster boxes, *Neolab*-Heidelberg, Germany) and left at room temperature for one hour for solidification. The plates were kept at 4°C until usage within 4 weeks.

1.2. Virus genotypes

CpGV-M	(Tanada, 1964)
CpGV-MCp5 (MCp5)*	(Jehle et al., 1995)

*CpGV-MCp5 is a mutant variant of CpGV-M virus, containing the TCl4.7 transposon

1.3. Chemicals and laboratory materials

Chemical substances and reagents used in this study and not specially mentioned in the text were purchased from: Sigma (Deisenhofen), Roth (Karlsruhe), Roche (Mannheim). All DNA and protein standard markers were purchased from Invitrogen (Karlsruhe), Fermentas (Leon-Rot) and Promega GmbH (Mannheim). For all media and buffers see Appendix I and for plasmids maps see Appendix II.

Enzymes

Taq DNA polymerase 1000 units, 5 U/µl	Axon Labotechnik

T4 DNA ligase 100 units, 1 U/µl	Invitrogen
Reverse Transcriptase 10,000 units, 200 U/µl	Invitrogen
Shrimp Alkaline Phosphatase (SAP) 500 units, 1 U/µl	Promega
Ribonuclase A 100 mg, 90 U/mg	ROTH
Proteinase K 10 mg, 30 U/mg	ROTH
*Pac*I recombinant endonuclease 250 units, 10 U/µl	Biolabs, New England
Other DNA endonucleases 10 U/µl	Fermentas

Antibodies

Anti-Rabbit IgG Peroxidase, Developed in Goat, 0.5 ml	Sigma
His.Tag® Monoclonal Antibody 100 µg	Novagene
Anti-Rabbit IgG Cp15 polyclonal antibody	Davids Biotechnology, Germany
Anti-Rabbit IgG Cp16 polyclonal antibody	Davids Biotechnology, Germany

Bacterial strains

Table 1. Bacterial strains which were used for cloning and protein expression.

Bacteria (E. coli)	***Function***	***Characteristics***	***Source***
DH5α	Cloning	F^- Φ80d*lac*ZΔ M15 Δ(*lac*ZYA) U169 *rec*A1 *end*A1 *hsd*R17 (r_k^-, m_k^+) *pho*A *sup*E44 λ^- *thi*$^-$ *gyr*A96 *rel*A1	Invitrogen
BL21-CodonPlus (DE3)-RP	Protein expression	*E. coli* B F^- *ompT hsdS*(r_B^- m_B^-) *dcm*$^+$ Tet^r *gal* λ(DE3) *endA* Hte [*argU* proL Cam^r)	Stratagene
TransforMax™-EPI300™	Cloning	F^- mcrA Δ(*mrr-hsdRMS-mcrBC*) Φ80d*lacZΔM15 ΔlacX74 recA1 endA1 araD139* Δ(*ara, leu*)7697 *galU galK* λ^- *rpsL nupG trfA dhfr*	EPICNTRE-Biotechnologies

Plasmids

Table 2. Plasmids which were used for cloning and protein expression, maps can be seen in (Appendix II).

Plasmid	***Resistance gene***	***Promoter***	***Tag***	***Company***
pGEM®-T Easy	Amp^r	T7 and Sp6	-	Promega
pET-28b(+)	Kan^r	T7	His-Tag /T7-Tag	Novagen
CopyControl pCC1BAC	Chl^r	T7	-	EPICENTRE
PIE1^{hr}/PA	Amp^r	ie1/early	-	Cartier et al., 1994

Oligonucleotides

Table 3. Overview of oligonucleotides (5'-3') used for PCR analysis and sequencing (synthesized by MWG Biotech AG., Germany). The introduced restriction endonucleases are under lines. The genome position of the oligonucleotides in CpGV-M in positive strand (+) or negative strand (-) are indicated in brackets.

1. Primers used for homogeneity detection of CpGV and MCp5 virus stocks		
PR-CpGV-LB	ctg gtt gga tgt gga gta tgt a	[12285-12306 nt (+)]
PR-CpGV-RB	cta agt tgg ggg aag taa tgt aa	[11796-11818 nt (-)]
PR-TCl4.7-int	tgc ttc gac aca aca gag aca g	
2. Primers used for RT-PCR detection of Cp15, Cp16 and F protein genes		
Cp15-rt_F	tcc ggtatc tgt gtc cca tca	[11178-11198 nt (+)]
Cp15-rt_R	acc gcg gac acc ttc aag tat	[11576-11596 nt (-)]
Cp16-rt_F	caa aaa cac cct cct ctg acg a	[12261-12282 nt (+)]
Cp16-rt_R	aat atc tgg ctt tgg acg gtg tt	[12699-12721 nt (-)]
F-Protein _F	gac agg gac gca gca cta ct	[25775-25794 nt (+)]
F-Protein _R	tcc gcc aca ctg tcc ttg at	[25946-25965 nt (-)]
3. Primers used for qReal-Time RT-PCR analysis of Cp15, Cp16 and F protein genes		
Cp15qRT_F	gca agt ttg atg gga cac aga tac	[11182-11205 nt (-)]
Cp15qRT_R	aaa cgc gtc aaa cac cac at	[11057-11076 nt (+)]
Cp16qRT_F	gaa gcg cct aaa aca gac cca cat	[12397-12420 nt (-)]
Cp16qRT_R	aca ccc tcc tct gac gat tta cat	[12266-12289 nt (+)]
F-Protein_F	gac agg gac gca gca cta ct	[25775-25794 nt (+)]
F-Protein_R	tcc gcc aca ctg tcc ttg at	[25946-25965 nt (-)]
4. Primers used for the amplification of Cp15 and Cp16 ORFs of CpGV		
Cp15-ORF_F	gaa aag ctt atg ggt gac aac tct gcc a	[11758-11776 nt (-)]
Cp15-ORF_R	cac ctc gag tta ata ttt tct tac aaa taa act	[10403-10426 nt (+)]
Cp16-ORF_F	cac aag ctt atg acc act acc aaa aaa tat ctg	[12714-12737 nt (-)]
Cp16-ORF_R	gaa ctc gag cta ttc act act aaa cgc gct	[12147-12167 nt (+)]
5. Primers used for the amplification of enhanced GFP ORF		
Egfp-orf_F	aaa ctg cag atg ggc aaa gga gaa gaa ctt	
Egfp-orf_R	tcc aag ctt tta ttt gta tag ttc atc cat	
6. Primers used for the amplification of IE1-GFP-PA cassette		
pIE1-gfp_F	ttt ctc gag ggg gat ccg gcg cgt aaa a	
pIE1-gfp_R	ttt ctc gag tta att aat ata ggg cga att gga gct cga at	
7. Primers used for construction of Cp15-null and Cp16-null Bacmids		
PCp15NL-F	ccc gca atg cgt cta gtt aca cct gtg tcg gta cct ctg aac gtg tcc atc ccg ggt gga cag	

	caa gcg aac cgg aat tg	*[5'-(50 bp) 10353-10402 nt (+)]
PCp15NL-R	tag ttt att aca tta ctt ccc cca act tag taa gtc att att tta taa aac ccg ggt cag aag aac	
	tcg tca aga agg cg	*[5'-(50 bp) 11776-11825 nt (-)]
PCp16NL-F	agg aaa aat ttt aaa att ttt aaa ttt tgc cga ata aac tca gct cgt gtc ccg ggt gga cag	
	caa gcg aac cgg aat tg	*[5'-(50 bp) 12097-12146 nt (+)]
PCp16NL-R	cca aca gta tat atg gtg act agg aat ata cta tta tca gtg tta caa cac ccg ggt cag aag	
	aac tcg tca aga agg cg	*[5'-(50 bp) 12738-12787 nt (-)]

8. Primers used for the detection of Cp15-null and Cp16-null Bacmids

B-Cp15-det_F (D1)	cgt gtt gag cgg gtt gaa gaa t	[10205-10226 nt (+)]
B-Cp15-det_R (D2)	gat atg ggc gca cgt aat gga cta	[12338-12261 nt (-)]
B-Cp16-det_F (D3)	ggt gtc cgc ggt ggc atc a	[11585-11603 nt (+)]
B-Cp16-det_R (D4)	ggt ttc cgg cga caa aaa cga ca	[12922-12944 nt (-)]

9. Primers used for Cp15 gene amplification with *Sma*I sites

Cp15-SmaI_F	tcg agc ccg ggg gta cct ctg aac gtg tcc at	[10383-10402 nt (+)]
Cp15-SmaI_R	tcg acc ccg ggc aga ctc gtg acg ccg cta t	[11895-11914 nt (-)]

10. Primers used for CpBAC^{Cp15KO} rescue

PCp15REP-F	tac agc cag tag tgc tcg ccg cag tcg agc gac agg gcg aag ccc tcg agg gta act gaa	
	gtt tta aat caa tct aaa gt	*[5'-(50 bp) 109627-109676 nt (+)]
PCp15REP-R	taa ttg tgt tta ata tta cat ttt tgt tga gtg cac tag tcg agg tcg acg gta act cgt atg ttg	
	tgt gga att gt	*[5'-(50 bp) 111317-111366 nt (-)]

11. Primers used for the construction of CpBAC$^{hr3/hr4KO}$ mutant bacmid

Phr3/hr4NL-F	aca gac aca caa aat acg tca aat gta caa tca aat gat ata gcg gcg tcc ccg ggt gga	
	cag caa gcg aac cgg aat tg	*[5'-(50 bp) 11856-11905 nt (+)]
Phr3/hr4NL-R	cag caa caa aaa gtg tgc tcc atg att gaa agc gcg ttt agt agt gaa tac ccg ggt cag	
	aag aac tcg tca aga agg cg	*[5'-(50 bp) 12148-12197 nt (-)]

12. Primers used for the construction of CpBAC$^{hr3\text{-}kan\text{-}hr4}$ mutant bacmid

Phr3-kan-hr4-F	tta gcg aaa aac ttt ttt tcg cta aaa tct cgg cgc aaa gcc aga ttc gtc ccg ggt gga cag	
	caa gcg aac cgg aat tg	*[5'-(50 bp) 11932-11981 nt (+)]
Phr3-kan-hr4-R	ttt aaa aat ttt aaa att ttt cct aaa tca gct aat aaa gtc ggc ctc gtc ccg ggt cag aag	
	aac tcg tca aga agg cg	*[5'-(50 bp) 12071-12120 nt (-)]

13. Primers used for the detection of CpBAC$^{hr3/hr4KO}$ and CpBAC$^{hr3\text{-}kan\text{-}hr4}$

Det-hr3/hr4-F (D5)	acc gtg gca gag ttg tca ccc at	[11754-11776 nt (+)]
Det-hr3/hr4-R (D6)	tg aaa gcg cgt tta gta gtg aat ag	[12147-12171 nt (-)]

* The homology sequence (50 bp) of the left and right border of the deleted DNA fragment

2. METHODS

2.1. Insects and viruses

2.1.1. Virus stock production

In order to produce pure virus stocks of CpGV-M and MCp5, late fourth instar of CM were inoculated by feeding them a small piece of medium inoculated with 1000 OB of either CpGV or MCp5. Only the larvae that had completely ingested the medium within 24 hour were transferred to a fresh virus free medium and reared individually at 26°C. Dead larvae succumbed from virus infection were collected in 2-ml Eppendorf tubes just after larval death and before liquefication, when they were still whitish. They were kept frozen at -20ºC until OB purification.

2.1.2. Virus OB purification from infected larvae

The OBs were purified from CM cadavers by grinding them in 0.5% sodium dodecyl sulphate (SDS) solution. The crude suspension was filtered through a piece of cotton wool and a tea filter into 50-ml Falcon tubes. The filter was rinsed with 30 ml of 0.5% SDS and the suspension was completely squeezed out of the filter. The suspension was centrifuged at 10,000xg (8900 rpm Eppendorf-Centrifuge 5810R) for 30 min at 10ºC and the pellet containing the OBs was resuspended in 2 ml of 0.5% SDS. The pellet was sonicated for 5 min and then loaded on the top of a 60%, 70% and 80% (v/v) glycerol layer gradient in 15-ml Falcon tubes. The gradient was centrifuged for 30 min at 3220xg (4000 rpm Eppendorf 5810R) at 10ºC in a swing-out rotor (A-4-62, Eppendorf). The 60% glycerol layer containing virus OB was transferred to a fresh 15-ml Falcon tube, diluted with a few ml of bidistilled water (bdH_2O) and then centrifuged for 30 min at 4000 rpm at 10ºC. The pellet was resuspended in 2 ml bdH_2O and applied for glycerol gradient centrifugation once more as described above. The whitish virus layer was then transferred to a 2-ml Eppendorf-tube using a long Pasteur pipette and centrifuged for 10 min at full speed 20,800xg (14,000 rpm Eppendorf-centrifuge 5417C) at room temperature. The OBs pellet was washed twice with bdH_2O and then resuspended in bdH_2O or TE buffer (Appendix I) and stored at -20ºC.

2.1.3. Virus OBs counting

The purified OBs obtained in (2.1.2) were counted in the dark field of Leica-DMRBE microscope with 400X magnification using a Petroff-Hauser counting chamber (depth 0.02 mm, Hausser Scientific). The counting chamber contains 25 big squares with a size of 0.004 mm^2, each square divided to 16 small squares. 10 µl of virus suspension were used for counting and the OBs were counted in 5 different big squares. The virus concentration was calculated using the formula: Mean of OBs in 5 big squares x 1250 x virus dilution = OBs/ml.

2.1.4. Infection of CM in a time course for RT-PCR and qRT-PCR

CM larvae (L4) were inoculated by feeding them a small piece of medium (approximately 3 mm^3) inoculated with 1000 OB of either CpGV-M or MCp5. Only the larvae that had completely ingested the medium within 24 hours were placed on fresh virus free medium and reared individually at 26°C. At each time point 0, 6, 12, 24, 48, 72 and 96 hour post infection (hpi), larval midguts were isolated by dissecting the CM larvae without damaging the midguts and then the midguts were removed from the insect body and rinsed in 1X PBS solution (Appendix I). The isolated midguts were cleaved using two forceps to detach the Pretrophic Membrane (PM) from midguts which may contains food and RNase residues. The midguts were briefly rinsed in 1X PBS and pooled as five larvae midguts in 2-ml Eppendorf tube for each time point. Isolated midguts were cooled immediately in liquid nitrogen and stored at -80ºC until usage. The isolated midguts were subjected to total RNA extraction and cDNAs synthesis for RT-PCR and quantitative real-time RT-PCR (qRT-PCR) using Cp15, Cp16 and F protein specific primers.

2.1.5. Injection experiments of CM larvae using CpGV-M bacmid DNA (CpBAC)

CpGV-M genome was manipulated as a bacmid in *E. coli* in order to generate mutant viruses from the bacmid. For transfection of the generated CpGV-M bacmid (CpBAC) into CM larval, bacmid DNA was mixed with lipofectin transfection reagent (Invitrogen) in sterile bdH_2O using a ratio of 500:250 (ng/µl) bacmid DNA: lipofectin. Before injecting larvae were treated with 0.4 Hyamin (Sigma) for desinfection and then anaesthetised with diethyl ether vapor for 2-3 min. One microliter of the mixture was injected into hemocoel of CM larvae (L4) through the third proleg of the larva using Microliter Syringes (25 µl) (HAMILTON, Switzerland). Twenty larvae were used for each treatment. After injection, larvae were transferred to a fresh diet and reared until larval death or pupation.

2.1.6. Peroral infection of CM larvae (L4) using CpBAC OBs

After the injection experiments using CpGV DNA or bacmid DNA, larvae that had died from virus infection were collected in 2-ml Eppendorf tubes and subjected to OBs purification and counting as described in 2.1.2 and 2.1.3. CM larvae (L4) were subjected to peroral infection using a small piece of medium inoculated with the purified CpBAC OBs (1000 OBs/larva). Only the larvae that had completely ingested the inoculated piece of medium within 24 hpi were transferred to a fresh virus free medium and reared individually at 26°C. Dead CM larvae succumbed from virus infection were collected in a 2-ml Eppendorf tubes just after larval death and kept frozen at -20ºC until OBs purification for the bioassay experiments.

2.1.7. Determination of LC_{50} and ST_{50} values of CpBAC and its mutants

First instar CM larvae were used to determine the median lethal concentration (LC_{50}) and median survival time (ST_{50}) for CpBAC OBs and its generated mutants using OBs collected from infected larvae 12-14 days post infection (dpi). Bioassays were performed in autoclavable 50-well plates containing 45 ml of diet mixed with 5 ml virus suspension. Except for the virus, the same diet was used as for the rearing (1.1). The LC_{50} was determined using OB concentrations of $3x10^2$, $1x10^3$, $3x10^3$, $1x10^4$, $3x10^4$, $1x10^5$ OB/ml as well as two virus free control plates, which were mixed with water instead of virus suspension. For the bioassays, half the amount of agar–agar was applied (10 g/liter) to assure that the diet could cool down to 40°C without solidifying. This prevented thermal inactivation of the virus while mixing the virus suspension with the diet. For each bioassay, 35 individually held larvae were used per concentration. Each bioassay was replicated three times independently using freshly made solutions each time. Larval mortality was determined at the day 1 following the experimental setup, to exclude those larvae which died from handling, at day 7 and at day 14. Larvae which did not react to tactile stimuli by touching with a needle were regarded as dead. The ST_{50} was determined by inoculating 35 individually held larvae in three replicates with the calculated LC_{80} for each tested virus, as well as three control plates which were mixed with water instead of virus suspension. Mortality of the larvae was monitored daily and every 8 hours starting at day 5 post infection until day 12 or larval death.

2.1.8. Statistical analysis

Estimation of the LC_{50} and slopes of regression lines were calculated by probit analysis (normal distribution) using the SAS software package. Significance testing of the LC_{50} was done by pairwise comparisons using non-overlapping 95% confidence intervals (CIs); $P < 0.05$ (Robertson and Preisler, 1992). The ST_{50} value was determined using the Kaplan-Meier estimator analysis method (Kaplan-Meier, 1958), and the NCSS statistical analysis and graphics software (NCSS statistical analysis software for windows).

2.1.9. Competition experiment between CpBAC and CpBAC$^{hr3\text{-}kan\text{-}hr4}$

To compare the proportion of each virus genotype in virus inoculum with that in virus offspring, co-infection experiments between CpBAC and CpBAC$^{hr3\text{-}kan\text{-}hr4}$ were performed in CM larvae. CM larvae (L4) were inoculated by feeding them a small piece of medium containing 1000 OB/larva in a mixture of CpBAC:CpBAC$^{hr3\text{-}kan\text{-}hr4}$ using five different viruses ratio in five replicates. Only the larvae that had completely ingested the medium within 24 hpi were transferred to a fresh virus free medium and reared individually at 26°C. CM larvae died from virus infection were collected in a 2-ml Eppendorf tubes just after larval death and subjected to OBs purification and DNA extraction as described by Jehle et al. (1992). The samples of isolated viral DNAs were digested using *Bam*HI restriction endonuclease, DNA restricted fragments were separated on 0.8% TAE agarose gel and stained with ethidium bromide (0.1 µg/ml). After staining, gels were photographed using INTAS Gel Documentation System and the optical density of the single DNA specific fragments for each genotype was quantified using the Imagemaster 1D software (Amersham Pharmacia Biotech). By correlating the sizes and the densities of the genotype-specific and genotype-shared restriction fragments, the molar proportions of the different DNA fragments were calculated. Using these molar proportions, the ratios of the CpBAC and mutant genotype CpBAC$^{hr3\text{-}kan\text{-}hr4}$ in the virus offspring were determined (see results 4.4).

2.1.10. Injection using mutant bacmids DNAs into CM larvae hemocoel

For transfection of the generated bacmids into hemocoel of CM larvae, bacmids DNA were mixed with lipofectin transfection reagent (Invitrogen) using sterile bdH_2O using a ratio of 500:250 (ng/µl) bacmid DNA: lipofectin and injected into larvae hemocoel as described in paragraph 2.1.5. After injection, larvae were transferred to a fresh diet and reared until death or pupation. The same methodology was used for transfection of each generated mutant

bacmid designed; $CpBAC^{Cp15KO}$ (Cp15-null), $CpBAC^{Cp16KO}$ (Cp16-null), $CpBAC^{hr3/hr4KO}$ (hr3/hr4-null) and $CpBAC^{hr3\text{-}kan\text{-}hr4}$ (with an insertion of Kan^R gene between hr3 and hr4).

2.1.11. Peroral infection of CM larvae (L4) using the generated mutant viruses

After transfection of mutant bacmid DNAs into CM larval hemocoel, larvae that had died from virus infection were collected in 2-ml Eppendorf tubes and subjected to OB purification and counting as described in 2.1.2 and 2.1.3. CM larvae (L4) were peroral infected using a piece of medium (approximately 3 mm^3) inoculated with the purified OBs (1000 OB/larva). Only the larvae that had completely ingested the medium within 24 hpi were transferred to a fresh virus free medium and reared individually at 26°C. Dead CM larvae resulted from virus infection were collected in a 2-ml Eppendorf tubes just after larval death and kept frozen at -20ºC until OB purification to be used for determining the LC_{50}.

2.2. DNA molecular analysis

2.2.1. DNA isolation of virus OBs

About 500 µl of the purified OBs ($1.5x10^{11}$ OB/µl) were pelleted and resuspended in autoclaved 500 µl 1X TE-buffer. CpGV-M virions were released from OBs by incubation in 0.1 M Na_2CO_3 at 37°C for 1 h. The solution was neutralized to pH 8.0 with 1.0 M HCl and was subsequently treated with 45 µg/ml RNaseA at 37°C for 10 min. To disrupt the virions, the solution was incubated in 1% SDS and treated with 250 µg/ml Proteinase K for 1 h at 37°C. The solution was extracted twice with a TE-saturated phenol:chloroform:isoamyl alcohol mixture [25:24:1 (v/v/v)], followed by chloroform:isoamyl alcohol [24:1 (v/v)] extraction. The DNA was precipitated in 2.5 volumes ice-cold 97% Ethanol in the presence of 1/10 volume 3 M NaAc, pH 5.2, for 10 min at full speed 20,800xg (14,000 rpm Eppendorf-centrifuge 5417C) at 4ºC. The DNA pellet was washed twice with 70% Ethanol and centrifuged again for 10 min at full speed 20,800xg at room temperature and finally eluted with 50 µl 1X TE buffer.

2.2.2. DNA restriction endonuclease analysis (REN)

Restriction endonuclease digestion of plasmids or virus genomic DNAs was performed by incubation of about 1-2 µg DNA with 5-10 units of the appropriate restriction endonucleases according to manufacturer's instruction. Reaction was performed using the

buffer recommended by the manufacture at the appropriate temperature for 2 h to over night. The sizes of fragments were determined on agarose gel using DNA size standard (e.g. Lambda DNA/*Hin*dIII Marker). The restriction endonuclease was inactivated if possible by incubation at 65°C for 15 min. If necessary, phenol:chloroform extraction and DNA precipitation was carried out.

2.2.3. Low melting agarose extraction

For the purpose of purification of the DNA fragments, the digested DNA fragments were loaded in a low melting agarose gel and agarose gel electrophoreses was done at 100 V and 50 mA. The desired bands were cut out under UV light (312 nm). The gel piece was put in an 1.5-ml Eppendorf tube and subjected to DNA extraction using GFX PCR and Gel Band Purification Kit (GE Healthcare, UK) according to the manufacturer's instruction.

2.2.4. Dephosphorylation of DNA 5' ends

To prevent religation of linearized plasmid DNA, phosphate groups were removed from the 5´ termini using Shrimp Alkaline Phosphatase (SAP) (Promega). For this, 30 µl of the REN digestion reaction were mixed with 5 µl of 10X SAP buffer, 1 µl of SAP dephosphorylation enzyme (1 U/µl) and the volume was completed to 50 µl with sterile bdH_2O. The reaction was incubated for 30 min at 37ºC; then the enzyme was deactivated by heating to 65°C for 15 min. The DNA was extracted with GFX PCR DNA and Gel Band Purification Kit following the manufacturer's instruction and the purified DNA was subjected to the ligation reaction. To test if the reaction was successful, a control ligation reaction was performed using SAP treated and untreated plasmid DNA.

2.2.5. Ligation of DNA REN fragments

To ligate DNA fragments into cloning vectors with compatible cohesive or blunt termini a reaction was performed containing DNAs with a molar ratio of 1:3 (vector : DNA fragment) using 1 µl T4 DNA ligase and 2 µl 10X ligation buffer in 20 µl total volume. The reaction was incubated at 16°C overnight and 2-3 µl of the ligation mixture was used directly for bacterial transformation.

2.2.6. Preparation of electro competent *E. coli* cells

Bacterial host strain was stroked on an LB plate containing appropriate antibiotics and grown at 37ºC overnight. A single colony was picked, inoculated in 5 ml of LB medium and the culture was grown at 37°C overnight with constant agitation at 250 rpm. On the next day, four Erlenmeyer flasks each containing 250 ml of pre-warmed LB without NaCl were inoculated with 1/100 volume of the overnight culture. The cultures were grown at 37°C with vigorous shaking until optical density at 600 nm (OD_{600}) reached 0.6-0.9. For cells harvest, the flasks were chilled on ice for 15-30 min, transferred to 250-ml centrifuge bottles and then centrifuged in a cold rotor (SLA-1500, SORVALL) at 4000 rpm at 4°C for 15 min. The supernatant was discarded and the cell pellets were resuspended in a total of 1 Liter of cold sterile bdH_2O and centrifuged as previously. The pellets were resuspended one time more using 0.5 Liter of cold sterile bdH_2O and centrifuged again. The resulting pellets were resuspended in 20 ml of 10% glycerol and then centrifuged as previously. Finally, the pellets were resuspended in 1-2 ml of 10% glycerol by gently pipetting back and forth. The cells were aliquoted in 50-100 µl volumes in 1.5-ml microcentrifuge tubes and frozen in liquid nitrogen before storing at -70°C. A 50 µl cells aliquot was used for each transformation reaction.

2.2.7. Transformation of *E. coli* cells

Frozen 50 µl aliquots of competent cells were thawed on ice for several minutes and mixed with 1 to maximum 5 µl of ligated plasmid DNA in a cold 1.5-ml Eppendorf-tube. The mixture was incubated on ice for 0.5 to 1 min and then electroporated using electroporation cuvettes of 1 mm gap size and a Gene Pulser apparatus at 25 µF and 2.5 kV with pulse controller 200 Ohm (*Bio-Rad*). One ml SOC or LB medium was added to the cells immediately after electroporation and the cells were resuspended using a Pasteur pipette. The suspension was transferred to sterile 15-ml Falcon tubes (Greiner Bio-One GmbH) and incubated for 90 min at 37°C with shaking at 225 rpm. After incubation, about 100-150 µl of the bacterial culture were plated on LB agar plates containing the appropriate antibiotics. The plates were incubated converted overnight at 37°C.

2.2.8. Blue/white selection of recombinant *E. coli* colonies

Blue/white selection for the presence of inserted DNA in cloning vectors containing the α-peptide coding region of the β-galactosidase gene (*lacZα*) was carried out by adding 20

µl of 100 mM IPTG and 40 µl of 40 mM X-Gal to the surface of the agar plates, spreaded on the plates and left to dry for 5-10 min. About 100 µl of the transformed bacterial culture was spreaded on the agar plates and after overnight incubation at 37°C, the white colonies that contained the recombinant plasmid were selected and applied for DNA restriction analysis.

2.2.9. Plasmid DNA preparation

For the isolation of small amounts of high copy number plasmid DNA for analytical purposes, a single colony was picked using a sterile toothpick and inoculated in 1.5-2.0 ml LB medium with the appropriate antibiotics and shacked vigorously overnight at 37°C. The next day, the culture was centrifuged for 1 min at 13,000 rpm (18,000xg) in a bench-top centrifuge (5417 C, Eppendorf), the supernatant was discarded and the precipitated bacterial pellet was used for plasmid DNA minipreparation using GFX Micro Plasmid Prep Kit (Amersham Biosciences) following the manufacturer's instruction. The typical yield of high copy number plasmids DNA prepared by this method was about 3-5 µg DNA per 1 ml of original bacterial culture. For low copy number cloning systems used in this study, e.g. BACs, the starting material was 50 ml of a bacterial overnight culture and bacmid DNA preparation was done using the User-Developed Protocol of QIAGEN® Plasmid Midi Kit (QIAGEN, USA) according to the manufacturer's instructions.

2.2.10. Agarose gel electrophoresis of nucleic acids

DNA fragments of plasmids DNA or PCR products were separated according to its molecular sizes in 0.8-1.5% (w/v) agarose gel dissolved in 1X TBE buffer (Appendix I). For separation of virus genomic DNA or virus DNA restriction fragments, 0.8% agarose gel dissolved in 1X TAE buffer (Appendix I) was used. Samples were mixed with DNA loading dye (Appendix I), loaded on the agarose gel and run using mini gel at 100 V and 50 mA for approximately 90 min. Virus genomic DNA restriction fragments were run in maxi gel at 25 V and 20 mA for 14-16 h. To determine the fragments size and estimate the DNA concentration, a suitable DNA marker was loaded close to the loaded samples in the gel lanes. After electrophoresis, gels were stained in Ethidium Bromide stain solution (0.5 µg/ml) for 30 min, destained for 10 min in water and the DNA fragments were visualized by illuminating with UV light (wavelength 312 nm). The photographs were taken using INTAS documentation system.

2.2.11. Polymerase Chain Reaction (PCR)

For all PCR analyses, the Mastercycler (Eppendorf) was used. The PCR reactions were done in a total reaction volume of 50 µl containing 1 µl of the appropriate upper-primer (10 pmol/µl), 1 µl of the appropriate lower-primer (10 pmol/µl), 1.5 µl $MgCl_2$ (50 mM), 1.5 µl of dNTPs mixture solution (10 mM), 2 µl of DNA template (0.1-0.5 µg), 5 µl of 10X PCR-reaction buffer and 0.5 µl of Taq DNA polymerase (5 U/µl). The reaction volume was completed to 50 µl using autoclaved bdH_2O. For a typical PCR the following programme was used: an initial 95°C for 3 min; a total of 30 cycles of denaturation at 95°C for 1 min, primer annealing at 50-60°C for 1 min and primer extension at 72°C for 1-3 min; final cycle at 72 ºC for 7 min to allow the completion of primer extension. PCR-amplified DNA was analyzed by electrophoresis on a 1% agarose gel prepared in 1X TBE buffer (Appendix I). The standard PCR reaction was used for all reactions with annealing temperature ranging from 50-60ºC and extension time ranging from 1-3 min/cycle according to the primers G+C% contents and the target fragment size, respectively.

2.2.12. Sequencing analysis

Sequence analysis of a targeted fragment was carried out using the following protocol. For 6 µl reaction about 1-2 µg of DNA was diluted in 5 µl of sterile bdH_2O and 1 µl of the appropriate primer (10 pmol/µl) was added. The samples were commercially sequenced by Genterprise GmbH, Mainz, Germany.

2.2.13. Direct cloning of CpGV-M as a bacmid

CpGV-M genomic DNA was purified using alkaline treatment of purified OBs using same method as described in 2.2.1. Two micrograms of CpGV-M DNA was linearized at the *Pac*I locus by overnight digestion with 10 U of *Pac*I endonuclease at 37°C. On the next day, the restriction enzyme was heat inactivated for 15 min at 65°C. One microgram of bacmid cloning vector pCC1-hr5-ie1-GFP was digested with 10 U of *Pac*I endonuclease in a total volume of 30 µl for 3 h at 37°C. The linearized vector was then dephosphorylated using 1 U of SAP as described in 2.2.4. The enzymes were heat inactivated for 15 min at 65°C prior to gel purification of the linearized plasmid DNA with GFX gel and solution purification kit (Amersham Biosciences). Ligation reaction was performed overnight at 16°C with approximately 500 ng of linearized CpGV-M DNA and 50 ng of linearized vector DNA in a total volume of 20 µl using 2 U of T4 DNA ligase (Invitrogen). Electrocompetent

TransforMax EPI300 *E. coli* (*EPICENTRE*) were transformed with 2 µl of the ligation mixture at 25 µF and 2.5 kV using a *Bio-Rad* Gene Pulser apparatus. The transformed cells were recovered in LB medium for 1 h at 37°C and spreaded on agar plates containing 12.5 µg/ml Chloramphenicol antibiotic. The colonies were screened for positive clones by restriction digestion of the isolated bacmid DNA from 10 ml inoculated LB overnight cultures.

2.2.14. Deletion of Cp15 and Cp16 ORFs using Red/ET-Recombination

In Red/ET-Recombination system (Quick and easy BAC recombination kit, Gene Bridge), target DNA molecules are precisely altered by homologous recombination in *E. coli* in the presence of pRedET expression plasmid (pSC101-BAD-gbaA-tet) (Appendix II), which expresses Redα and Redβ from λ phage as essential recombination proteins for homologous recombination process. pRedET is a derivative of a thermo-sensitive pSC101 replicon, which is a low copy number plasmid dependent on oriR101 (Miller et al., 1995). It carries the phage redγβα operon expressed under the control of the arabinose-inducible pBAD promoter and confers tetracycline resistance (Guzman L.M. et al., 1995). Redα is a 5`-3` exonuclease, and Redβ is a DNA annealing protein. A functional interaction between Redα and Redβ is required in order to catalyze the homologous recombination reaction. Recombination occurs through homologous sequences, which are 50-bp stretches of DNA shared by the two molecules to recombine (Fig. 6). Transformation of *E. coli* hosts with pRedET plasmid is selected for by acquisition of tetracycline resistance at 30ºC and the expression of the Red/ET recombination proteins is induced by L-arabinose activation of the BAD promoter at 37ºC. Using this strategy, a PCR product containing a Kan^R cassette flanked by sequences homologous to either Cp15 or Cp16 region at both ends was generated using two 80-mer oligonucleotides and used to delete and replace the target ORF (Cp15 and Cp16) in CpGV-M bacmid (CpBAC) (see results 3).

2.2.14.1. Generation of a Tn5-neo (Kan^R) PCR product

For deletion of Cp15 and Cp16 ORFs from CpBAC, two specific primers were designed for each target ORF with homologous arms of 50 bp at the 5' end of each oligo directly adjacent to either side of the target region to be deleted from CpBAC. The 3' end of these nucleotides contained the necessary sequence for amplification of the Tn5-neo (Kan^R) cassette of the provided template (Gene Bridges) (Fig. 6). To replace Cp15, the Kan^R cassette

was amplified using two long oligonucleotides; the forward primer PCp15NL-F contained the Cp15 gene flanking sequence from 10.353 to 10.402 nt and the reverse primer PCp15NL-R contained the Cp15 gene flanking sequence from 11.776 to 11.825 nt according to the CpGV-M complete genome sequence (Luque et al., 2001). To replace Cp16, the Kan^R cassette was amplified using two long oligonucleotides: the forward primer PCp16NL-F contained the Cp16 gene flanking sequence from 12.097 to 12.146 nt and the reverse primer PCp16NL-R contained the Cp16 gene flanking sequence from 12.738 to 12.787 nt (Luque et al., 2001). The PCR amplification of Kan^R cassette was performed using Taq DNA polymerase according to the manufacturer's protocol (Axon, Labtechnik). The PCR products were purified using the GFX gel and solution purification kit (Amersham Biosciences) prior to use for transformation into EPI300 *E. coli* cells.

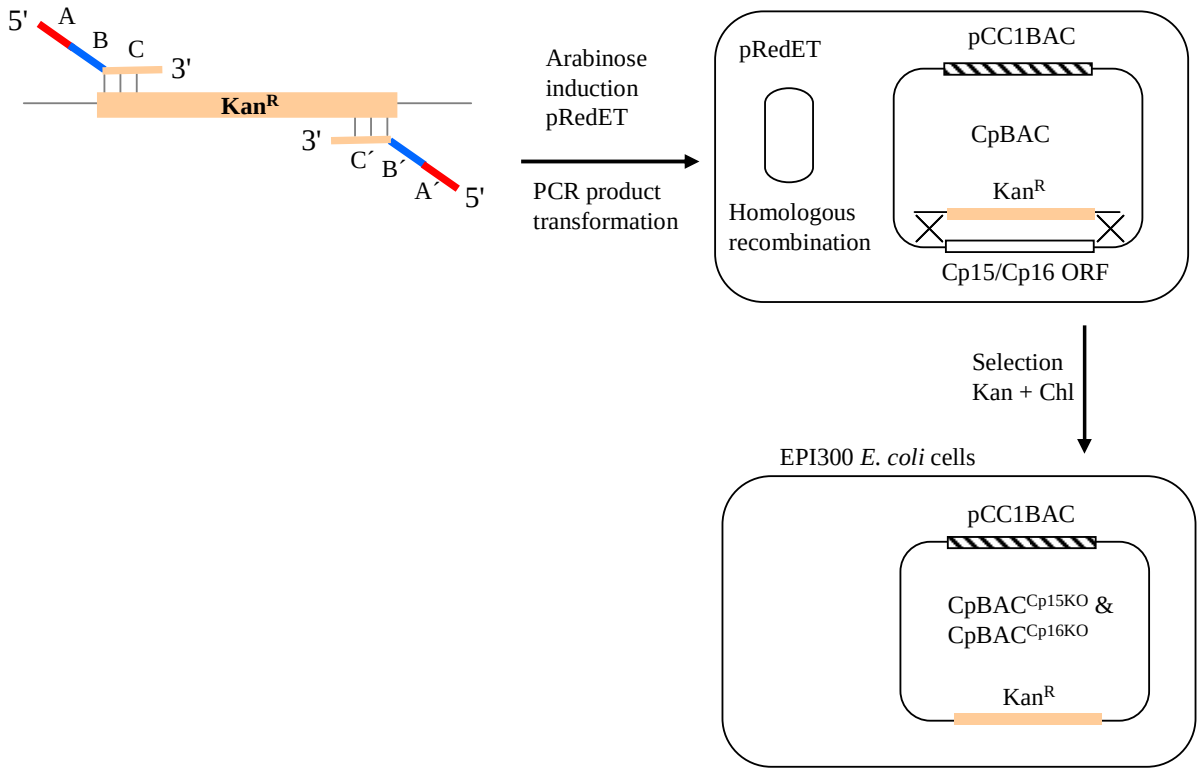

Fig. 6. Deletion of ORFs Cp15 and Cp16 from CpBAC by Red/ET-Recombination technology. The long arms primers (5'-ABC-3', 5'-A´B´C´-3') used for PCR amplification of Kan^R cassette typically consisted of in its 5'-end a homologous region of 50 bp flanking the region to be deleted (A, A´), a selectable restriction site sequence (B, B´) followed by an 24 bp region homologous to the Kan^R cassette (C, C´) in its 3'-end. The PCR product was transformed to EPI300 *E. coli* cells and the homologous recombination between either Cp15 or Cp16 ORFs in CpBAC and the Kan^R PCR fragment was carried out in the presence of the pRedET plasmid expressing the recombination proteins. The deletion of either Cp15 and Cp16 resulting in the generation of the mutant CpBAC^{Cp15KO} and CpBAC^{Cp16KO} that were selected in LB agar plates in the presence of Chloramphenicol and Kanamycin antibiotics.

2.2.14.2. Transformation of pRedET plasmid DNA into EPI300 *E. coli* cells

TransforMax EPI300 *E. coli* cells containing CpBAC were inoculated in 1.0 ml LB medium containing 12.5 µg Chloramphenicol antibiotic in 15-ml Falcon tube and incubated at 37ºC overnight with shaking. Next day, 1.4 ml LB medium with the same antibiotic was inoculated with 30 µl of the overnight culture in a 15-ml Falcon tube and cultured for 2-3 hours at 37ºC with vigorous shaking (290 rpm). The cells were harvested for 30 s at 11,000 rpm (11,228xg, Centrifuge 5417 R, Eppendorf) at 2ºC and washed three times with 1 ml chilled sterile bdH_2O. The cells were transformed with 1 µl pRedET plasmid DNA (20 ng/µl) and incubated at 30ºC for 70 min with shaking at 290 rpm according to the manufacturer's instruction (Gene Bridges). About 100 µl cultured cells were plated on LB agar plates containing Tetracycline (3 µg/ml) plus chloramphenicol (12.5 µg/ml). The plates were protected from light, because of Tetracycline light sensitivity, by wrapping them up and incubated at 30ºC overnight. Transformation of *E. coli* cells with this plasmid was selected for by acquisition of tetracycline resistance at 30°C.

2.2.14.3. Replacing of the target region with the Tn5-neo cassette

Colonies were picked from the plate obtained in 2.2.14.2 and inoculated in 1 ml LB medium containing Tetracycline (3 µg/ml) plus Chloramphenicol (12.5 µg/ml) and incubated overnight at 30ºC with shaking. The next day, two sterile 15 ml Falcon-tubes with 1.4 ml LB medium containing the same antibiotics were inoculated using 30 µl of the overnight culture. After vigorous shaking (290 rpm) for ~ 2 h at 30°C until, OD_{600} reached ~ 0.3, 50 µl of 10% L-arabinose was added to one tube to give a final concentration of 0.3% - 0.4% which will induce the expression of pRed/ET recombination proteins. The other tube was left without induction as a negative control. The cells were incubated at 37ºC with vigorous shaking (290 rpm) for 45 min to 1 h and subsequently made electrocompetent by three washes with ice-cold sterile bdH_2O. The prepared electrocompetent cells (~30 µl) were transformed with 5 µl of the purified PCR product (100 ng/µl) in 2-mm-diameter electroporation cuvettes (Eurogentec) at 2.5 kV using a Bio-Rad Gene Pulser. The cells were resuspended in 1 ml of LB medium and shacked for 70 min at 37°C and subsequently 100 µl culture was spreaded on agar plates containing 15 µg/ml Kanamycin and 12.5 µg/ml Chloramphenicol. The plates were incubated overnight at 37ºC and the induced colonies containing mutant bacmids were analyzed. The altered genotype of the recombinant bacmids was confirmed by *Bam*HI restriction digestion and PCR analysis.

2.3. RNA Molecular analysis

2.3.1. Total RNA extraction and RT-PCR analysis

For gene transcription analysis, reverse transcription PCR (RT-PCR) were carried out using isolated total RNA from infected CM larvae. Total RNA was extracted from 5 pooled fourth instar larval midguts using 50-100 mg of tissue using Trizol reagent according to manufacturer's protocol (Invitrogen). The collected midguts tissue was homogenized in 1 ml Trizol in a 2-ml Eppendorf tube and the insoluble material was removed from the homogenate by centrifugation at 12,000xg for 10 min at 4ºC in a benchtop centrifuge (5417 R, Eppendorf). The homogenized samples were incubated at room temperature for 5 min, and then 200 µl chloroform was added to each sample followed by vigorously shaking and subsequently centrifugation at 12,000xg for 15 min at room temperature. The aqueous phase was removed to fresh tube and 500 µl of isopropanol was added. The samples were incubated at room temperature for 10 min, then centrifuged at 12,000xg for 10 min at 4ºC. The supernatant was removed and the RNA pellet was washed once with 1 ml of 75% ethanol. Total RNA was dissolved in an appropriate amount of Diethylprocarbonate (DEPC)-treated bdH_2O and quantified by optical density measurement at 260 nm (OD_{260}). RT-PCR was performed using 1 µg total RNA as a template for each time-point. Extracted RNA was treated with DNase 3-5 U/µg of total RNA to digest any potential genomic DNA contamination. First-strand cDNA was synthesized from DNase treated RNA in 20 µl reaction volume containing; 1 µl Oligonucleotide $(dT)_{12-18}$ (500 µg/ml), 1 µg total RNA, 2 µl 10 mM dNTPs mixture solution and sterile bdH_2O to 20 µl. The mixture was heated to 65°C for 5 min and quickly chilled on ice. Then, the following contents were added: 4 µl 5X First-strand buffer, 2 µl 0.1 M DTT, 1 µl RNase OUT™ Recombinant Ribonuclease Inhibitor (40 units/µl) and 1 µl (200 units) of cloned SuperScript™ II was added to the mixture. The contents were mixed gently and then incubated for 50 min at 45°C. Finally, the reaction was inactivated by heating to 80°C for 5 min. The synthesized first-strand cDNA was amplified by PCR using specific sets of primers Cp15-rt_F/Cp15-rt_R, Cp16-rt_F/Cp16-rt_R and F-Protein_F/F-Protein_R designed for Cp15, Cp16 and F protein ORFs, respectively (Table 3).

2.3.2. RNA (glyoxal) electrophoresis

Total RNA electrophoresis was performed using Glyoxal (40%) (Sambrook et al., 1989). Electrophoresis equipment was thoroughly cleaned with detergent, rinsed with water,

incubated in 3% H_2O_2 for 10 minutes and rinsed again with bdH_2O and then 1.5% agarose gel was prepared in 10 mM sodium phosphate buffer (Appendix I).

For preparation of the RNA samples, 5.4 µl of 8 M glyoxal was mixed with 10 µl DMSO, 3.0 µl 0.1 M sodium phosphate and 5.4 µl total RNA (up to 10 µg). Samples were incubated at 50°C for 60 min and chilled on ice for 2-3 min. About 4 µl of glyoxal loading dye (Appendix I) was added to the cooled RNA samples and mixed well. Samples were loaded on the agarose gel and run at 80 V and 40 mA until the bromophenol blue dye migrated 2/3 through the gel. Running buffer was circulated during the run from time to time. The RNA fragments were visualized by illuminating with UV light (312 nm).

2.3.3. Quantitative Real Time RT-PCR (qRT-PCR)

The fluorescence-based quantitative real-time reverse transcription PCR (qRT-PCR) was used for the quantification of Cp15, Cp16 and F protein mRNA using the synthesized cDNAs. The reaction and fluorescence detection was performed using the DNA Engine Opticon™ System (MJ Research, Biozym Diagnostik GmbH) using QuantiTect SYBR green (Qiagen). SYBR Green I dye is a highly specific double-stranded DNA binding dye to detect PCR products as they accumulate during the PCR cycles. To quantify Cp15, Cp16 and F protein cDNA levels for each time point, three sets of primers were designed to amplify ~150 bp region within each ORF, using primer pairs Cp15qRT_F/Cp15qRT_R for Cp15, Cp16qRT_F/Cp16qRT_R for Cp16 and F-Protein_F/F-Protein_R for F protein ORF, respectively (Table 3). The reaction was performed with a total volume of 40 µl in 0.2 ml Thin-Wall tubes (Biozyems) using the following conditions: denaturation at 95ºC for 15 min for the initiation of HotStarTaq DNA polymerase, followed by 50 cycles of 95ºC for 30 s, 55ºC for 30 s and 72ºC for 30 s. At the end of the reaction, a melting curve was produced by continuously monitoring fluorescence while slowly heating the samples from 50 to 95ºC at intervals of 0.5ºC. The melting curve analysis was performed for specificity control of the PCR. Specific reactions should result in a single melting peak corresponding to the PCR product being amplified. Serial dilutions of CpGV-M DNA ranging from 50 to 0.0005 ng/reaction were applied to generate standard quantification curves for all reactions, which were used to calculate the cDNA concentration by Opticon Monitor™ software.

2.4. Protein expression analysis

2.4.1. Induction of Cp15 and Cp16 His-Tagged fusion proteins

The target CpGV-M Cp15 and Cp16 ORFs were cloned behind the T7 promoter in pET-28b(+) expression vector (Novagen), which carry an N-terminal His-Tag fusion protein and can be induced for target protein expression in the presence of 1 mM IPTG (Isopropyl β-D-1-thiogalactopyranoside). Cp15 and Cp16 ORFs were PCR amplified from CpGV-M genomic DNA using two sets of primers designed Cp15-ORF_F/Cp15-ORF_R and Cp16-ORF_F/Cp16-ORF_R, respectively (Table 3). The PCR products of ORFs Cp15 and Cp16 were purified with GFX gel and solution purification kit to remove primer dimers and any impurity from the amplification reaction, then digested with *Hin*dIII and *Xho*I endonucleases and subsequently cloned in *Hin*dIII/*Xho*I cloning sites of pET28b(+) expression vector. The BL21 (DE3) codon plus *E. coli* (Novagen) was used as an expression host for Cp15 and Cp16 bacterial protein expression. After screening of the recombinant clones containing pET28-Cp15 or pET28-Cp16 plasmids, a single colony of each plasmid was inoculated in 2 ml 2X YT medium supplemented with 30 µg/ml Kanamycin in 15-ml Falcon tube and incubated with shaking overnight at 37°C. On the next day, the overnight culture was diluted 1:100 with fresh medium supplemented with 30 µg/ml Kanamycin and then incubated with shaking at 250 rpm at 37°C until OD_{600} reached 0.6 - 0.9. Then, IPTG was added to a final concentration of 1 mM and the culture was continued for shaking in a time course experiment for 0, 1, 2, 3 hours. At each time point, 1 ml culture was taken, centrifuged for 30 s at 13,000 rpm (18,000xg) in a bench-top centrifuge (5417 C, Eppendorf) and the pellets were applied for 12% SDS-PAGE gel analysis in order to determine the maximal over protein expression time point.

2.4.2. SDS-PAGE

Total protein extracts were separated according to its molecular mass using Sodium Dodecyl Sulfate Polyacrylamide Gel Electrophoresis (SDS-PAGE). For the experiments, the Bio-Rad mini-protein II dual slab gel was used with 10 ml of 15% separating gel containing 5 ml of 30%/ 0.8% (v/v) acrylamid/bisacrylamid (Carl Roth GmbH, Germany), 2.3 ml bdH_2O, 2.5 ml of 1.5 M Tris-HCL (pH 8.8), 0.1 ml of 10% SDS, 0.1 ml of 10% ammonium persulfate (APS) and 0.004 ml of TEMED (N,N,tetramethylethylenediamine). The mixture was poured slowly between two glass plates and overlaid with 1-2 ml of bdH_2O saturated Butanol. After

complete polymerization of the gel (15-20 min), the overlay was removed and the surface was rinsed with 1X SDS-PAGE running buffer (Appendix I, A.4.1). About 2 ml of 5% stacking gel containing 0.33 ml of 30%/ 0.8% acrylamid/bisacrylamid, 1.4 ml bdH_2O, 0.25 ml of 1 M Tris-HCL (pH6.8), 0.02 ml of 10% SDS, 0.02 ml of 10% APS and 0.002 ml of TEMED was poured onto the separating gel and then the combs were placed. Electrophoresis was carried out in 1X SDS-PAGE running buffer. For preparation of the protein samples, four volume of protein lysis buffer (Appendix I, A.4.2) and 0.1 volume of ß-mercaptoethanol were added to each sample and boiled for 10 min. About 0.25 volume of 4X SDS protein sample buffer (Appendix I, A.4.3) was added and the samples were re-boiled for further 5 min. The samples were loaded and the gel was run at 75 V until the dye reached the separating gel and then the gel was run at 150 V for 90 min. After running, the gels were stained in coomassie brilliant blue protein stain solution (Appendix I, A.4.4) with gentle shaking for 30-45 min and then destained overnight in protein destaining solution (Appendix I, A.4.5).

2.4.3. Generating of anti-Cp15 and anti-Cp16 polyclonal antibodies

Gel purified Cp15 and Cp16 bacterial expressed proteins were used for production of polyclonal antibodies (pABs). For preparation of protein antiserum, total bacterial expressed proteins were subjected to electrophoresis on 12% SDS-PAGE as described in 2.4.2 followed by gel light staining for 10 min in 0.05 % coomassie brilliant blue stain solution to locate the position of the protein bands. After destaining, ~53 kDa (Cp15) and ~23 kDa (Cp16) protein bands were excised from the gel and rinsed in appropriate amount of bdH_2O three times for 10 min followed by an overnight wash. The prepared gel pieces containing proteins were sent for anti-rabbit pAB production to Davids Biotechnology, Germany.

The produced anti-Cp15 and anti-Cp16 pABs were used for the production of mono-specific pABs specific for Cp15 and Cp16 proteins. The Cp15 and Cp16 bacterial expressed proteins were subjected to SDS-PAGE electrophoresis, transferred to PVDF membrane and the exact band for each protein was excised from the membrane. The prepared membrane pieces containing protein bands were kept in blocking buffer (Appendix I, A.4.10) for 1 h followed by washing in PBS-T (Appendix I, A.4.9) three times for 5 min. The membrane pieces were incubated with the produced anti-rabbit pAB for 1 h in 2-ml Eppendorf tube followed by washing for 10 min with 1X PBS + 0.5%Tween-20 and for 10 min with 1X PBS (Appendix I). The mono-specific pAB was eluted from the membrane using 1 ml of Glycin-HCl buffer, pH 2.0 (Appendix II, A.4.7) for 2 min then the pH was adjusted to 7.0 using 1 N

NaOH. The prepared mono-specific pABs were used as a specific antibody to detect Cp15 and Cp16 temporal protein expression in infected CM larvae using Western blot analysis.

2.4.4. Infection of CM in a time course for protein expression

CM larvae (L4) were infected by feeding them a small piece of medium (approximately 3 mm^3) inoculated with 1000 OB of either CpGV-M or MCp5. Only the larvae that had completely ingested the medium within 24 hours were placed on fresh virus free medium and reared individually at 26°C. At each time point 24, 48, 72 and 96 and 120 hpi, larval fat bodies were isolated by dissecting the CM larvae without damaging the midguts or the fat bodies and then the fat bodies were removed carefully from the insect body, rinsed in 1X PBS solution and pooled as five larval fat bodies for each time point. Isolated fat bodies were cooled immediately in liquid nitrogen and stored at -80ºC until use for total protein extraction. The isolated fat bodies were subjected to total protein extraction and SDS-PAGE electrophoresis as described above in 2.4.2. After elechtrophoresis, the electrophoresed proteins were transferred to PVDF membrane as described in 2.4.5 and analyzed by Western blot using anti-Cp15 and anti-Cp16 monospecific pABs.

2.4.5. Western blot

Western blot was performed as described by Sambrook et al. (1989). For protein blotting, the PVDF membrane was rewetted in methanol for 1 min before soaking in blotting transfer buffer (Appendix I, A.4.6) with two filter papers (Blot paper, Protein XL size Cat. Nr: 1703969, *Bio-Rad*) for 15 min before applying to blotting. The electrophoresed protein gels were also soaked in blotting transfer buffer for 5 min before applying to protein transfer. The protein transfer to PVDF membrane was performed using the TRANS-BLOT® SD (Semi-dry transfer cell) and the transfer cassette was assembled according to the manufacturer's instruction (*Bio-Rad*). The electro blotting was run for 30 min at 20 V. Following the transfer, the membrane was blocked by shaking in blocking buffer (Appendix I, A.4.10) for 60 min at room temperature. The membrane was incubated with the primary rabbit-derived mono-specific pAB 1:1000 diluted in blocking buffer at room temperature for 90 min with gently agitation. After washing 3 times with PBS-T each for 10 min, the membrane was incubated with secondary antibody goat anti-rabbit IgG conjugated with Horse-Radish Peroxidase (diluted 1:10,000) for 60 min at room temperature to detect the reactive bands. The peroxidase activity was developed by adding a substrate mixture of equal amounts of

Enhanced Luminol Reagent and Oxidizing Reagent (Western Lighting, PerkinElmer) to the membrane and allowed to react for 1 min. Membrane was laid between two transparency films, the X-ray film exposure was done for 1-30 min and protein signals were developed using Developing and Fixing solutions according to manufacturer's instruction (Sigma-Aldrich Chemise GmbH).

IV. RESULTS

1. Transcription and translation analysis of ORFs Cp15, Cp16 and F protein

1.1. Preparation of MCp5 and CpGV-M virus stocks

In order to produce genetically homogenous virus stocks of CpGV-M and its mutant MCp5 carrying the TCl4.7 transposon, fourth instar CM larvae were infected with about 1000 OBs for the propagation of each virus genotype. After larval death, 7-10 days post infection (dpi) viral OBs were isolated, purified and applied for DNA extraction. Then, *Bam*HI restriction endonuclease digestions (REN) were carried out using 1.5 µg of viral DNA to confirm the viruses' genotype homogeneity. *Bam*HI digestion of CpGV-M and MCp5 DNA resulted in a 6.8 kb fragment specific for CpGV-M and an 11.6 kb fragment specific for MCp5. The latter corresponded to the insertion of the 4.7 kb transposon between two *Bam*HI loci at nucleotide positions (nt) 5739 and 12586 (Fig. 7) (Jehle et al., 1995). No submolar bands in the REN profile were observed suggesting that both virus preparations were homogeneous.

In addition, PCR analysis was performed in order to confirm the genotype homogeneity of the virus stocks. Two different primer pairs were designed, which selectively amplified MCp5 and CpGV-M specific fragments. The diagnostic PCR for CpGV-M was achieved using CpGV-M specific primers PR-CpGV-LB and PR-CpGV-RB adjacent to the TA transposon insertion site (Fig. 8A). PCR resulted in a ~ 500 bp fragment as expected from the CpGV sequences. No ~ 500 bp fragment was observed with MCp5 DNA confirming the purity of MCp5 and lack of contamination with CpGV-M (Fig. 8B). Theoretically, PCR using PR-CpGV-LB and PR-CpGV-RB primers should results a 5.237 bp fragment for MCp5 DNA. This was not observed due to the short extension time of 30 second applied in the PCR.

For the specific amplification of MCp5 sequence, PR-CpGV-LB and the transposon specific primer PR-TCl4.7-int were used (Fig. 8A). As expected the PCR resulted in an 850 bp fragment for MCp5 DNA and no amplification product for CpGV-M DNA (Fig. 8B). This indicated the purity of the CpGV-M virus preparation from MCp5 contaminant. Hence, restriction analyses and the PCR analysis revealed that the purified MCp5 and CpGV-M virus stocks were free of cross contamination and could be used for the downstream work.

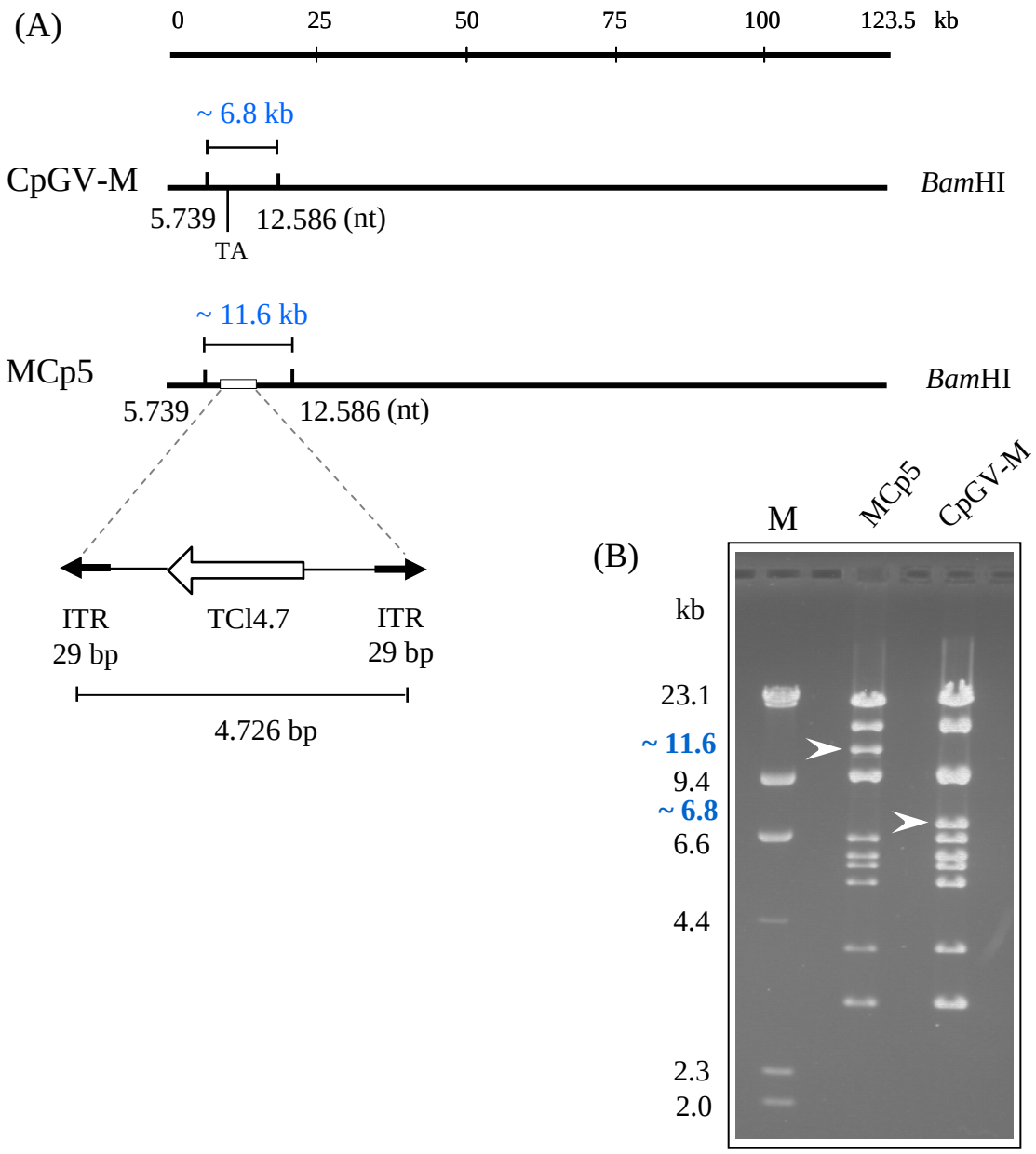

Fig. 7. (A) Schematic drawing of the genomes of CpGV-M and MCp5 indicating the *Bam*HI sites flanking the TCl4.7 insertion site. The TA transposon insertion site is flanking by two *Bam*HI sites at nucleotide position of 5739 and 12586 (according to Luque et al., 2001) resulting in a 6.8 kb specific fragment for CpGV-M and a 11.6 kb specific fragment for MCp5 which carrying TCl4.7 (4.7 kb) transposon. **(B)** Gel electrophoresis of CpGV-M and MCp5 genotypes *Bam*HI restriction profiles show the specific fragments of 6.8 kb and 11.6 kb for each virus genotype, respectively. Fragment sizes (kb) are given to the left. M indicates λ *Hin*dIII size marker.

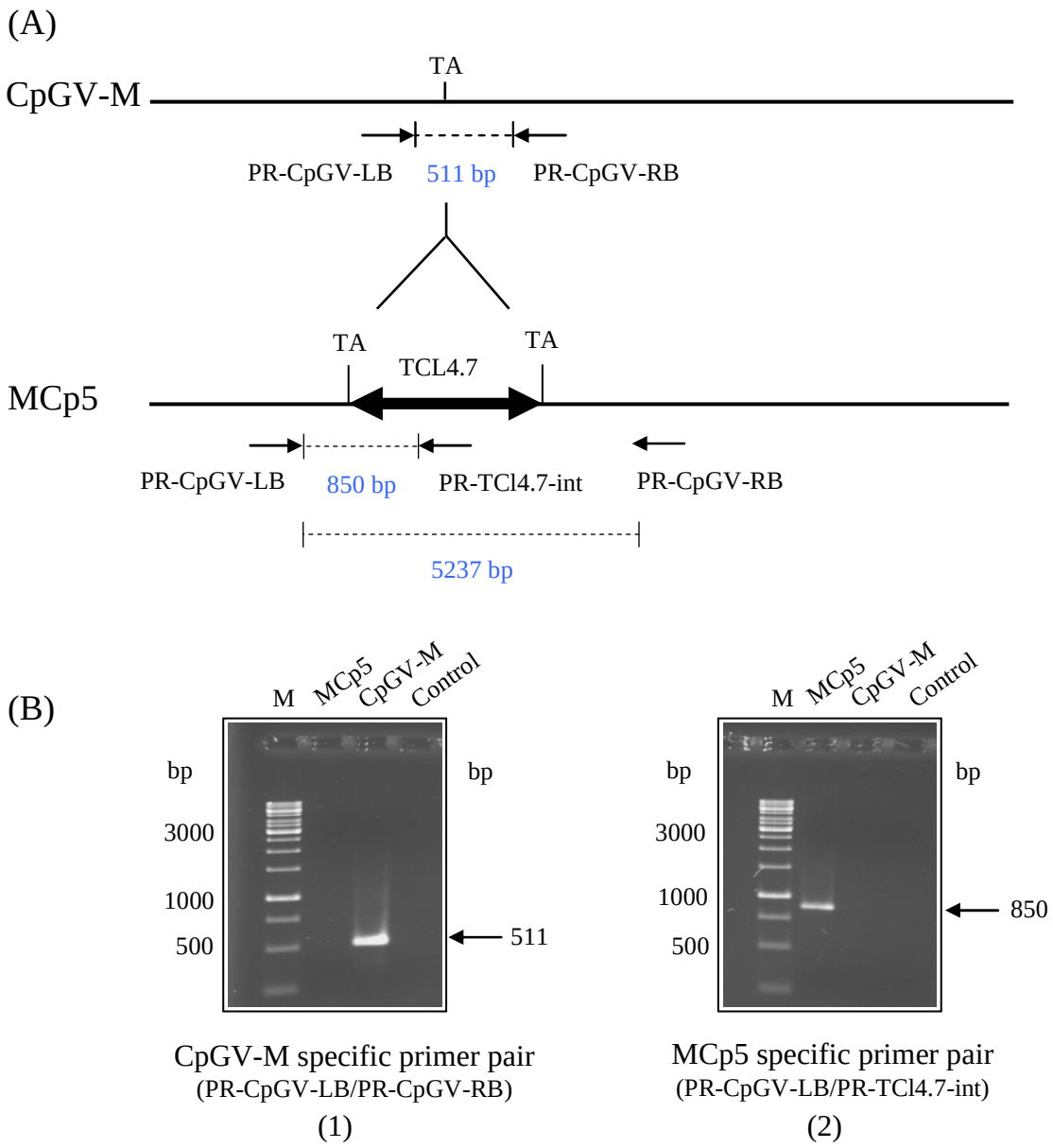

Fig. 8. PCR analysis for homogeneity of the MCp5 and CpGV-M virus stocks**. (A)** Schematic drawing shows the binding sites of primer pairs used for amplification of MCp5 and CpGV-M specific fragments (not to scale). The TA target site of TCl4.7 transposon is shown in CpGV-M genome and its duplication in MCp5 genome upon insertion of the TCl4.7 transposon. **(B)** Gel electrophoresis of PCR products using; (1) CpGV-M specific primers, (2) MCp5 specific primers. Control = negative control. M = 1-kb DNA standard marker. The fragments sizes (bp) are given to the left and to the right.

1.2. Temporal transcriptional analysis of Cp15, Cp16 and F protein

To examine the potential influence of TCl4.7 transposon insertion on the transcription regulation of the neighbouring Cp15 and Cp16 genes, RT-PCR and quantitative real-time RT-PCR (qRT-PCR) analyses were performed on CpGV-M and MCp5 infected CM larvae. RT-PCR and quantitative real-time RT-PCR were carried out using cDNA synthesized from total

RNA extracted from pooled larval midguts of five CM fourth instars infected either with CpGV-M or MCp5. Moreover, the temporal transcriptional regulation of the envelope fusion protein F protein gene (Cp31) was also analyzed as a control.

1.2.1. RT-PCR

The RT-PCR analysis was applied using different time points at 0, 6, 12, 24, 48, 72 and 96 hours post infection (hpi) using two primer pairs designed Cp15-rt_F/Cp15-rt_R for detection of Cp15 gene and Cp16-rt_F/Cp16-rt_R for detection of Cp16 gene. Using Cp15 specific primers a single band was detected with the predicted size of 419 bp in both CpGV-M and MCp5 infected larvae (Fig. 9). The Cp15 transcripts was first detected in CpGV-M infected larvae at 12 hpi and remained detectable until 96 hpi. Using cDNA synthesized from MCp5 infected larvae the Cp15 transcription was first detected at 6 hpi and remained detectable until 96 hpi with a low intensity of PCR product compared to CpGV-M transcripts (Fig. 9). The detection of Cp15 transcripts at early stage of CpGV-M virus infection (12 hpi) until late stage (96 hpi) suggest that Cp15 is probably transcribed from both early and late promoter motifs located within 120 bp upstream from the first ATG start codon throughout the viral infection cycle (Luque et al., 2001).

Using Cp16 specific primers, a RT-PCR fragment of the predicted size of 461 bp was detected in CpGV-M infected larvae at 12 hpi and remained detectable until 96 hpi. In MCp5 infected larvae, the same band was detected at 6 hpi until 48 hpi with a significant decreasing of PCR product intensity (Fig. 9). The detection of Cp16 transcripts at early stage of CpGV-M virus infection (12 hpi) suggest that it is possibly an early gene since a consensus TATA box and a consensus early gene motif CAGT located within 120 bp upstream from the first ATG start codon (Luque et al., 2001). However, an accumulation of Cp16 transcription was observed at late stage of infection (96 hpi), which means the presence of Cp16 transcripts until late stage of virus infection.

The RT-PCR detected a strong band at 6 hpi in MCp5 infected CM larvae in both Cp15 and Cp16 transcription profile. Since this band was not observed in CpGV-M infected CM larvae at the same time point this observation may attributed to a possible presence of virus genomic DNA residues, although all samples were treated with DNAase before syntheses of cDNAs. The temporal RT-PCR analysis clearly showed that the mRNA transcription of Cp15 and Cp16 genes in MCp5 infected larvae was significantly lower than

that of the wt CpGV-M. These observations suggest that the transcription of both Cp15 and Cp16 in MCp5 was delayed or reduced.

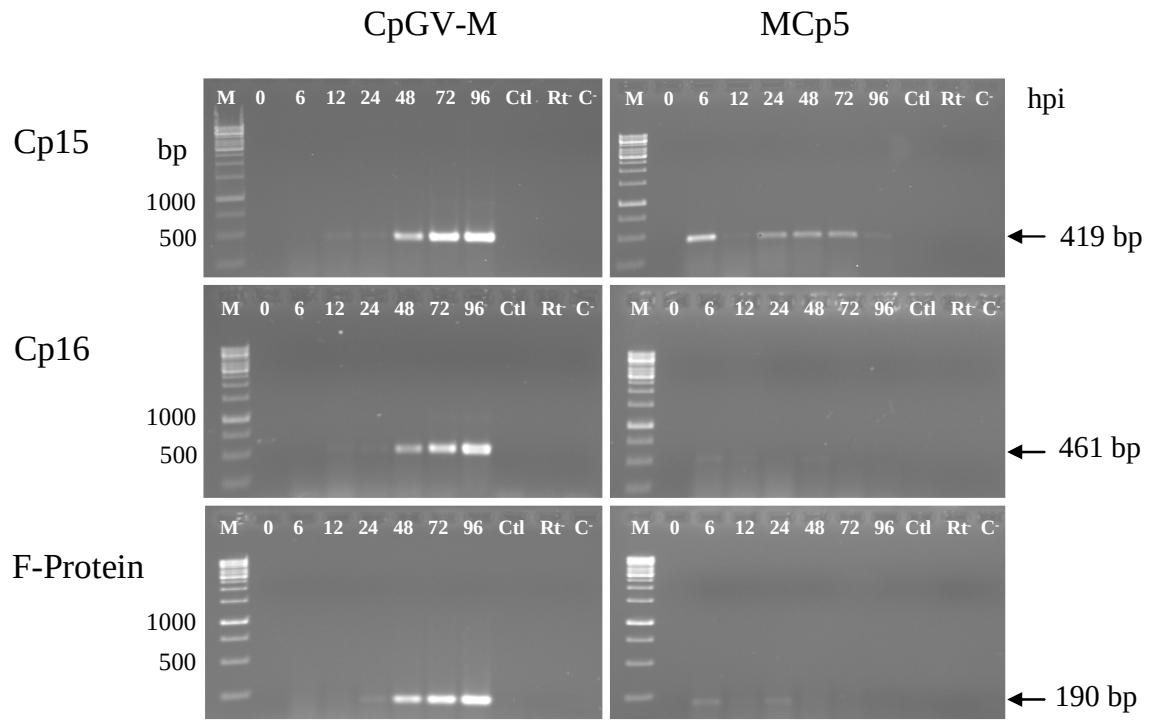

Fig. 9. Analysis of Cp15, Cp16 and Cp31 (F protein) ORFs transcription using RT-PCR. The RT-PCR analysis was performed on infected CM larvae at 0, 6, 12, 24, 48, 72 and 96 hour post infection (hpi) as shown on the top of the gels, by using Cp15, Cp16 and F protein specific primer pairs. The arrows show the detected RT-PCR product of each ORF synthesized cDNA with its predicted size. Lanes: (Ctl) show the result of the RT-PCR using cDNA synthesized from uninfected larvae. The results of the PCR when the reverse transcriptase is omitted are shown in lanes (Rt^-). Lanes (C^-) show the PCR negative control reaction. M= DNA standard marker.

In order to determine whether there is a general delay or reduction in genes transcription of MCp5, the temporal transcription of the envelope fusion protein (F protein; Cp31) was analyzed by RT-PCR using specific oligonucleotides F-Protein_F and F-Protein_R and CpGV-M and MCp5 infected CM larvae at the same time points as for Cp15 and Cp16 analyses (Fig. 9). The F protein is the major envelope fusion protein of group II NPVs and GVs. Using F protein specific primers, a band of 190 bp corresponding to the predicted F protein PCR product was detected as early as 24 hpi in CpGV-M infected larvae and remained detectable with accumulation until 96 hpi. At 6 hpi, a faint band of 190 bp was detected in MCp5 samples and remained detectable until 24 hpi (Fig. 9). Though no putative early or late promoter motives were detected 120 nt upstream from the first ATG start codon of F protein (Luque et al., 2001), conventional RT-PCR revealed that F protein may

transcribe at early and late stages of virus infection, since its transcripts were detected at 24 hpi and sustained until 96 hpi in case of the wt CpGV-M. The RT-PCR transcription analysis suggested a significantly low mRNA transcription level of Cp15, Cp16 and F protein genes in CM larvae infected with MCp5 mutant virus carrying TCl4.7 transposon compared to the wt CpGV-M in all investigated time points.

1.2.2. Quantitative Real-Time RT-PCR (qRT-PCR)

To substantiate the results obtained by the RT-PCR, quantitative real-time RT-PCR (qRT-PCR) was performed using cDNAs generated from the same RNA extracts that used for RT-PCR analysis; the qRT-PCR was applied in order to quantify the cDNA of Cp15, Cp16 and F protein from CM larvae infected with MCp5 and CpGV-M at the designated time points. For every qRT-PCR, a control measurement was performed in order to demonstrate that the detected amplified PCR fragments originated from synthesized cDNA and not from contaminating DNA. As a negative control, a sample in which a first strand synthesis reaction was carried out with the same RNA isolated from CpGV-M infected larvae at 96 hpi but no reverse transcriptase was added to these samples. In these control reactions, the quantified Cp15, Cp16 or F protein ORFs template molecules were at least 5000 times lower than that in the CpGV-M cDNA containing samples (data not shown).

This showed that the amount of DNA in the samples was negligible compared to the amount of cDNA template molecules and confirmed that the reaction was sensitive to cDNA but not to viral DNA in the samples. With this approach it was possible to determine the potential differences in the transcription levels among the infected larvae using CpGV-M and MCp5 mutant virus carrying the TCl4.7 transposon. The strategy used to quantify the level of mRNA transcription involved designing one primer pair specific for each ORF that would amplify about 150 bp genomic fragment. The primers were designed Cp15qRT_F/Cp15qRT_R, Cp16qRT_F/Cp16qRT_R and F-Protein_F/F-Protein_R for amplification of Cp15, Cp16 and F protein genes, respectively. The relative amount of synthesized cDNA was calculated from a standard calibration curve obtained by using log dilutions of duplicate samples of CpGV-M DNA serially diluted from 50 to 0.0005 ng/reaction allowing an accurate estimation of viral cDNA presents in each time point (Fig. 10A). To confirm the specificity of the PCR products, a melting curve analysis was performed which showed that all PCR products were denatured to single stranded DNA at about 79°C indicating specific amplification of a homogenous DNA sequence (Fig. 10B). The quantified

cDNAs of Cp15, Cp16 and F protein are presented by the bar graph in Fig. 10C, D and F, respectively. A steady increase in the transcription levels of Cp15, Cp16 and F protein was detected in CpGV-M infected larvae resulted in about 4.5-, 6.25- and 7.86-fold increase at 48 hpi up to 10.2 x 10^3, 12.1 x 10^3 and 24.7 x 10^3-fold increase at 96 hpi, respectively. In contrast, quantification of gene transcripts of MCp5 revealed 2.8, 0.62, and 4.30-fold increases at 48 hpi up to 2.0, 1.07 and 3.26-fold increase at 96 hpi for Cp15, Cp16 and F protein, respectively. The qRT-PCR analyses showed dramatically reduction in gene transcription of Cp15 and Cp16 genes as well as F protein in larvae infected with MCp5 compared to the wt CpGV-M suggest a general delay or reduction in gene transcription in MCp5. Similar to the RT-PCR observations, the qRT-PCR analyses resulted in less cDNA amounts detected for Cp15, Cp16 and F protein in CM larvae infected with MCp5 compared to the CpGV-M. These observations suggest a general delay or reduction of MCp5 gene transcription compared to wt CpGV-M in all investigated time points, at least during midgut infection.

Fig. 10. (**Next page**) Quantitative Real-Time RT-PCR analysis of CpGV-M and MCp5 Cp15, Cp16 and Cp31 (F protein) cDNAs of infected CM larvae. Total RNA was isolated from ~5 pooled larval midguts of infected CM larvae for each time point; the cDNAs were synthesized and then quantified using qRT-PCR. **(A)** A standard calibration curve generated from duplicate samples of purified CpGV-M DNA serially diluted from 50 to 0.0005 ng/reaction. The cycle threshold C(T) corresponds to the number of cycles needed to reach a fluorescence level above the background level and has been shown to be inversely proportional to the initial amount of target DNA (correlation coefficient = 0.994). **(B)** Melting curve of amplified PCR products. The curve was generated by subjecting PCR products to a step-wise increase in temperature and monitoring fluorescence levels. The single peak at ~ 79ºC indicates a single PCR product was produced. The bar graphs show the quantitative analyses of CpGV-M and MCp5 viral mRNA transcripts of **(C)** Cp15, **(D)** Cp16 and **(F)** Cp31 (F protein) in infected fourth instar CM larvae. The bars heights indicate the average and the error bars represent the standard deviation between two replicates for each time point.

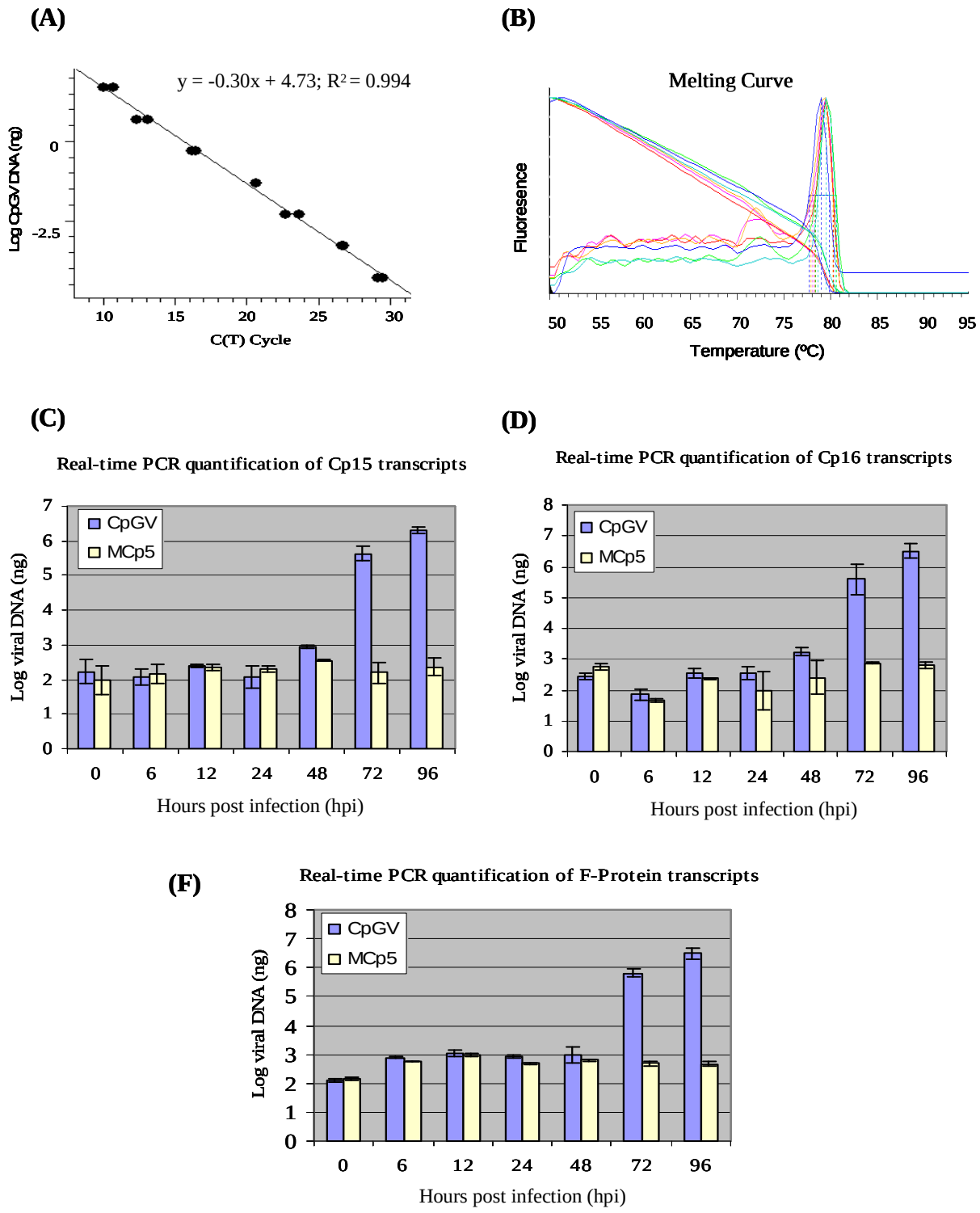

Fig. 10. Legand see page before.

1.3. Western blot analysis of Cp15 and Cp16 temporal protein expression

1.3.1. Generation of anti-Cp15 and anti-Cp16 polyclonal antibodies

In an attempt to examine the expression pattern of Cp15 and Cp16 proteins in CpGV-M and MCp5 infected CM larvae, anti-Cp15 and anti-Cp16 polyclonal antibodies (pABs) were produced by rabbit immunization against His-tagged Cp15 and His-tagged Cp16 fusion proteins expressed in *E. coli* using pET-expresssion system (Novagen). The target ORFs of Cp15 and Cp16 were cloned in the pET-28b (+) vector under control of strong bacteriophage T7 transcription and translation signals fused with N-terminal His-Tag protein.

For the generation of PCR fragments containing the Cp15 and Cp16 ORFs, a PCR reaction using specific sets of primers for each ORF (Cp15-ORF_F/Cp15-ORF_R for Cp15 and Cp16-ORF_F/Cp16-ORF_R for Cp16) was performed. The primers were designed to contain restriction sites compatible with the pET-28b (+) vector (*Hin*dIII and *Xho*I) (Fig. 11). The amplification of the target ORFs was carried out using CpGV-M genomic DNA as a template. After generation of the PCR products, Cp15 and Cp16 DNA fragments were electrophoresed in 1% TBE agarose gel and analysed for the specific PCR amplification (data not shown).

The results showed that the PCR was successful and gave specific products. The PCR products were purified and then digested with *Hin*dIII and *Xho*I. The resulted fragments were ligated into pET-28b (+) expression vector which was digested with the same enzymes. The ligated plasmids were transformed to *E. coli* (DH5α) competent cells and plated on a LB agar plates in the presence of Kanamycin. Putative positive colonies were analyzed by plasmid DNA minipreparation followed by DNA restriction digestion analysis. After verification of the identity of the correct clones, the plasmids were transformed to the expression host BL21 (DE3) codon plus *E. coli* (Novagen) for protein expression. Expression of Cp15 and Cp16 proteins were induced in a time course experiment using 1 mM IPTG for 1 h, 2 h and 3 h to determine the suitable induction time in which the target proteins were expressed in a high yield and not degraded. As shown in Fig. 11, incubation until 3 h post induction was the best time point for protein expression for both Cp15 and Cp16. The predicted molecular mass of Cp15 and Cp16 proteins fused with His-Tag was examined in total protein extracts of bacterial cultures after induction of proteins expression for 1, 2 and 3 hours by Western blot analysis (Fig. 12).

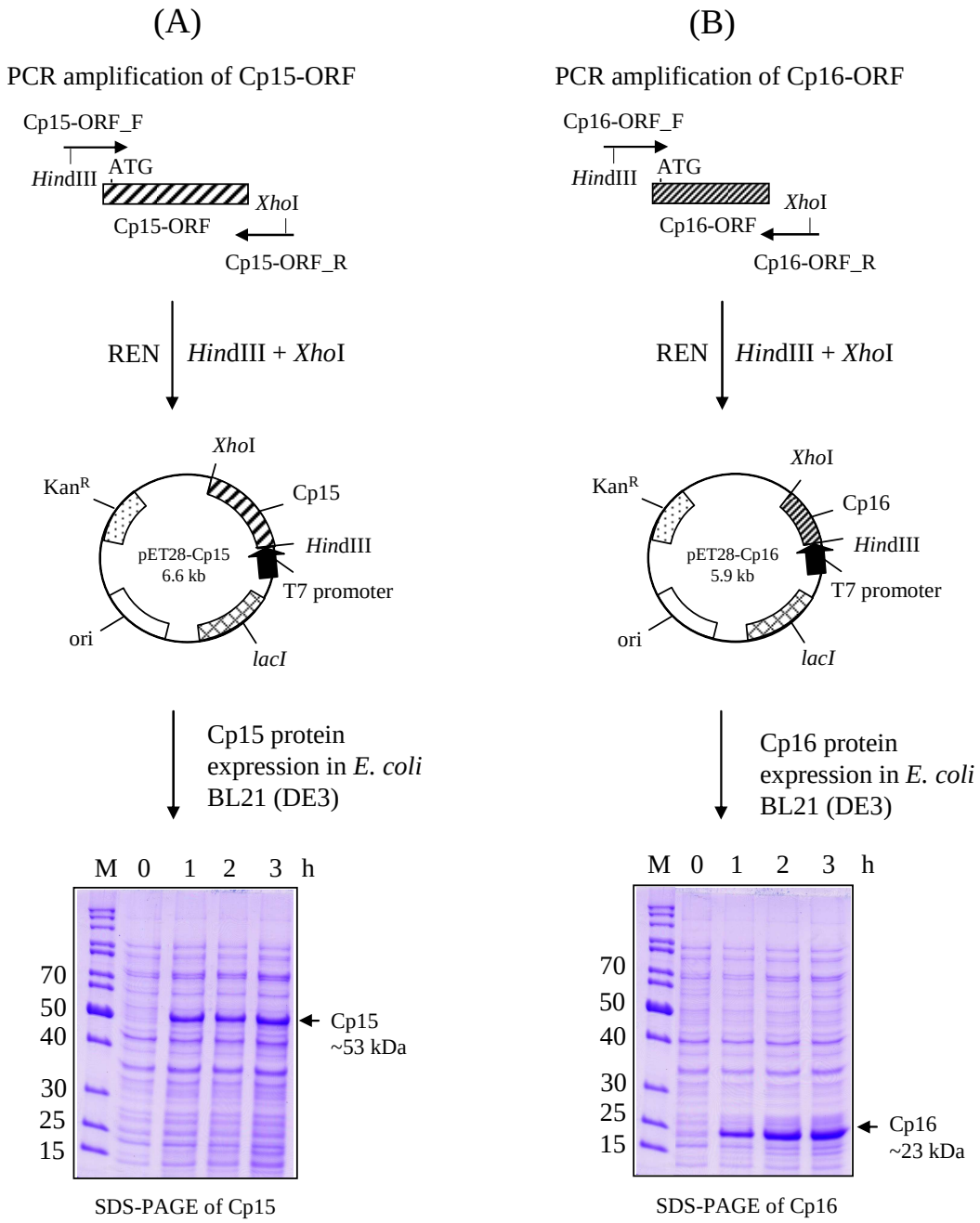

Fig. 11. Cloning and protein expression of ORFs Cp15 **(A)** and Cp16 **(B)**. The target Cp15 and Cp16 ORFs were PCR amplified from CpGV-M genome using specific set of primers designed Cp15-ORF_F/Cp15-ORF_R and Cp16-ORF_F/Cp16-ORF_R for Cp15 and Cp16 ORFs, respectively. The primers were designed to introduce *Hin*dIII and *Xho*I restriction sites to the PCR product compatible to ligate in pET-28b(+) vector. The drawing shows the cloning of Cp15 and Cp16 as *Hin*dIII/*Xho*I fragments into pET-28b(+). The cloning resulted in the recombinant plasmids pET-Cp15 and pET-Cp16 which were subsequently used for Cp15 and Cp16 bacterial protein expression in a time course for 1, 2 and 3 hours in the presence of 1mM IPTG as expression inducer. The gel band specific for each protein at 3 h was excised from the gel and used for commercial polyclonal antibody production. The numbers on the right show the predicted molecular mass of Cp15 (~53 kDa) and Cp16 (~23 kDa). Lane 0 shows the protein lysate before adding of 1mM IPTG. Lanes 1, 2 and 3 show the protein lysate obtained 1, 2 and 3 hours after adding of 1mM IPTG, respectively. M= Protein standard marker.

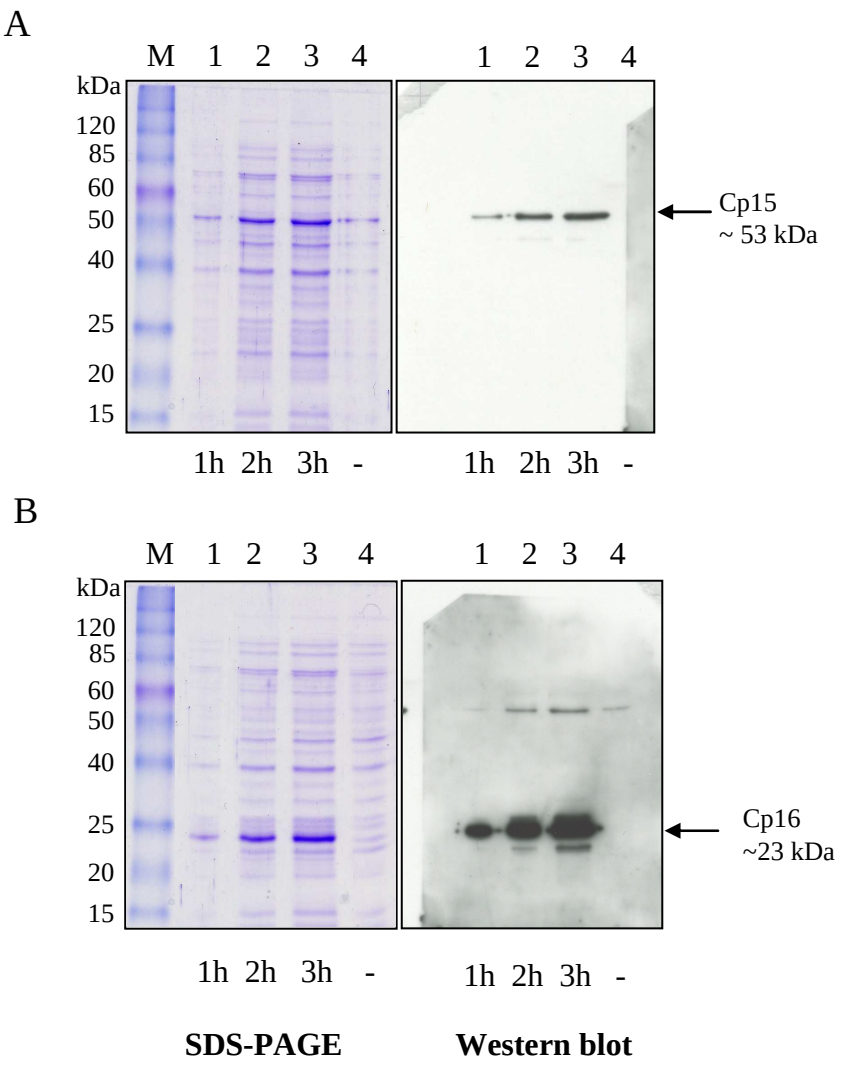

Fig. 12. Bacterial expression and Western blot detection of His-tagged Cp15 (**A**) and His-tagged Cp16 (**B**) fusion proteins using His-Tag Monoclonal antibody. The recombinant plasmids pET-28-Cp15 and pET-28-Cp16 were induced with 1 mM IPTG for His-tagged Cp15 and His-tagged Cp16 fused protein expression for 1 h (lane 1), 2 h (lane 2) and 3 h (lane 3). Lane 4 shows the non-induced bacterial culture for both Cp15 and Cp16. Arrows indicate the predicted molecular mass of Cp15 (~53 kDa) and Cp16 (~23 kDa) as observed in SDS-PAGE and detected by His-Tag Monoclonal antibody in the Western blot. M= protein standard marker

The results showed that the predicted molecular mass of His-tagged Cp15 (~53 kDa) and His-tagged Cp16 (~23 kDa) was successfully detected using His-Tag Monoclonal antibody suggesting the correct molecular mass of Cp15 and Cp16 using bacterial protein expression pET-28 system (Fig. 12).

The Ni-NTA column (Qiagen) was used for purification of Cp15 and Cp16 His-tagged fusion proteins based on the selective binding of the Ni-NTA resin to the histidine residues. Since also non-specific cell lysate proteins were co-purified with the Cp15 and Cp16 His-

tagged fusion protein (data not shown), the expressed bacterial protein bands were visualized on SDS-PAGE and the specific Cp15 and Cp16 bands were directly excised from the gels and used for immunization of rabbits to generate anti-Cp15 and anti-Cp16 pABs.

In order to investigate whether the Cp15 protein is a structural component of OB, the generated anti-Cp15 pAB was tested against viral OB protein extracts. The anti-Cp15 pAB showed binding to ~60 kDa and ~29 kDa proteins (Fig. 13). The binding signal observed with 29 kDa can be attributed to the unspecific binding to the granulin protein which has the same molecular mass (29 kDa). Also it was not clear whether the binding that was observed with 60 kDa is a specific binding to Cp15 (53 kDa) with a Posttranslational modification, which may have altered its molecular mass, or it is also unspecific protein binding. In order to invistigate these observations and also to avoid the background formation or the unspecific protein binding, which may happen when using the polyclonal antibody, mono-specific pABs were generated from the anti-Cp15 and anti-Cp16 antisera.

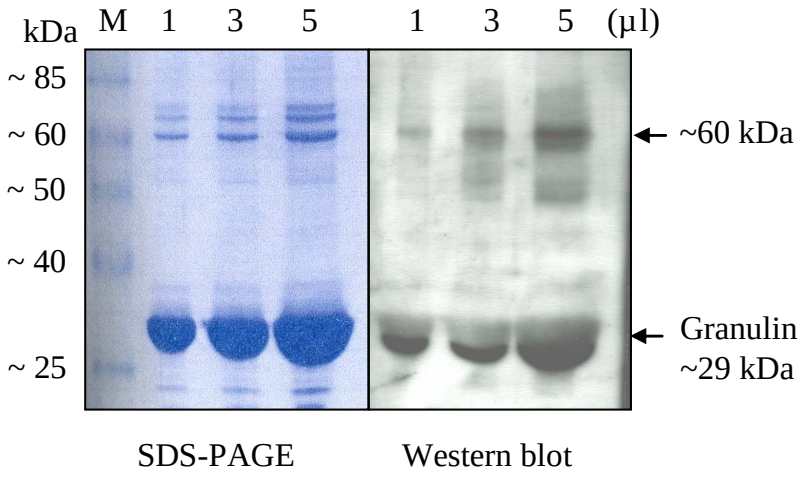

Fig. 13. Testing the specificity of the generated anti-Cp15 antiserum to OB protein lysates. 1, 2 and 3 µl of purified CpGV-M OBs protein extracts (~1 µg/µl) were sampled in SDS-PAGE and applied to anti-Cp15 antiserum for immuno detection. Arrow shows a non-specific detection of the granulin protein at the molecular mass ~29 kDa and at protein band of ~60 kDa.

Therefore, a preparative SDS-PAGE of bacterial lysates was performed and the Cp15 and Cp16 proteins lysates were subjected to SDS-PAGE gel electrophoresis and transferred to PVDF membrane. The exact band for each protein Cp15 and Cp16 was excised from the membrane, respectively. The membrane pieces were incubated with the produced anti-rabbit antisera to allow the specific antibodies to bind to Cp15 and Cp16, respectively. Then the

mono-specific pABs were eluted from the membrane and used for Western blot analysis of Cp15 and Cp16 temporal protein expression using CM larvae infected either with MCp5 or CpGV-M.

1.3.2. Detection of Cp15 and Cp16 temporal protein expression

A time course infection of fourth instar CM larvae infected with MCp5 and CpGV-M was performed, respectively, by feeding them a small plug of semi-artificial diet inoculated with 1000 OB/larva of the viruses. Only the larvae that completely ingested the plug were transferred to a fresh diet and sampled every 24 h for 5 days. A group of 5 larval midguts and fat bodies tissues were pooled in separate 2-ml Eppendorf tubes and applied for total protein extraction and SDS-PAGE followed by Western blotting analysis using mono-specific anti-Cp15-pAB and anti-Cp16-pAB. Neither extracts of MCp5- nor CpGV-infected larvae showed immuno-reactive response when using the mono-specific pABs with midguts samples (data not shown). In order to increase the protein amount in the infected tissues, samples of larval fat bodies were tested as these were expected to contain a higher amount of virus structural and non-structural proteins.

As shown in Fig. 14, the mono-specific anti-Cp15-pAB only reacted with a protein of ~29 kDa at 72 h and at late time points in CpGV-M samples (Fig. 14A). In MCp5 infected larvae, a faint signal was also observed at ~29 kDa late at 96 hpi and 120 hpi (Fig. 14B). The size of the detected protein bands (~29 kDa) differed from the predicted molecular mass of Cp15 (~53 kDa) based on its sequence. Since the same results were observed using extracts of a purified CpGV-M OBs (Fig. 13), it is most likely that the detected ~29 kDa protein in both CpGV-M and MCp5 infected fat bodies samples can be attributed to a non-specific binding of anti-Cp15-pAB to the granulin protein (29 kDa), which is expressed at a high amounts at a very late stage of virus infection. Using the mono-specific anti-Cp16-pAB, no specific protein signals were observed in both CpGV-M and MCp5 infected fat bodies of CM larvae (Fig. 15).

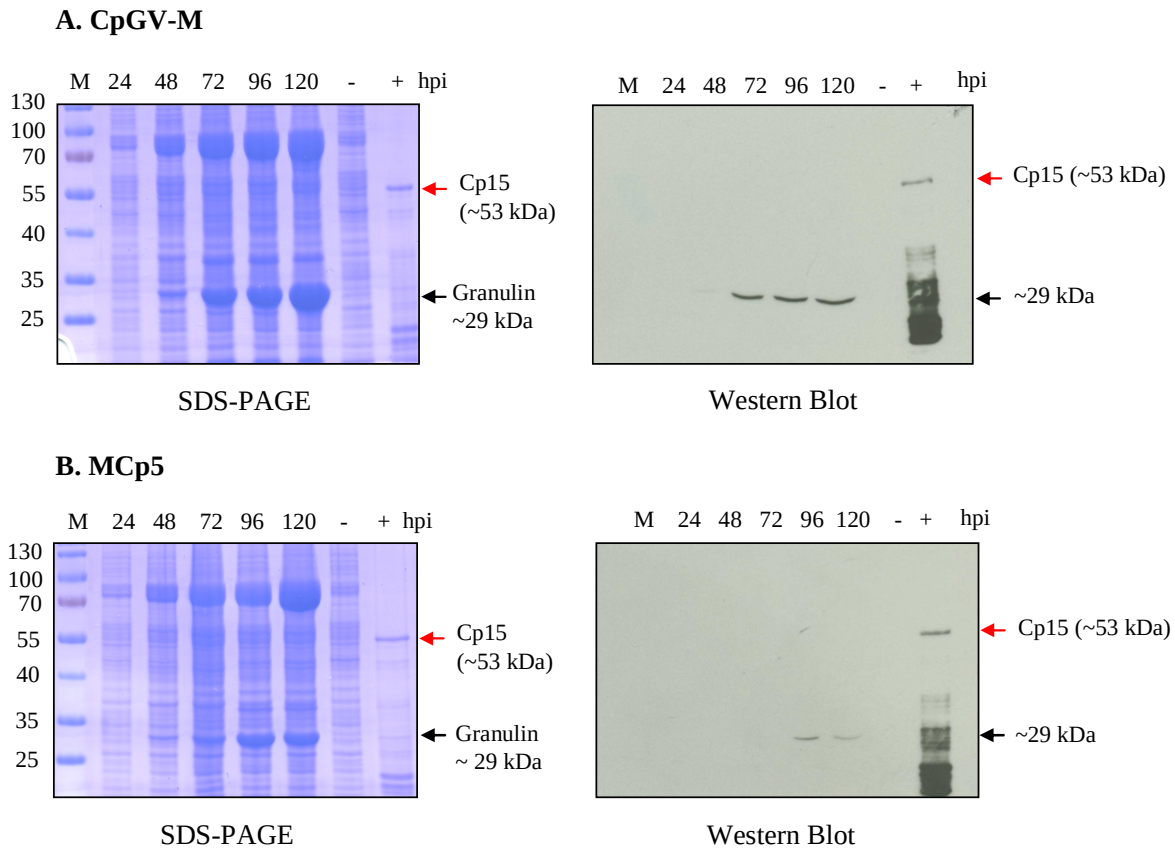

Fig. 14. SDS-PAGE and Western blot analysis of temporal protein expression of Cp15 in CM infected larvae using **(A)** CpGV-M and **(B)** MCp5 viruses. About 10 µg of total protein isolated from larval fat bodies was loaded per lane, separated in 12% SDS-PAGE, transferred to PVDF membrane and detected using a mono-specific anti-Cp15-pAB. The analyses were performed in a time course of CM larvae at different time points at 24, 48, 72, 96 and 120 hpi. Lane (-) shows the total protein extracted from mock infected larvae. Lane (+) shows the bacterial expressed Cp15 protein marked by red arrows in both gel and blot. The position of the granulin protein (~ 29 kDa) in lanes 72, 96, and 120 is marked by black arrows on the right.

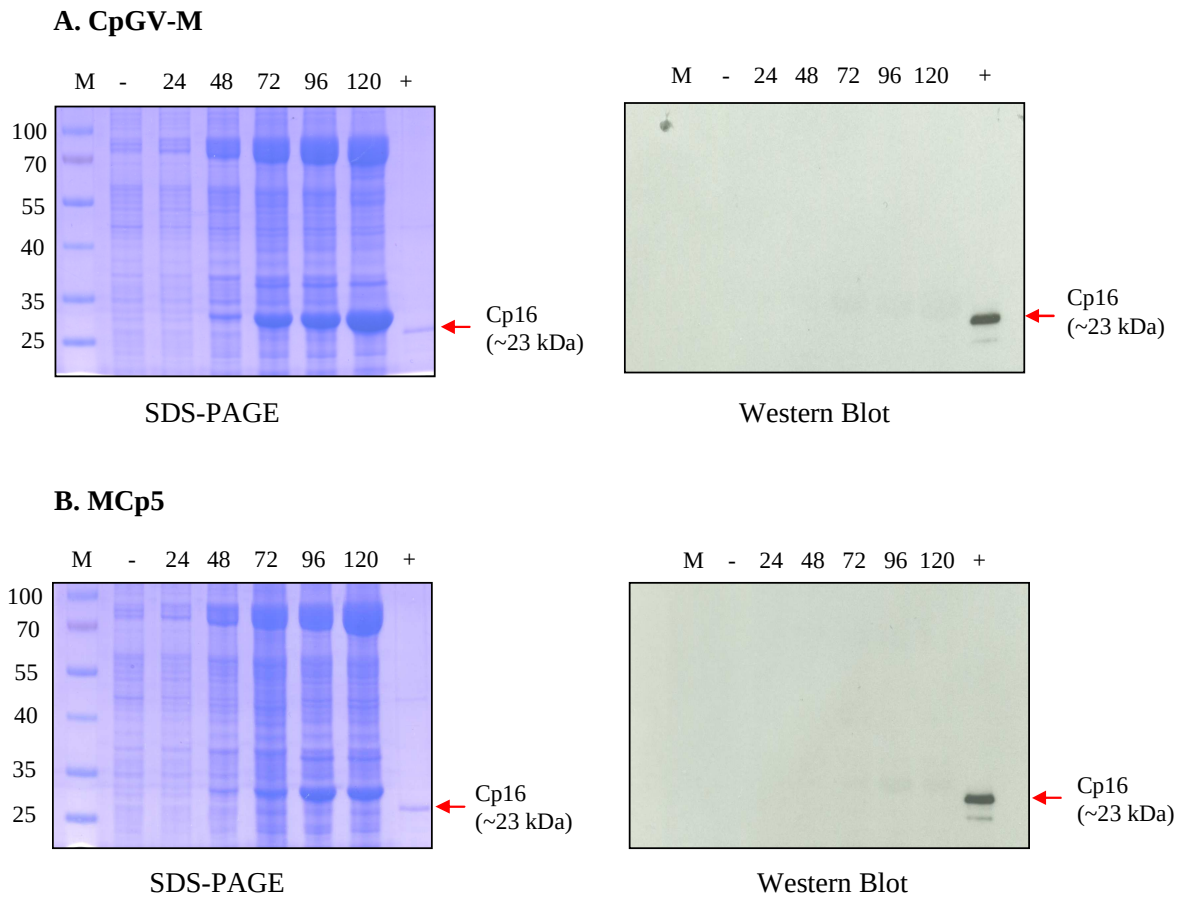

Fig. 15. SDS-PAGE and Western blot analysis temporal protein expression of Cp16 in CM infected larvae using **(A)** CpGV-M and **(B)** MCp5 viruses. About 10 µg total protein isolated from larval fat bodies was loaded per lane, separated in 12% SDS-PAGE, transferred to PVDF membrane and detected with anti-Cp16-pAB. The analyses were performed in a time course of CM larvae at different time points at 24, 48, 72, 96 and 120 hpi. Lane (-) shows the total protein extracted from mock infected larvae. Lane (+) shows the bacterial expressed Cp16 protein marked by red arrows on the right in both gel and blot.

When using different dilutions of the mono-specific anti-Cp16-pAB together with longer incubation times, specific protein signal for Cp16 could not be detected. These observations suggested that both Cp15 and Cp16 temporal protein expression in both CpGV-M and MCp5 infected larvae were probably too low to exceed the detection level of the generated antibodies and/or the affinity of the antiserum to Cp15 and Cp16 proteins were too low.

2. Generation and characterization of CpGV-M bacmid (CpBAC)

2.1. Construction of CpBAC

In order to further characterize the gene function of Cp15 and Cp16, the generation of CpGV-M mutants with a deletion of Cp15 and Cp16, respectively, was designed by using bacmid technology. In order to facilitate the generation of knockout mutants, the production of a CpGV-M shuttle vector (bacmid) that is capable of propagation in *E. coli* and also infectious for CM larvae is required. The bacmid construction should contain a selectable resistant gene and mini-F replicon single-copy origin of replication to maintain stability of the generated bacmid DNA. Moreover a second high copy origin of replication (oriV) for induction of higher yields of bacmid DNA is also required to facilitate the identification of the bacmid colonies using restriction digestion analysis. For this purpose, the Copy Control pCC1BAC cloning vector was used for direct cloning of CpGV-M genome. The pCC1BAC cloning vector with a cassette that includes a chloramphenicol resistant gene (Chl^R) as an antibiotic selectable marker, *lacZα* region derived from a pUC-based plasmid, *E. coli* F factor single-copy origin of replication (ori2) and a second origin of replication (oriV) which can be selectively induced to high copy number (Appendix II)

In order to monitor the CpGV-M bacmid replication and infection process in the infected CM larvae, the enhanced green florescent protein (*egfp*) was introduced into the pCC1BAC cloning vector. The *egfp* ORF (717 bp) was PCR amplified from pGEM-Z11-GFP plasmid kindly provided by Dr. H. Wang, Wuhan Institute of Virology, Chinese Academy of Sciences, Wuhan, China. Using two specific primers Egfp-orf_F and Egfp-orf_R, the *egfp* was PCR amplified introducing *Pst*I and *Hin*dIII restriction sites compatible with $Pie1^{hr}$/PA plasmid (Cartier et al., 1994) (Table 3 and Appendix II). The cloning strategy is outlined in Fig. 16. The *egfp* PCR fragment was digested with *Pst*I and *Hin*dIII endonucleases, and cloned as a *Pst*I/*Hin*dIII fragment under the control of AcMNPV ie-1 early promoter enhanced with the AcMNPV transcriptional enhancer hr5 into the $Pie1^{hr}$/PA expression vector generating the recombinant plasmid $pIE1^{hr}$-GFP-PA. The IE1-GFP-PA cassette was PCR

amplified from pIE1^{hr}-GFP-PA plasmid using two specific primers pIE1-gfp_F and pIE1-gfp_R introducing a *Xho*I restriction site in the upper primer (pIE1-gfp_F) and two *Pac*I and *Xho*I restriction sites in the lower primer (pIE1-gfp_R) compatible with the Copy Control pCC1BAC vector (Table 3, Fig. 16). The IE1-GFP-PA PCR product (~2.0 kb) was digested using *Xho*I endonuclease and subsequently cloned as *Xho*I fragment in pCC1BAC vector in *Xho*I locus generated the bacmid cloning vector pCC1-hr5-ie1-GFP.

Genomic viral DNA isolated from the purified CpGV-M OBs and linearized in *Pac*I locus was directly cloned in pCC1-hr5-ie1-GFP bacmid cloning vector *Pac*I locus and was transformed into electrocompetent Transformax EPI300 *E. coli* competent cells. *Pac*I locus in CpGV-M was chosen for cloning since it is located in a non-coding region of the virus genome. It was therefore expected not to affect the virus replication process. Transformants were distinguishable as light blue colonies on agar plates containing Chloramphenicol, X-Gal and IPTG. In order to maintain genotype stability of the clones, bacmid clones were grown at single-copy number during the initial cloning and screening processes. Then, before DNA purification, clones were induced to 10-20 copies per cell within 2 hours of adding Copy Control induction solution (*EPICENTRE*) to the culture for higher yield of bacmid DNA purification. Yields of pure bacmids DNAs were 20-30 µg per 100 ml of *E. coli* grown overnight in LB medium. Thus the yields were 50 to100-fold lower than that observed for high copy number plasmids. No transformants were observed when CpGV-M viral DNA was introduced into *E. coli.* Generated CpGV-M bacmid DNA was isolated from *E. coli* colonies and examined by digestion with *Pac*I and *Bam*HI endonucleases and the restriction patterns were compared to the REN pattern of purified CpGV-M DNA (Fig. 17).

The CpGV-M bacmid with the correct restriction profile was selected from 74 putative bacmid clones and was designated CpBAC. The CpBAC DNA isolated from *E. coli* and digested with *Bam*HI endonuclease exhibited no structural difference from the corresponding viral DNA isolated originally from purified CpGV-M OBs except for the presence of the pCC1-hr5-ie1-GFP cloning vector fragments (Fig. 17).

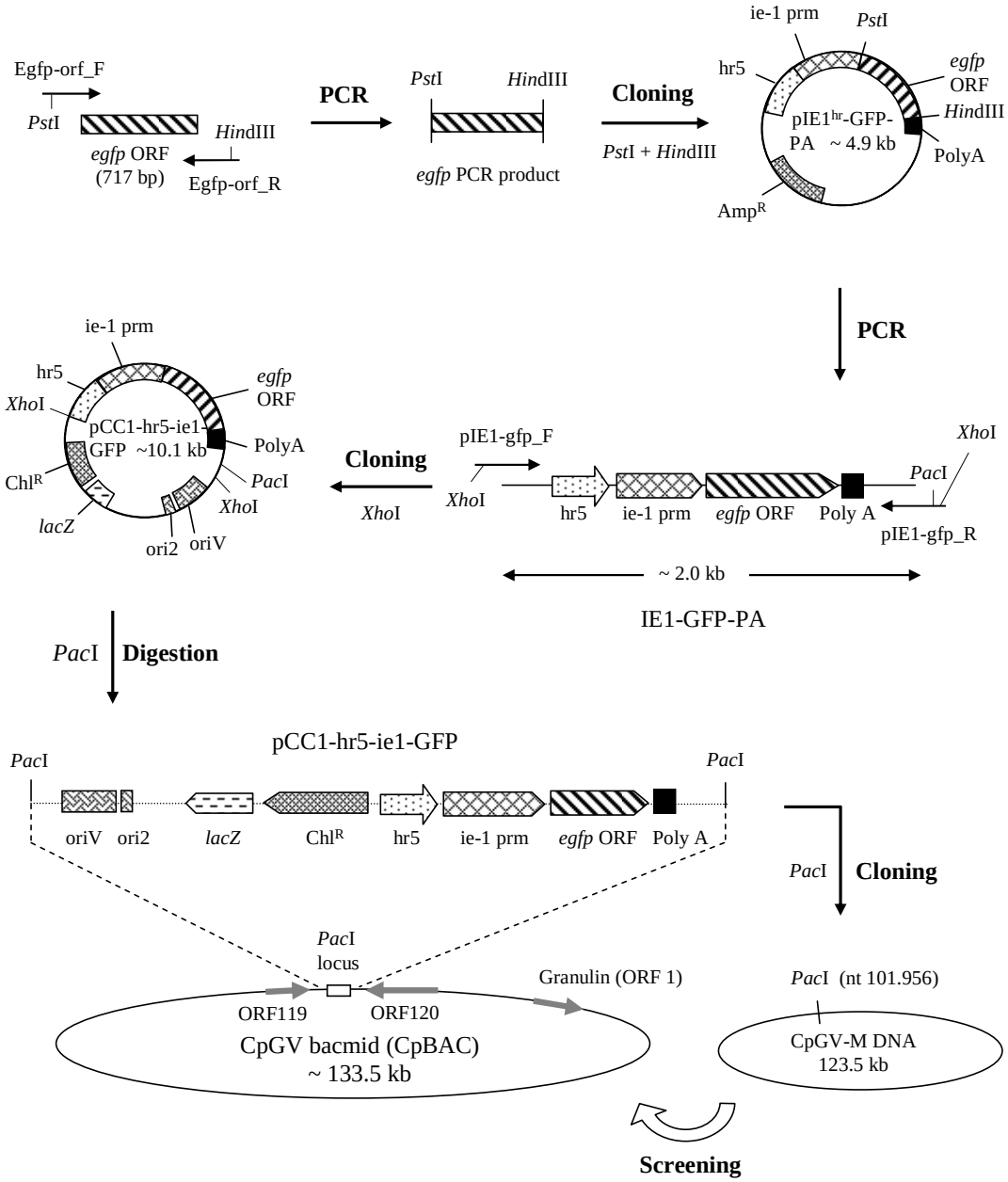

Fig. 16. Schematic outline for the generation of CpGV-M bacmid (CpBAC) and the construction of the enhanced GFP cassette (*egfp*). The *egfp* ORF was PCR amplified using Egfp-orf_F and Egfp-orf_R specific primers and subsequently ligated as 717 bp *Pst*I/*Hin*dIII-cleaved PCR fragment into pIE1^{hr}/PA vector to generate the pIEI^{hr}-GFP-PA recombinant plasmid (upper construct). The *egfp* cassette (IE1-GFP-PA) contains AcMNPV hr5 transcriptional enhancer, ie-1 promoter-driven *egfp* ORF and AcMNPV Polyadenylation signal was PCR amplified using pIE1-gfp_F and pIE1-gfp_R primer set and subsequently ligated as 2.0 kb *Xho*I-cleaved PCR fragment into the copy control pCC1BAC vector to generate the bacmid cloning vector pCC1-hr5-ie1-GFP (middle construct). The construct as shown containing the introduced *egfp* cassette in addition to a chloramphenicol resistance marker, *lacZ*α region of pUC-based plasmid, *E. coli* F factor single-copy origin of replication (ori2) and a high-copy origin of replication (oriV). The CpGV-M genomic DNA linearized at the *Pac*I site was ligated into the introduced *Pac*I site in pCC1-hr5-ie1-GFP plasmid to generate the CpGV-M bacmid (CpBAC) (lower construct). The drawing is not to scale.

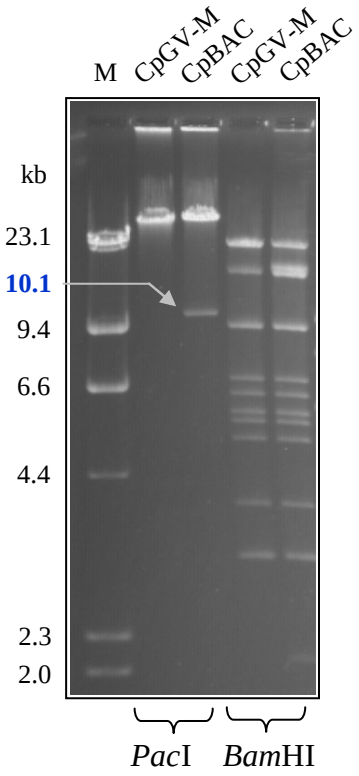

Fig. 17. Restriction digestion analysis of CpBAC and the parental CpGV-M using *Pac*I and *Bam*HI endonucleases. The 10.1 kb *Pac*I-fragment corresponding to the pCC1-hr5-ie1-GFP bacmid cloning vector is indicated by gray arrow in CpBAC lane after digestion with *Pac*I endonuclease. *Bam*HI restriction digestion shows the correct profile of the generated bacmid (CpBAC) compared to CpGV-M. M= lambda *Hin*dIII marker.

Fig. 18. Injection of fourth-instar CM larva with 1 µl of CpBAC DNA/lipofectin complex using HAMILTON Microliter Syringe.

2.2. Analysis of the infectivity of CpBAC

Since the CpBAC was constructed by direct cloning of CpGV-M genome in pCC1-hr5-ie1-GFP cloning vector, it was important to confirm its infectivity to CM larvae in order to be able to reliably use this construct. Confirmation of infectivity was a prerequisite for subsequently analyzing the influence of the Cp15 and Cp16 ORFs deletion on the *in vivo* infection capacity of the virus. In order to test the infectivity of CpBAC and to obtain viable viruses, CpBAC DNA isolated from *E. coli* cells was assembled into liposome using lipofectin (Invitrogen) and injected into the hemocoel of fourth instar CM larvae (Fig. 18). The controls included animals injected with CpGV-M DNA solution with out lipofectin, lipofectin solution alone (to test toxicity), TE-buffer in a lipofectin (to test TE-buffer viral contamination) and untreated animals. As a positive control experiment, CM larvae were injected with CpGV-M DNA/lipofectin using the same ratio used with the CpBAC DNA. All experiments were performed using 20 animals for each experimental group (Table 4).

Seventeen out of twenty injected CM larvae with CpBAC DNA/lipofectin complex died of viral infection about 9-12 days post injection. By using the CpGV-M DNA/lipofectin complex, nineteen injected larvae died of viral infection 9-12 days post infection. Those animals injected with CpGV-M DNA in the absence of lipofectin remained healthy underscoring the importance of liposome in this *in vivo* transfection process. Larvae injected with lipofectin alone or TE-buffer in lipofectin complex showed initially signs of a mild toxic effect, but they all quickly recovered. No virus infection symptom was observed on untreated larvae. From the diseased animals injected with CpBAC or CpGV-M DNA, the OBs were isolated and fed to 100 early fourth instar larvae of CM to test their biological activity. All animals died of viral infection providing evidence that OBs isolated from lipofected larvae were biologically active and that the CpBAC constituted a viable virus.

Table 4. Analysis of the infectivity of CpBAC against CM larvae (L4)

Virus	Number of injected larvae	Dead larvae (12 dpi)
CpBAC/lipo	20	17
CpGV-M/lipo	20	19
CpGV-M	20	0
lipofectin	20	0
TE-buffer/lipo	20	0
Untreated	20	0

2.3. Median lethal concentration (LC_{50}) of CpBAC

In order to test the biological activity of CpBAC virus, its median lethal concentration (LC_{50}) was determined. Groups of about 35 CM larvae (L1) were exposed to 5 different concentrations (300-100.000 OBs/ml) in a bioassay using OBs isolated from infected CM larvae with CpBAC or CpGV-M viruses. The experiments were performed in 3 replicates, the mortality was determined after 7 days and the LC_{50} was calculated using probit analysis (Table 5). The LC_{50} were 1698 and 1740 OB/ml for CpBAC and CpGV-M, respectively. The analysis showed no significant difference between the LC_{50} value of CpBAC and CpGV-M, confirming that the CpBAC virus obtained from direct cloning of CpGV-M genome in pCC1-hr5-ie1-GFP cloning vector had a similar biological activity of the virus it self.

Table 5. Median lethal concentration (LC_{50}) of CM first instar larvae infected either with CpBAC or CpGV-M viruses after 7 days. Nr = Number of tested larvae. The LC_{50} of probit analysis, as well as the slopes of the probit lines, are given. Cl, 95% confidence interval; SE, standar error. LC_{50} value and confidence limits are given in OB/ml. All Wald χ^2 tests (DF=1) were significant at P <0.0001. Different superscript letters indicate statistical differences between LC values (P <0.05) according to Robertson and Preisler (1992).

Virus	Nr. larvae	LC_{50} (Cl)	Slope (SE)	χ^2
CpBAC	625	1698[a] (1389 – 2058)	1.63 (0.12)	190.35
CpGV-M	627	1740[a] (1421-2113)	1.60 (0.12)	191.5

2.4. Visual expression profile of GFP

During the injection experiments of CpBAC viruses, however, it was noticed that infected CM larvae did not show EGFP expression as it would have been expected from the CpBAC construct. Therefore, the expression of EGFP in CpBAC-infected CM larvae was investigated in detail. Time course of larvae samples were placed, with uninfected control larvae, on a UV table (312 nm) and photographed. Until 4 days post infection, no green fluorescence signals were observed in the infected larvae. The *egfp* cassette in the CpBAC was applied to nucleotide sequencing in order to investigate the reason for missing the EGFP expression. The nucleotide sequencing of the *egfp* cassette revealed one point mutation on the ATG start codon of the *egfp* ORF (Fig. 19). This point mutation in the *egfp* ORF was detected in the position of the forward primer sequence that was used for PCR amplification of *egfp* ORF. This point mutation could be attributing to a mistake in the primer synthesis which altered the ATG start codon and thus the *egfp* translation and expression. These results

indicated that the GFP system could not be used as a marker for the infection spreading of the CpBAC virus.

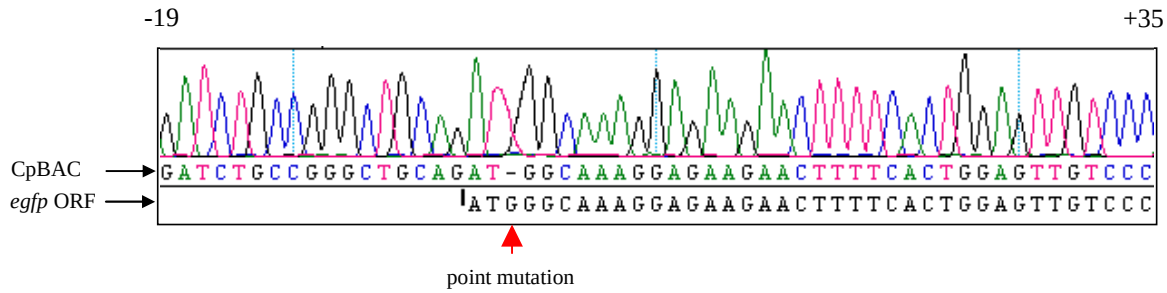

Fig. 19. Sequence alignment of the *egfp* ORF and the nucleotide sequence of the CpBAC *egfp* cassette. The missing G nucleotide (point mutation) of the ATG start codon in the CpBAC *egfp* cassette is shown indicated by red arrow.

3. Generation of CpBAC^{Cp15KO} and CpBAC^{Cp16KO} bacmids

In order to elucidate the function of Cp15 and Cp16 in the CpGV-M genome, either Cp15 or Cp16 were deleted from the CpGV-M bacmid (CpBAC) by using the Red/ET-Recombination technology (Stewart et al., 1998). Two 80-mer oligonucleotides for each target ORF were synthesized and used to generate a Kan^R PCR product from plasmid PGK-Tn5-neo of ~1.0 kb (Gene Bridges). The PCR product contained a kanamycin resistance gene (Kan^R) flanked by sequences homologous to (i) a region immediately upstream of ATG start codon of either Cp15 (H1 in Fig. 20A) or Cp16 (H3 in Fig. 21A) and (ii) a region immediately downstream of the stop codon of either Cp15 (H2 in Fig. 20A) or Cp16 (H4 in Fig. 21A). The PCR product was purified and co-transfected along with CpBAC DNA into electrocompetent Transformax EPI300 *E. coli* cells expressing the λ phage recombination proteins Redα and Redβ. Colonies harboring recombinant bacmids were selected on medium containing Kanamycin and Chloramphenicol.

The selected Cp15-null bacmid (CpBAC^{Cp15KO}) was expected to contain a deletion of Cp15 ORF (nt 10403 to 11776), and the selected Cp16-null bacmid (CpBAC^{Cp16KO}) was expected to contain a deletion of Cp16 ORF (nt 12147-12737) in the CpBAC. Replacement of either Cp15 or Cp16 ORFs with the Kan^R was confirmed by PCR using two specific oligonucleotides flanking the Kan^R insertion site for detection of predicted recombinant junction regions.

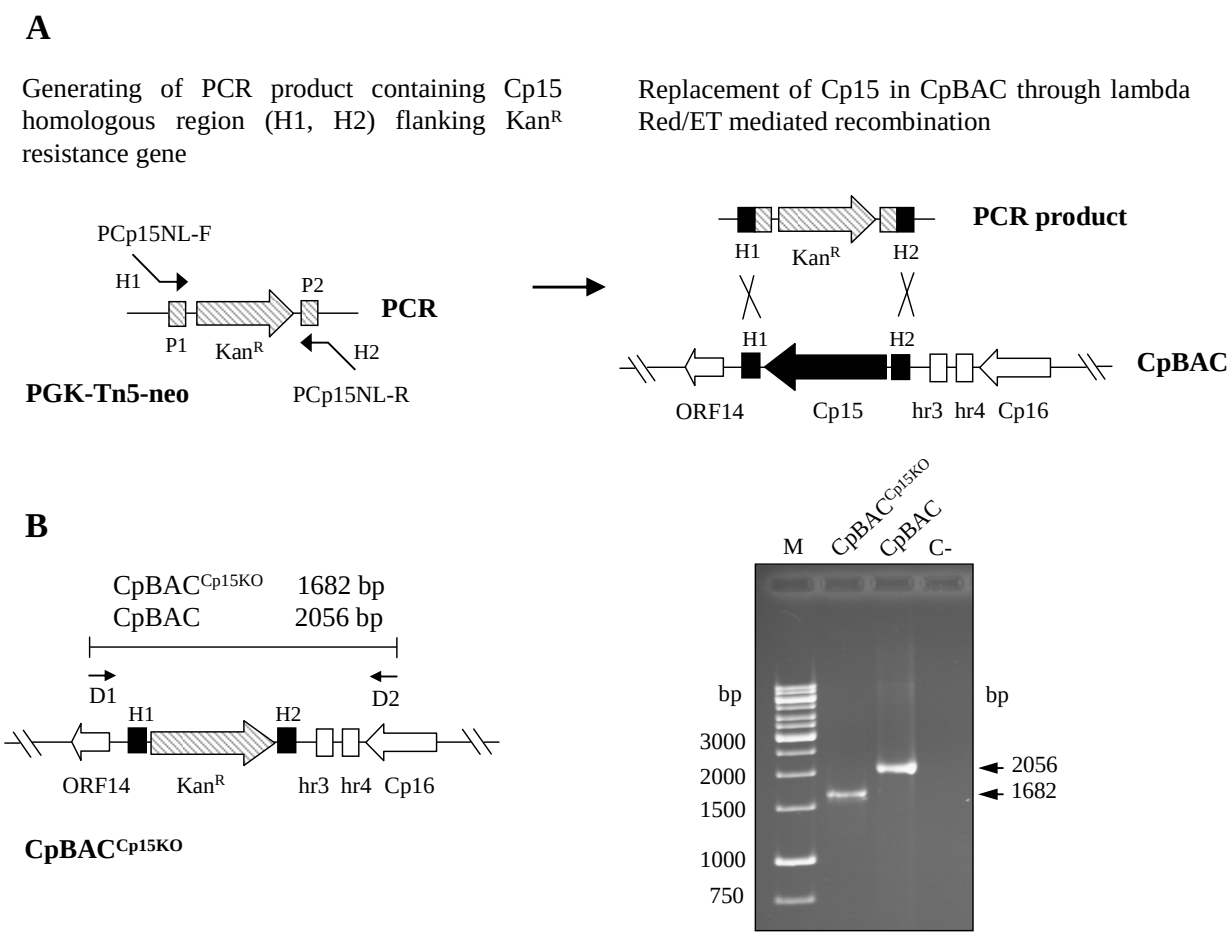

Fig. 20. Flow chart of Cp15 deletion strategy. **(A)** A PCR product containing Kan^R cassette flanked by sequences homologous to the Cp15 region at both ends was generated using two 80-mer oligonucleotides (PCp15NL-F and PCp15NL-R [Table 3]). Each oligonucleotide consisted of a 24-nt P1 or P2 priming site sequences flanking the Kan^R in PGK-Tn5-neo, 6-nt of *Sma*I site and a 50-nt Cp15 homology region complementary to sequences upstream of the Cp15 start codon (H1) or downstream of Cp15 stop codon (H2). The PCR product was used to replace the Cp15 in CpBAC using the Red/ET-Recombination system to generate the mutant virus CpBAC^{Cp15KO}. **(B)** PCR analysis was used to confirm the correct replacement of Cp15 with the Kan^R cassette in CpBAC^{Cp15KO}. The relative locations of the oligonucleotides used in the analysis of Cp15 locus are indicated by arrows designated B-Cp15-det_F (D1) and B-Cp15-det_R (D2) (Table 3). The expected PCR product sizes in the presence or absence of Cp15 are indicated by numbers above the primer pairs. The PCR analysis of the generated bacmid is shown below in an ethidium bromide stained agarose gel. The amplified PCR products are indicated by arrows to the right. The gel shows the expected PCR products of 1682 bp using CpBAC^{Cp15KO} and 2056 bp using CpBAC as a template using D1+D2 primer pairs. C- is a PCR negative control without DNA. Lane M corresponds to the 1-kb DNA ladder (Invitrogen).

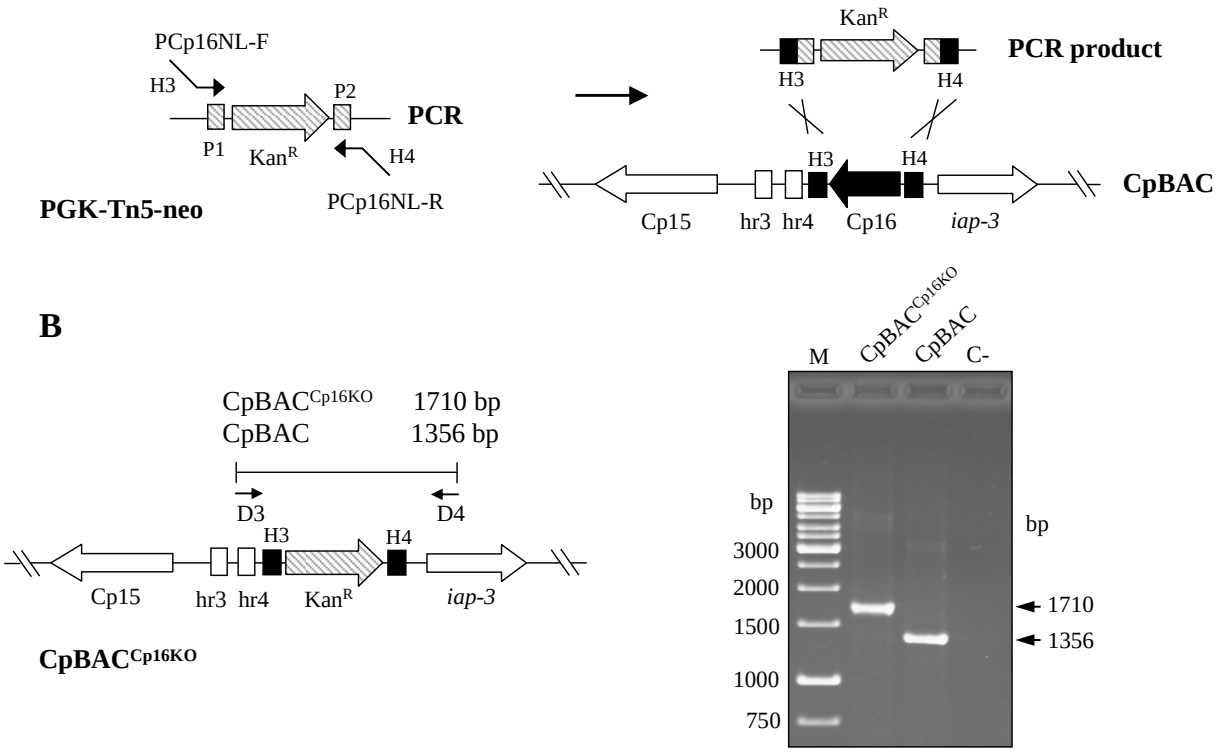

Fig. 21. Flow chart of Cp16 deletion strategy. **(A)** A PCR product containing Kan^R cassette flanked by sequences homologous to the Cp16 region at both ends was generated using two 80-mer oligonucleotides (PCp16NL-F and PCp16NL-R [Table 3]). Each oligonucleotide consisted of a 24-nt P1 or P2 priming site sequences flanking the Kan^R in PGK-Tn5-neo, 6-nt of *Sma*I site and a 50-nt Cp16 homology region complementary to sequences upstream of the Cp16 start codon (H3) or downstream of Cp16 stop codon (H4). The PCR product was used to replace the Cp16 in CpBAC using the Red/ET-Recombination system to generate the mutant virus $CpBAC^{Cp16KO}$. **(B)** PCR analysis was used to confirm the correct replacement of Cp16 with the Kan^R cassette in $CpBAC^{Cp16KO}$. The relative locations of the oligonucleotides used in the analysis of Cp16 locus are indicated by arrows designated B-Cp16-det_F (D3) and B-Cp16-det_R (D4) (Table 3). The expected PCR product sizes in the presence or absence of Cp16 are indicated by numbers above the primer pairs. The PCR analysis of the generated bacmid is shown below in an ethidium bromide stained agarose gel. The amplified PCR products are indicated by arrows to the right. The gel shows the expected PCR products of 1710 bp using $CpBAC^{Cp16KO}$ and 1356 bp using CpBAC as template using D3+D4 primer pairs. C- is a PCR negative control without DNA. Lane M corresponds to the 1-kb DNA ladder (Invitrogen).

The PCR analysis showed the expected product of 1682 bp with CpBAC^{Cp15KO} mutant and 2056 bp with the original CpBAC corresponded to the deletion of Cp15 and insertion of the Kan^{R} (Fig. 20B). For CpBAC^{Cp16KO}, the amplified PCR product was 1710 bp compared to that with the CpBAC, which was 1356 bp corresponding to the deletion of Cp16 and insertion of the Kan^{R} (Fig. 21B). The PCR analyses confirmed the correct replacement of either Cp15 or Cp16 with the Kan^{R} in CpBAC^{Cp15KO} and CpBAC^{Cp16KO}, respectively.

3.1. REN analysis of CpBAC^{Cp15KO} and CpBAC^{Cp16KO}

After putative positive clones were identified by PCR, the correct construction of CpBAC^{Cp15KO} and CpBAC^{Cp16KO} was analyzed by REN using *Bam*HI. As Cp15 ORF was located in fragment *Bam*HI-F (6.8 kb) of the CpGV-M genome, the replacement of Cp15 (1374 bp) with the Kan^{R} cassette (~ 1 kb), which has no *Bam*HI sites, resulted in a *Bam*HI fragment of 6.4 kp in the CpBAC^{Cp15KO} restriction profile (Fig. 22). Since CpGV-M genome contains a *Bam*HI site at 12.5 kb (nt 12586) within the Cp16 ORF, the *Bam*HI-F and *Bam*HI-J fragments in the CpGV-M should be replaced by a fragment of 12.4 kb in the CpBAC^{Cp16KO} restriction profile resulted from the replacement of Cp16 ORF with the Kan^{R} cassette and deletion of *Bam*HI locus at 12.5 kb (nt 12586) (Fig. 22). Therefore, REN analyses and the PCR analyses confirmed the correct deletion of Cp15 and Cp16 ORFs from the CpBAC and replacement with the Kan^{R} cassette in CpBAC^{Cp15KO} and CpBAC^{Cp16KO} viruses, respectively.

3.2. Analysis of the infectivity of CpBAC^{Cp15KO} and CpBAC^{Cp16KO}

The generated bacmids CpBAC^{Cp15KO} and CpBAC^{Cp16KO} were checked for their infectivity against CM larvae by injection. Fourth instar of CM larvae were injected with CpBAC^{Cp15KO} and CpBAC^{Cp16KO} DNA using lipofectin complex. The bacmid DNAs and the lipofectin were mixed and the mixture was injected into CM larval hemocoel. The controls included animals injected with CpBAC DNA solution without lipofectin, TE-buffer in a lipofectin (to test TE-buffer viral contamination) and untreated animals. As a positive control experiment, CM larvae were injected with CpBAC DNA mixed with lipofectin using the same ratio that was applied with the mutant bacmids. All experiments were performed using 20 animals for each experimental group. As shown in Table 6, the CM larvae injected with lipofected CpBAC^{Cp16KO} as well as CpBAC DNA showed viral infection symptoms after 7-9 days post injection.

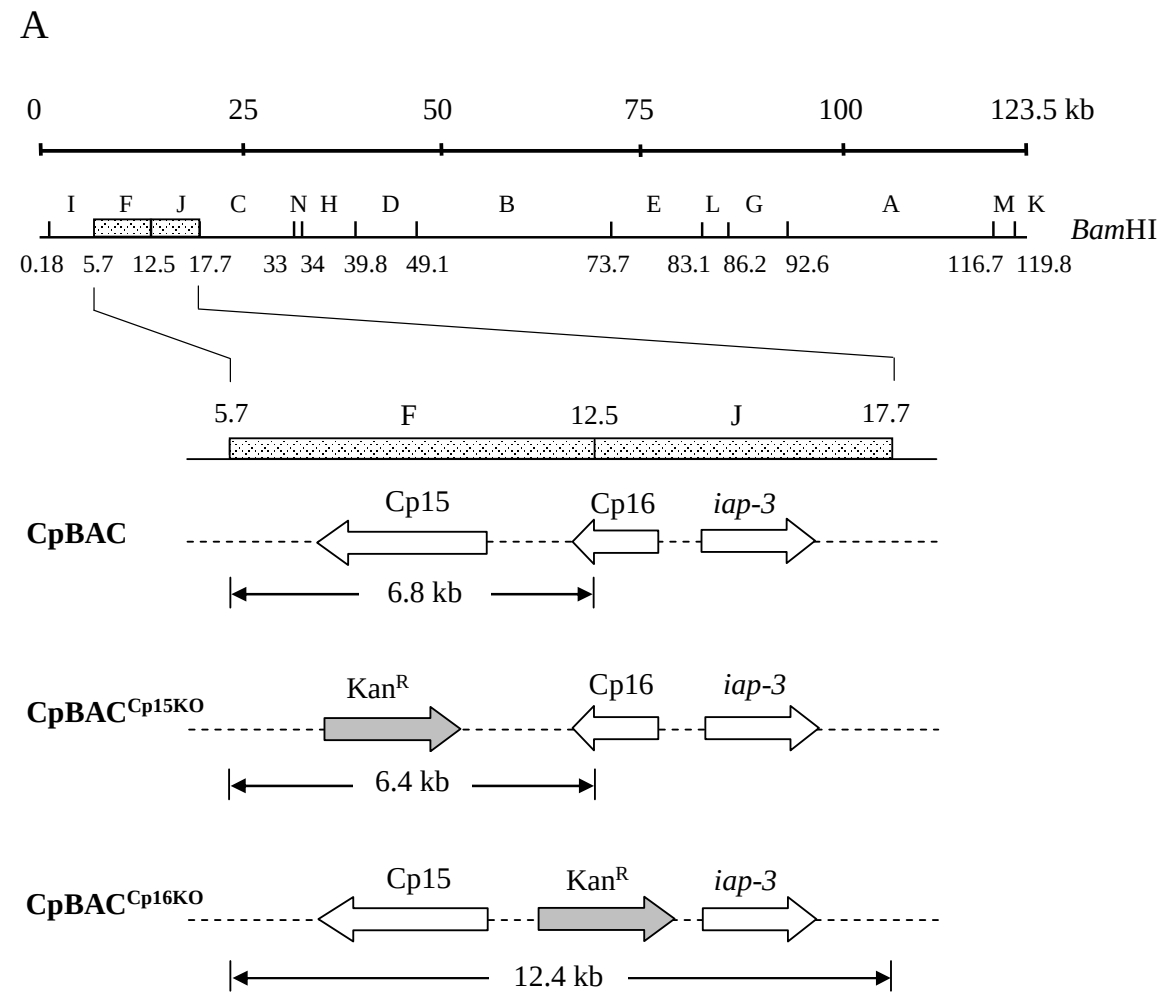

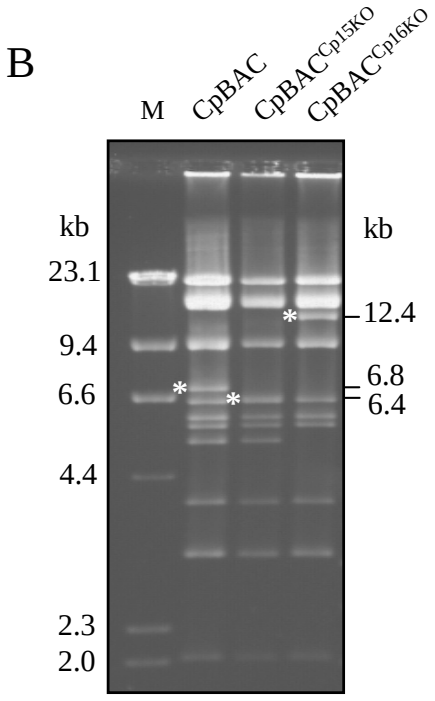

Fig. 22. *Bam*HI restriction map of CpGV-M according to Luque et al. (2001) and the corresponding regions in kb in CpBAC, CpBAC^{Cp15KO} and CpBAC^{Cp16KO}. **(A)** The expected size (kb) of the diagnostic *Bam*HI-F fragments in CpBAC, CpBAC^{Cp15KO} and CpBAC^{Cp16KO} are shown under each construct. **(B)** Restriction analysis of CpBAC, CpBAC^{Cp15KO} and CpBAC^{Cp16KO} viral DNA using *Bam*HI endonuclease. The different sizes (kb) of the *Bam*HI-F fragment in CpBAC^{Cp15KO} and CpBAC^{Cp16KO} due to the replacement of either Cp15 or Cp16 with a Kan^R cassette are indicated by asterisks. Their expected fragment sizes are given on the right. M: Lambda *Hin*dIII standard marker.

Most of the treated larvae died 9-12 days post injection and produced virus OBs. In contrast, larvae injected with CpBAC^{Cp15KO} DNA/lipofectin complex did not show any viral infection symptoms under the same condition. Those larvae injected with CpBAC DNA alone or TE-buffer in lipofectin complex as well as untreated animals remained healthy and did not show any symptoms of viral infection confirming the purity of these solutions of any virus contaminants. The OBs were isolated from the diseased animals injected with CpBAC or CpBAC^{Cp16KO} DNA and fed to 100 early fourth instar larvae of CM to test their peroral infectivity and to produce virus OBs. All animals died of granulosis providing evidence that OBs derived from larvae injected with CpBAC or CpBAC^{Cp16KO} were peroral infectious. These observations suggested that the deletion of Cp15 from the CpGV-M genome affected the viral infection cycle in CM larvae and did not allow virus replication *in vivo*. In contrast, the deletion of Cp16 from CpGV-M genome did not impair viral infection and the mutant virus CpBAC^{Cp16KO} produced OBs. Thus, the Cp16 is not essential gene for virus *in vivo* infection.

Table 6. Analysis of the infectivity of the CpBAC^{Cp15KO} and CpBAC^{Cp16KO} against CM larvae (L4)

Virus	Number of injected larvae	Dead larvae (12 dpi)
CpBAC^{Cp15KO}/lipo	20	0
CpBAC^{Cp16KO}/lipo	20	17
CpBAC/lipo	20	18
CpBAC	20	0
TE-buffer/lipo	20	0
Untreated	20	0

3.3. Generation of CpBAC^{Cp15KO} rescue bacmid

In order to confirm that the Cp15 knockout was responsible for the loss of infectivity of CpBAC^{Cp15KO}, it was aimed to rescue the mutant bacmid by reinsertion of Cp15 gene under the control of its own promoter region in CpBAC^{Cp15KO} using the Red/ET-Recombination system (Fig. 23). Due to the defect of the *egfp* expression, the locus of *egfp* cassette was chosen for the reinsertion of the Cp15 cassette for rescuing of the CpBAC^{Cp15KO}. This was accomplished by PCR amplification of the Cp15 ORF with its own putative promoter region (nt 10382-11914) from CpGV-M DNA using two specific primers Cp15-SmaI_F and Cp15-SmaI_R introducing *Sma*I restriction sites in their 5' ends.

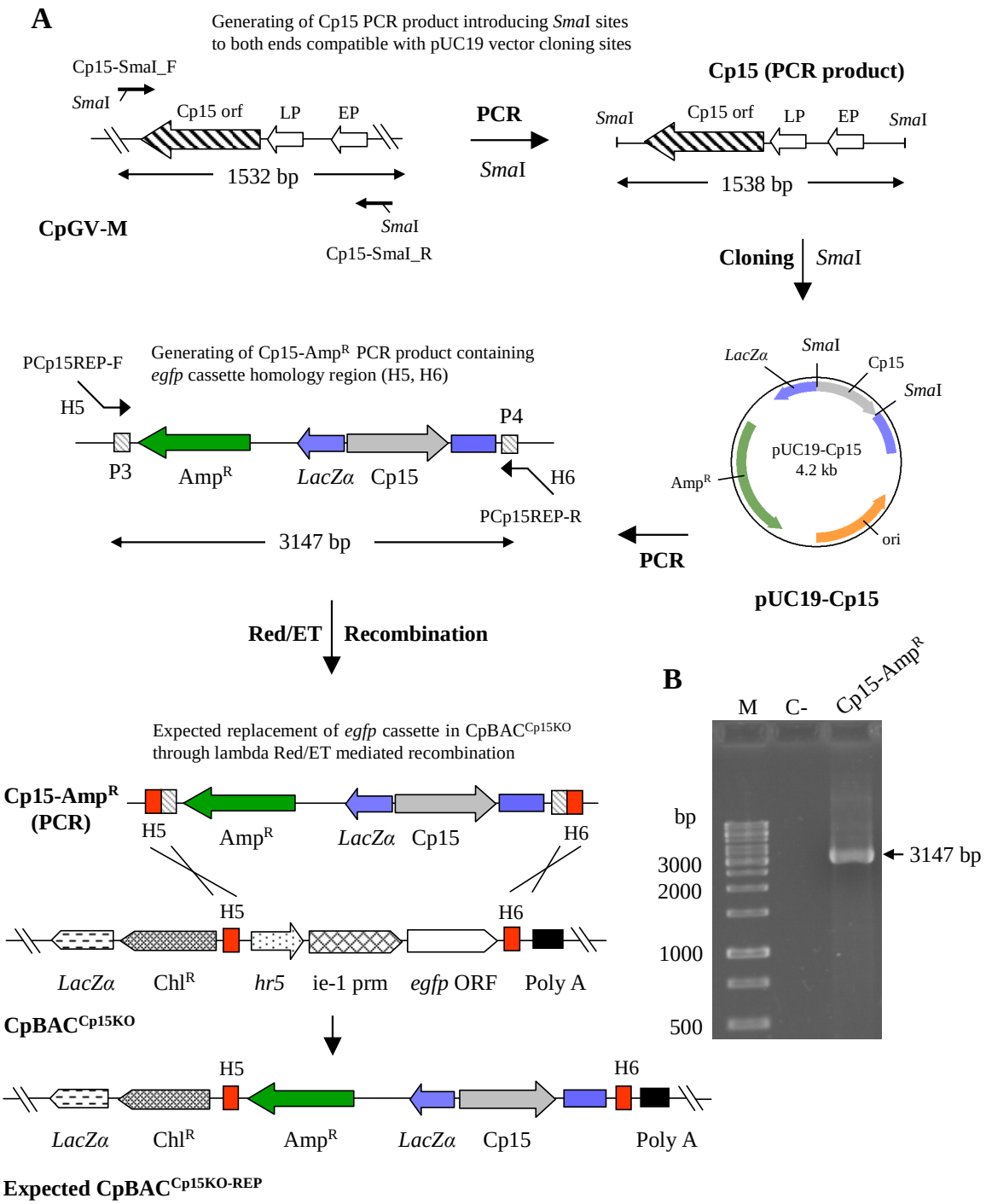

Fig. 23. Flow chart of CpBAC^{Cp15KO} rescue strategy. **(A)** The Cp15 with its promoter region putative late and early promoters (LP) and (EP), respectively, was PCR amplified using oligonucleotides Cp15-SmaI_F and Cp15-SmaI_R introducing *Sma*I sites to both ends of the generated product (upper construct). The digested Cp15-*Sma*I fragment was cloned into pUC19 *Sma*I site generated the pUC19-Cp15 plasmid. From the recombinant plasmid pUC19-Cp15, a PCR product containing Cp15-Amp^R cassette flanked by sequences homologous to *egfp* region at both ends was generated using two 80-mer oligonucleotides (PCp15REP-F and PCp15REP-R [Table 3]). Each oligonucleotide consisted of a 24-nt P3 or P4 priming site sequences flanking the Cp15-Amp^R cassette, 6-nt of *Kpn*I site and a 50-nt *egfp* homologous region complementary to sequences upstream of the hr5 transcriptional enhancer (H5) or downstream of *egfp* ORF (H6) (middle construct). The PCR

product (3147 bp) was used to replace the *egfp* cassette in CpBAC^{Cp15KO} using the Red/ET-Recombination system to generate the rescued bacmid CpBAC$^{Cp15KO-REP}$. The construction of the pUC19-Cp15 plasmid after cloning of the Cp15-Amp^{R} fragment is indicated and also the relative location of the Cp15-Amp^{R} fragment that was expected to replace the *egfp* cassette in the expected rescued CpBAC$^{Cp15KO-REP}$ (lower construct). The relative location of oligonucleotides used for PCR amplification of Cp15 gene or for generation of Cp15-Amp^{R} cassette are indicated below the constructs together with the expected sizes of the PCR products**. (B)** Ethidium bromide stained agarose gel with the expected PCR product (3147 bp) of Cp15-Amp cassette and the PCR negative control (C-). Lane M corresponds to the 1-kb DNA standard marker.

The Cp15 covering PCR fragment was digested using *Sma*I enzyme and subsequently cloned as *Sma*I fragment (~1532 bp) into *Sma*I locus of pUC19 vector to generate the recombinant plasmid pUC19-Cp15 (4.2 kb). The resulted plasmid pUC19-Cp15 was used as a template to generate a fusion product consisting of the Cp15 gene and the β-lactamase gene (Amp^{R}). For this, two 80-mer oligonucleotides named PCp15REP-F and PCp15REP-R were synthesized and used to generate a PCR product from plasmid pUC19-Cp15. The PCR product contained an Amp^{R} cassette fused to the Cp15 gene and flanked by sequences homologous to (i) a region immediately upstream of hr5 AcMNPV transcriptional enhancer (H5 in Fig. 23A) and (ii) a region immediately downstream of *egfp* ORF (H6 in Fig. 23A). These oligonucleotides were designed that they leave the AcMNPV polyadenylation signal in the *egfp* cassette and only replace the *egfp* ORF together with hr5 AcMNPV transcriptional enhancer and ie-1 promoter in CpBAC^{Cp15KO} by the Cp15-Amp^{R} cassette (Fig. 23A). The PCR product (3147 bp) was purified and co-transfected together with CpBAC^{Cp15KO} DNA into electrocompetent Transformax EPI300 *E. coli* cells to allow the homologous recombination between Cp15-Amp^{R} cassette and *egfp* cassette in CpBAC^{Cp15KO} through Red/ET-Recombination. Although, the generation of the Cp15-Amp^{R} PCR fragment was successful and produced the expected 3147 bp (Fig. 23B), the replacement of the *egfp* cassette with the Cp15-Amp^{R} in CpBAC^{Cp15KO} did not succeed using Red/ET-Recombination system. No bacterial colonies were observed in the presence of Ampicillin, Chloramphenicol and Kanamycin even by increasing the incubation time from 24 h to 48 h at 37ºC.

3.4. Median lethal concentration (LC_{50}) of CpBAC^{Cp16KO}

In order to compare the biological activity of CpBAC^{Cp16KO} and CpGV-M viruses, the median lethal concentration (LC_{50}) was determined. Groups of about 35 CM (L1) larvae were subjected to a bioassay using OBs isolated from infected CM larvae with CpBAC^{Cp16KO} or CpGV-M viruses and the mortality was determined. The experiments were performed in 3 replicates and the LC_{50} value was calculated using probit analysis (Table 7). The LC_{50} were

1151 OB/ml for CpBAC^{Cp16KO} and 1297 OB/ml for CpGV-M. Both viruses showed an almost complete overlapping of their fiducial limits and were hence not significantly different. CpBAC^{Cp16KO} also not different to CpBAC and CpGV-M tested previously (Table 5). The LC_{50} suggested that the deletion of ORF Cp16 did not affect the virus virulence against CM larvae based on the LC_{50} value analysis. Apparently, Cp16 gene is not required for *in vivo* infection of CM larvae.

Table 7. Median lethal concentration (LC_{50}) of first instar CM larvae infected either with CpBAC^{Cp16KO} or CpGV-M viruses after 7 days. Nr = Number of tested larvae. The LC_{50} of probit analysis, as well as the slopes of the probit lines, are given. Cl, 95% confidence interval; SE, standard error. LC_{50} value and confidence limits are given in OBs/ml. All Wald χ^2 tests (DF=1) were significant at P <0.0001. Different superscript letters indicate statistical differences between LC values (P< 0.05) according to Robertson and Preisler (1992).

Virus	Nr. larvae	LC_{50} (Cl)	Slope (SE)	χ^2
CpBAC^{Cp16KO}	620	1151^a (925 – 1407)	1.59 (0.12)	163.42
CpGV-M	625	1297^a (1076 – 1550)	1.87 (0.14)	164.04

4. Determining the function of hr3 and hr4 in CpGV virus infection cycle

4.1. Generation of CpBAC$^{hr3/hr4KO}$ and CpBAC$^{hr3\text{-}kan\text{-}hr4}$ bacmids

In MCp5, the TCl4.7 transposon is located between the ORFs Cp15 and Cp16 and separates two palindromes hr3 and hr4, which have been recently shown to function as CpGV ori (Hilton and Winstanley, 2007). Previous competition experiment had demonstrated, that MCp5 had a significant replication disadvantage when CM larvae or CpDW14R cells were co-infected with the wt CpGV-M (Arends et al., 2005). An effect of TCl4.7 insertion on the function of hr3 and hr4 ori is one of the possible reasons for this observation. To investigate this possibility, two mutant bacmids were generated, one with a deletion of hr3 and hr4 (CpBAC$^{hr3/hr4KO}$), and the second with an insertion of the Kan^R cassette between hr3 and hr4 (CpBAC$^{hr3\text{-}kan\text{-}hr4}$) as a mimic construct for MCp5 carrying TCl4.7 transposon between hr3 and hr4. The latter construct may tell whether the separation of hr3 and hr4 will influence the virulence and virus competitiveness as was observed previously with MCp5 (Arends et al., 2005).

The Red/ET-Recombination system was used to delete the hr3 and hr4 region in CpBAC to generate the mutant bacmid CpBAC$^{hr3/hr4KO}$, and to insert the Kan^R cassette between hr3 and hr4 to generate the mutant bacmid CpBAC$^{hr3\text{-}kan\text{-}hr4}$. For deletion of hr3 and

hr4, two 80-mer oligonucleotides Phr3/hr4NL-F and Phr3/hr4NL-R were synthesized and used to generate a PCR product of ~1.0 kb from plasmid PGK-Tn5-neo. The PCR product contained a kanamycin resistance cassette (Kan^R) flanked by sequences homologous to the flanking sequence of hr3 (nt 11906-11981) and hr4 (nt 12071-12145) region (H7 and H8 in Fig. 24A) corresponding to the CpGV-M nucleotide sequence (Luque et al., 2001). For insertion of the Kan^R cassette in the region between hr3 and hr4, two 80-mer oligonucleotides Phr3-kan-hr4-F and Phr3-kan-hr4-R were synthesized and used to generate a PCR product of ~1.0 kb from plasmid PGK-Tn5-neo. According to the CpGV-M nucleotide sequence, the distance between hr3 and hr4 is 90 bp (Luque et al., 2001). The PCR product was generated to contain a kanamycin resistance cassette (Kan^R) flanked by sequences homologous to the flanking sequence of the 90 bp (H9 and H10 in Fig. 24B). The generated PCR products were purified and contransfected, along with CpBAC DNA, into electrocompetent Transformax EPI300 *E. coli*. Colonies harboring recombinant bacmids were selected on medium containing Kanamycin and Chloramphenicol. The correct construction of both mutant bacmids was confirmed by PCR using two specific oligonucleotides (D5+D6) flanking the Kan^R insertion site for detection of predicted recombinant junction regions (Fig. 24C). The PCR analysis showed the expected product of 1249 bp for $CpBAC^{hr3/hr4KO}$, which corresponded to the deletion of hr3 and hr4 region and insertion of the Kan^R, and 1402 bp for $CpBAC^{hr3\text{-}kan\text{-}hr4}$, which corresponded to the insertion of the Kan^R cassette between hr3 and hr4 (Fig. 24C). Thus, the PCR analysis gave evidence of the correct construction of both bacmids $CpBAC^{hr3/hr4KO}$ and $CpBAC^{hr3\text{-}kan\text{-}hr4}$.

Fig. 24. (Next page) Flow chart for construction of $CpBAC^{hr3/hr4KO}$ and $CpBAC^{hr3\text{-}kan\text{-}hr4}$ bacmids. **(A)** A PCR product containing a Kan^R cassette flanked by sequences homologous to the hr3/hr4 region at both ends was generated using two 80-mer oligonucleotides (Phr3/hr4NL-F and Phr3/hr4NL-R [Table 3]). Each oligonucleotide consisted of a 24-nt P1 or P2 priming site sequences flanking the Kan^R in PGK-Tn5-neo, 6-nt of *Sma*I site and a 50-nt hr3/hr4 homologous region complementary to the right border sequences of hr3 (H7) or left border sequences of hr4 (H8). The PCR product was used to replace the hr3/hr4 region in CpBAC using the Red/ET-Recombination system to generate the mutant virus $CpBAC^{hr3/hr4KO}$. **(B)** A PCR product containing Kan^R cassette flanked by sequences homologous to the 90 bp region that located between hr3 and hr4 at both ends was generated using two 80-mer oligonucleotides (Phr3-kan-hr4-F and Phr3-kan-hr4-R [Table 3]). Each oligonucleotide consisted of a 24-nt P1 or P2 priming site sequences flanking the Kan^R in PGK-Tn5-neo, 6-nt of *Sma*I site and a 50-nt homologous region complementary to the right border (H9) or left border (H10) sequences flanking the 90 bp region. The PCR product was used to insert the Kan^R cassette between hr3 and hr4 in CpBAC using the Red/ET-Recombination system to generate the mutant virus $CpBAC^{hr3\text{-}kan\text{-}hr4}$. The relative locations of the oligonucleotides used in the analysis of the Kan^R locus are indicated by arrows designated Det-hr3/hr4-F (D5) and Det-hr3/hr4-R (D6). The expected PCR product sizes in $CpBAC^{hr3/hr4KO}$ and $CpBAC^{hr3\text{-}kan\text{-}hr4}$ as well as

CpBAC are indicated by numbers above the primer pair. **(C)** PCR analysis of the generated bacmids is shown below in an ethidium bromide stained agarose gel and the amplified PCR products are indicated by arrows. The gel shows the expected PCR products of 1249 bp for CpBAC$^{hr3/hr4KO}$, 1402 bp for CpBAC$^{hr3\text{-}kan\text{-}hr4}$ and 417 bp for the parental CpBAC using D5+D6 primer pair. Lane (M) corresponds to the 1-kb DNA ladder.

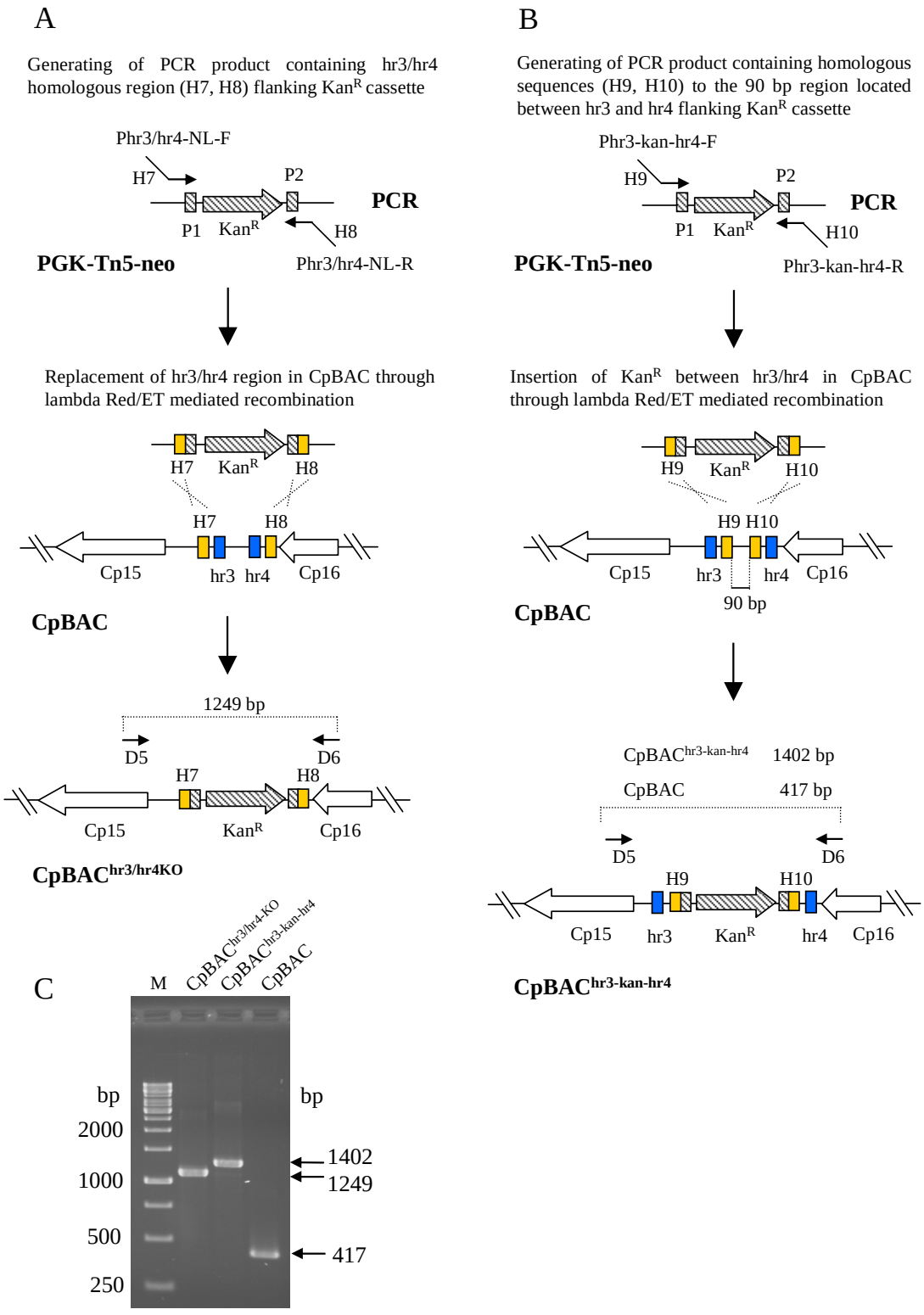

Fig 24. Legand see page before.

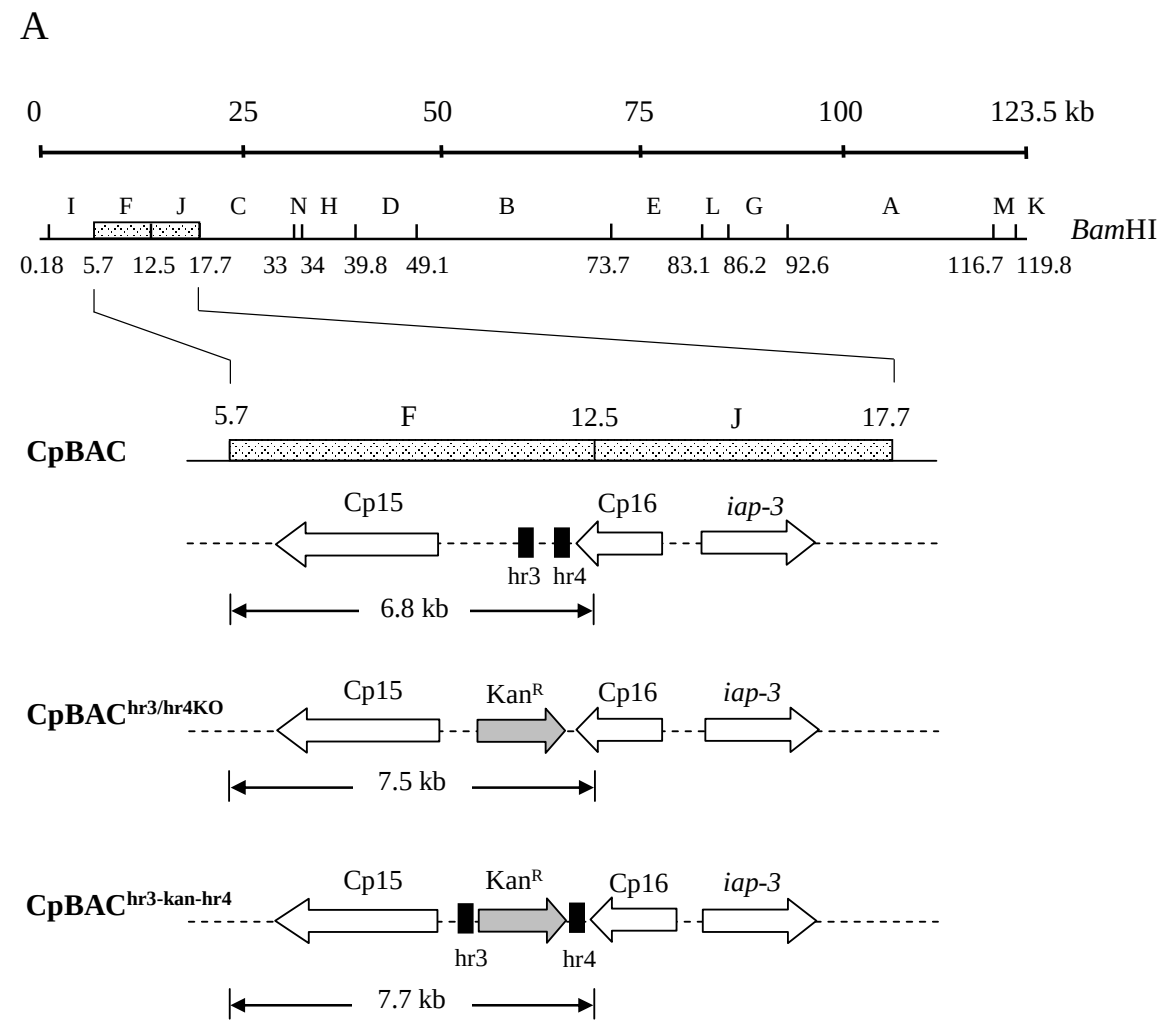

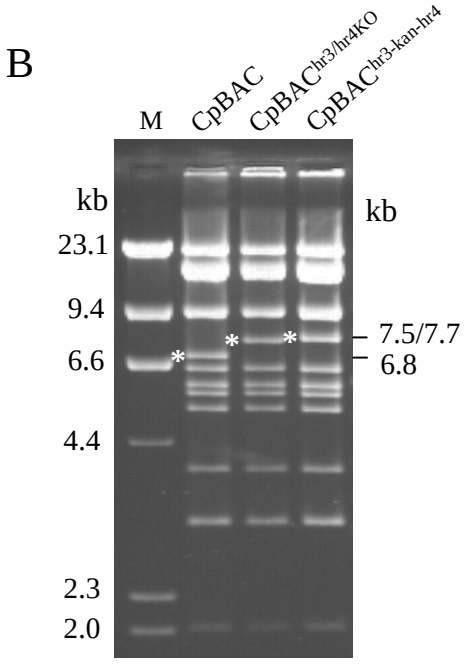

Fig. 25. *Bam*HI restriction analysis of CpGV-M according to the corresponding regions in CpBAC, CpBAC$^{hr3/hr4KO}$ and CpBAC$^{hr3\text{-}kan\text{-}hr4}$. **(A)** Top: *Bam*HI map of CpGV-M (Luque et al., 2001). The corresponding region in *Bam*HI-F and -J is shown for CpBAC, CpBAC$^{hr3/hr4KO}$ and CpBAC$^{hr3\text{-}kan\text{-}hr4}$. The expected size (kb) of the diagnostic *Bam*HI-F fragment in CpBAC, CpBAC$^{hr3/hr4KO}$ and CpBAC$^{hr3\text{-}kan\text{-}hr4}$ are shown under each construct. **(B)** Ethidium bromide stained agarose gel of *Bam*HI digestion of CpBAC, CpBAC$^{hr3/hr4KO}$ and CpBAC$^{hr3\text{-}kan\text{-}hr4}$ DNA. The different sizes (kb) of the *Bam*HI-F fragment in each bacmid construct due to the insertion of Kan^R are indicated by asterisks with its expected fragment sizes on the right. M: Lambda *Hin*dIII standard marker.

In order to confirm the results of the PCR analyses, a REN analysis of the generated mutant bacmids was done using *Bam*HI. Since hr3 and hr4 are located within the 6.8 kb *Bam*HI-F fragment (Luque et al., 2001), the replacement of hr3/hr4 region by the Kan^R cassette in $CpBAC^{hr3/hr4KO}$ was expected to result in a specific fragment of 7.5 kb (Fig. 25A). Whereas, the insertion of Kan^R between hr3 and hr4 in $CpBAC^{hr3\text{-}kan\text{-}hr4}$ should result in a specific fragment of 7.7 kb (Fig. 25A). The REN digests resulted in the expected patterns (Fig. 25B) confirming the correct construction of $CpBAC^{hr3/hr4KO}$ and $CpBAC^{hr3\text{-}kan\text{-}hr4}$ bacmids.

4.2 Analysis of the infectivity of $CpBAC^{hr3/hr4KO}$ and $CpBAC^{hr3\text{-}kan\text{-}hr4}$

In order to test the replication capacity of $CpBAC^{hr3/hr4KO}$ and $CpBAC^{hr3\text{-}kan\text{-}hr4}$ bacmids and to produce viral OBs, the purified DNA of each bacmid was injected into the hemocoel of fourth instar CM larvae as a liposome complex. The control experiments included animals injected with CpBAC DNA solution without lipofectin, TE-buffer in lipofectin (to test TE-buffer viral contamination) and untreated animals. CM larvae were injected with a CpBAC DNA/lipofectin complex as a positive control. All experiments were performed using 20 animals for each experimental group (Table 8).

The CM larvae injected with $CpBAC^{hr3/hr4KO}$ and $CpBAC^{hr3\text{-}kan\text{-}hr4}$ as well as CpBAC DNA in a lipofectin complex showed viral infection symptoms after 7-9 days post injection. All treated larvae died 9-12 days post injection and produced viral OBs. Those larvae injected with CpBAC DNA alone or TE-buffer in Lipofectin complex as well as untreated animals remained healthy and did not show any symptoms of viral infection confirming the purity of these solutions of any virus contaminants.

From the diseased animals injected with $CpBAC^{hr3/hr4KO}$, $CpBAC^{hr3\text{-}kan\text{-}hr4}$ or CpBAC, the OBs were isolated and fed to 100 early fourth instar of CM larvae to test their *per os* infectivity and to produce OBs. All animals died of granulosis providing evidence that OBs derived from larvae injected with $CpBAC^{hr3/hr4KO}$ and $CpBAC^{hr3\text{-}kan\text{-}hr4}$ as well as CpBAC were biologically active *per os*. Thus, neither the separation of hr3 and hr4 nor their complete deletion from the CpBAC did affect viral infection and the resulted mutant viruses $CpBAC^{hr3/hr4KO}$ and $CpBAC^{hr3\text{-}kan\text{-}hr4}$ produced infective OBs and were still infectious *per os* for CM larvae.

Table 8. Analysis of the infectivity of the CpBAC$^{hr3/hr4KO}$ and CpBAC$^{hr3\text{-}kan\text{-}hr4}$ against CM larvae (L4)

Virus	Number of injected larvae	Dead larvae (12 dpi)
CpBAC$^{hr3/hr4KO}$/lipo	20	20
CpBAC$^{hr3\text{-}kan\text{-}hr4}$/lip	20	20
CpBAC/lipo	20	20
CpBAC	20	0
TE-buffer/lipo	20	0
Untreated	20	0

4.3. Median lethal concentration (LC_{50}) and survival time (ST_{50}) analysis

In order to compare the biological activity of CpBAC$^{hr3/hr4KO}$, CpBAC$^{hr3\text{-}kan\text{-}hr4}$ and the parental CpBAC, the LC_{50} and the ST_{50} were determined for neonate CM larvae. For the LC_{50} determination, groups of about 35 larvae in three replicates were exposed to 5 different concentrations (300-100.000 OBs/ml) of each virus OBs for 7 days and the mortality was determined. The calculated values of LC_{50} and the slopes of the probit regression lines are given in Table 9. The analysis showed that LC_{50} value of CpBAC$^{hr3/hr4KO}$ (5044 OB/ml) was slightly higher than that of CpBAC (2439 OB/ml) and CpBAC$^{hr3\text{-}kan\text{-}hr4}$ (2837 OB/ml). However, there was no statistically significant difference between the LC_{50} values of CpBAC$^{hr3/hr4KO}$ and CpBAC or between those of CpBAC$^{hr3\text{-}kan\text{-}hr4}$ and CpBAC.

Table 9. Median lethal concentration (LC_{50}) of CM first instar larvae infected with OBs derived from CpBAC$^{hr3/hr4KO}$, CpBAC$^{hr3\text{-}kan\text{-}hr4}$ or CpBAC viruses after 7 days. Nr = Number of tested larvae. The LC_{50} of probit analysis and the slopes of the probit lines are given. Cl, 95% confidence interval; SE, standard error. LC_{50} value and confidence limits are given in OBs/ml. All Wald χ^2 tests (DF=1) were significant at P <0.0001. Different superscript letters indicate statistical differences between LC values (P <0.05) according to Robertson and Preisler (1992).

Virus	**Nr. larvae**	**LC_{50} (Cl)**	**Slope (SE)**	**χ^2**
CpBAC$^{hr3/h4KO}$	828	5044^a (2901 – 8938)	1.34 (0.16)	69.82
CpBAC$^{hr3\text{-}kan\text{-}hr4}$	850	2837^a (1819 – 4429)	1.33 (0.13)	102.95
CpBAC	804	2439^a (1299 – 4588)	1.30 (0.17)	56.94

Table 10. Kaplan-Meier estimation of ST_{50} for CM larvae infected with OBs derived from CpBAC$^{hr3/hr4KO}$, CpBAC$^{hr3\text{-}kan\text{-}hr4}$ or CpBAC viruses.

Virus	**Nr. tested larvae**	**LC_{80} (OB/ml)**	**ST_{50}**	**Cl (lower-upper)**
CpBAC$^{hr3/hr4KO}$	103	2.13×10^4	150	150-158
CpBAC$^{hr3\text{-}kan\text{-}hr4}$	105	1.21×10^4	142	142-150
CpBAC	105	1.07×10^4	150	150-158

ST_{50} and 95% confidence interval (CI) are given in hpi.

The ST_{50} was determined by inoculating 35 individually held larvae in three replicates with the calculated LC_{80} for each tested virus. Mortality of the larvae was monitored daily and every 8 hours starting at day 5 post infection until day 12 or larval death. The ST_{50} was calculated using the Kaplan-Meier survival time estimator analysis (Table 10). The calculated ST_{50} values were 150 h for CpBAC$^{hr3/hr4KO}$, 142 h for CpBAC$^{hr3\text{-}kan\text{-}hr4}$ and 150 h for CpBAC. As shown in Fig. 26, the observed survival plots for the mutant viruses were closed to each other as well as the parental CpBAC. No significant difference was observed between the mutant viruses, which had more or less the same speed of kill as the parental CpBAC. During the bioassays, no differences were observed in the disease symptoms of the CM larvae infected either with CpBAC$^{hr3/hr4KO}$, CpBAC$^{hr3\text{-}kan\text{-}hr4}$ or CpBAC. These observations indicated that the deletion of hr3/hr4 or separation of hr3/hr4 by insertion of Kan^{R} did not significantly affect their biological fitness compared to CpBAC based on LC_{50} and ST_{50} values.

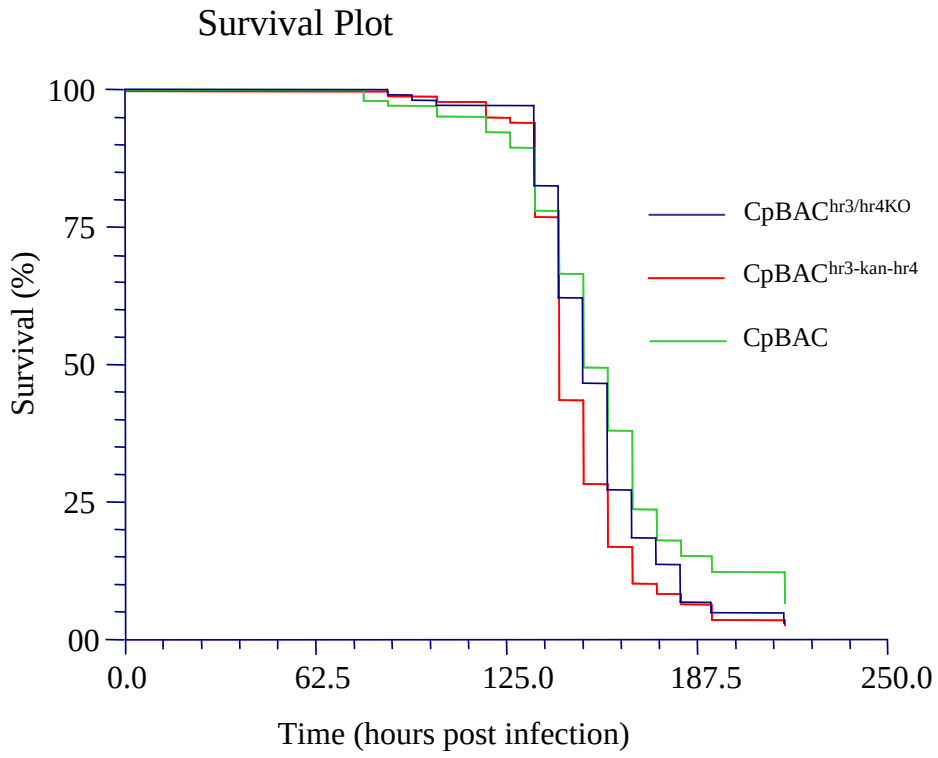

Fig. 26. Survival plots using NCSS statistical analysis software Kaplan-Meier curves (NCSS statistical analysis software for windows) showing the survival time analysis of CpBAC$^{hr3/h4KO}$, CpBAC$^{hr3\text{-}kan\text{-}hr4}$ and CpBAC as observed on infected CM larvae.

4.4. Co-infection of CM larvae using CpBAC and CpBAC$^{hr3\text{-}kan\text{-}hr4}$

The CpBAC$^{hr3\text{-}kan\text{-}hr4}$ bacmid carrying Kan^{R} was generated as a mimic construction for the mutant virus MCp5 carrying TCl4.7 transposon at the same integration region between hr3 and hr4. In order to compare the propagation efficacy of the mutant virus CpBAC$^{hr3\text{-}kan\text{-}hr4}$ in the presence of the parental CpBAC and to investigate whether CpBAC had a selection advantage over CpBAC$^{hr3\text{-}kan\text{-}hr4}$, co-infection experiments using both viruses were carried out on CM larvae (L4). A potential selection advantage of one of the genotypes was investigated by comparing the virus ratio in the inoculum in the co-infection experiment with the virus ratio in the offspring. In order to determine the viruses' genotype ratios, the relative amounts of CpBAC and the mutant CpBAC$^{hr3\text{-}kan\text{-}hr4}$ in the virus offspring were quantified by comparing the intensity of the pure genotype *Bam*HI specific restriction fragments with the intensity of the specific restriction fragments in the shared genotypes in a co-infection experiment.

In the co-infection experiments, the CM larvae (L4) were orally inoculated using different ratios of CpBAC to CpBAC$^{hr3\text{-}kan\text{-}hr4}$ virus OBs in order to exclude possible dose effects on the infection progress. Five different virus ratios of CpBAC:CpBAC$^{hr3\text{-}kan\text{-}hr4}$ were applied to inoculate single CM larvae (1000 OB/Larve) in five replicates. After larval death, virus OBs were isolated from single larvae and applied for DNA extraction, DNA electrophoresis on agaros gels stained with ethidium bromide and subsequently photographed under UV light. *Bam*HI restriction digests of pure virus genotype resulted in a 6.8 kb specific fragment for CpBAC and 7.7 kb specific fragment for CpBAC$^{hr3\text{-}kan\text{-}hr4}$ (Fig. 25B). Using the Imagemaster ID software (Pharmacia Biotech), the volumes (the amounts of pixels) of the bands representing the *Bam*HI genotype specific fragments were quantified. The genotype ratios in the virus offspring (shared genotypes) of the co-infection experiment were determined by quantifying the diagnostic *Bam*HI REN fragments. For pure genotype, the molarity of each REN fragment is equal. Therefore the amount of DNA per individual band is directly proportional to the fragment size. Thus, regression of molar bands can lead for determination of molar ratios of sub-molar bands in the shared genotype restriction fragments and thus determination of the genotype ratios in the virus offspring. Molar proportions of the genotypes were determined for each infection ratio of CpBAC: CpBAC$^{hr3\text{-}kan\text{-}hr4}$ used in the co-infection experiments by densitometry quantification of genotype-specific restriction fragments in the virus offspring.

An example how the CpBAC:CpBAC$^{hr3\text{-}kan\text{-}hr4}$ virus ratio in the offspring of a CpBAC: CpBAC$^{hr3\text{-}kan\text{-}hr4}$ virus ratio inoculum of 33:67 (%) in a co-infection experiment was determined, is shown in Fig. 27. All single bands (bands 1, 6, 7, 8, 9, 10 and 12) represented one-molar fragments (M=1), double bands (bands: 3 = *Bam*HI-E/F and 11 = *Bam*HI-M/N) represented two-molar fragments (M=2) and triple bands (band 2 = *Bam*HI-B/C/D) represented triple-molar fragment (M=3). The pixel volumes of the double and triple bands were divided by 2 and 3, respectively, in order to obtain the fragment specific pixel volume equal to one-molar fragment.

For all fragments the following relation between volume (V), fragment size (L), and a constant factor (C) is expected: V = L x M x C (Arends, 2003). By using this formula, the molar ratio of the genotype specific and genotype shared restriction fragment in a virus mixture can be determined. The digest contains only two bands that were diagnostic to CpBAC$^{hr3\text{-}kan\text{-}hr4}$ (band 4 = *Bam*HI-G1) and CpBAC (band 5 = *Bam*HI-G2) (Fig. 27A-C). The other fragments where present in equal molar concentration (Fig. 27C). Linear regression analysis of CpBAC:CpBAC$^{hr3\text{-}kan\text{-}hr4}$ virus offspring for the genotype shared *Bam*HI restriction fragments (bands/peaks 2, 3, 6-12) within a size range of 2-16 kb demonstrated a strong correlation (R^2=0.99) between fragment size and volume density (Pixel) (Fig. 27B). Since the CpBAC genotype specific fragments (6.8 kb) and CpBAC$^{hr3\text{-}kan\text{-}hr4}$ genotype specific fragment (7.7 kb) to be quantified were in this size range of the regression line, their molar ratio was determined as follow: By using the regression formula V = 4938L – 4649, the calculated volume was 28929 pixels for CpBAC specific fragment (6.8 kb) and 33374 pixels for CpBAC$^{hr3\text{-}kan\text{-}hr4}$ specific fragment (7.7 kb). Since the obtained virus offspring was a mixture of both genotypes, the molar proportion of CpBAC and CpBAC$^{hr3\text{-}kan\text{-}hr4}$ in the virus offspring was determined by dividing the actual measured volume by the calculated volume. In this example, the CpBAC genotype proportion makes up 0.83 (23985/28929) and the CpBAC$^{hr3\text{-}kan\text{-}hr4}$ genotype proportion makes up 0.40 (13454/33374) of the virus offspring. Since the virus offspring only consists of CpBAC and CpBAC$^{hr3\text{-}kan\text{-}hr4}$ genotypes, the sum of the quantified ratios of CpBAC and CpBAC$^{hr3\text{-}kan\text{-}hr4}$ should theoretically be 1.0. Although, with 1.23 (0.83 + 0.40) the total amount of actually quantified virus was slightly higher, it was shown that the quantification method was fairly accurate. More over, in order to calculate the molar proportion of each genotype in the virus offspring with more accuracy way, the calculated ratios were nominated to 1.0 by dividing the specific ratios by the total amount.

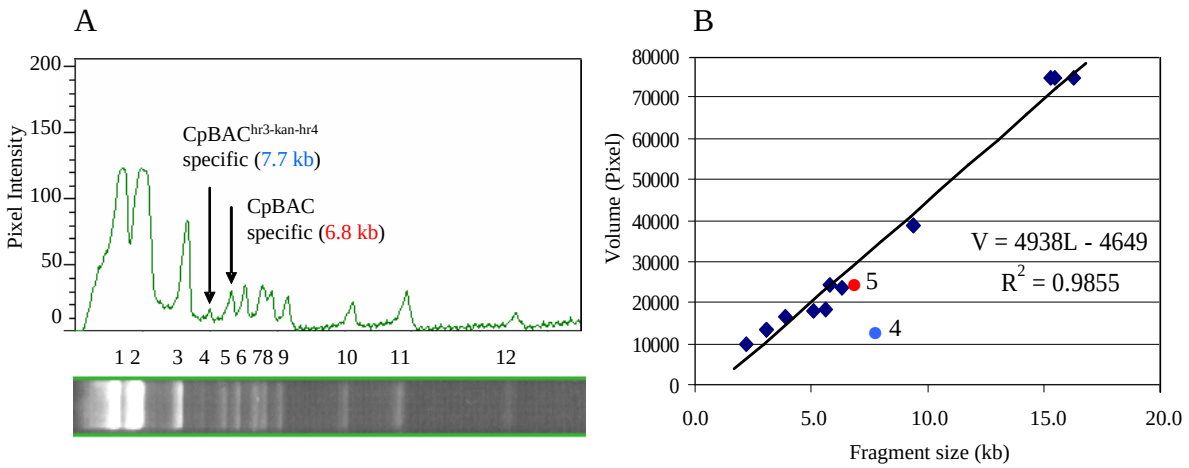

(C)

Peak	*Bam*HI Fragment	Fragment size (kb)	Volume (Pixel)
1	A	24.5	186746
2	B + C+ D	16.3 + 15.5 + 15.3	224116 (74705)
3	E + F	9.4 + 9.4	77200 (38600)
4	G1	7.7	13454
5	G2	6.8	23985
6	H	6.3	23638
7	I	5.8	24321
8	J	5.6	18408
9	K	5.1	17993
10	L	3.9	16423
11	M + N	3.1 + 3.1	26489 (13245)
12	O	2.2	9711

Fig. 27. Quantification of CpBAC:CpBAC$^{hr3\text{-}kan\text{-}hr4}$ ratio in the virus offspring of a co-infection experiment using an inoculum ratio of 33:67 (%) CpBAC:CpBAC$^{hr3\text{-}kan\text{-}hr4}$, respectively. **(A)** Determination of the pixel volumes of the *Bam*HI fragments on an ethidium bromide stained agarose gel using the Imagemaster 1D software. Arrows show the detected genotype specific bands 4 (7.7 kb) and 5 (6.8 kb) specific for CpBAC$^{hr3\text{-}kan\text{-}hr4}$ and CpBAC, respectively. **(B)** Linear regression analysis of the measured volume pixels of the CpBAC and CpBAC$^{hr3\text{-}kan\text{-}hr4}$ genotype shared *Bam*HI restriction fragments. The formula of the regression line and the regression quotient (R^2) are plotted in the graph. The numbered dots represent CpBAC$^{hr3\text{-}kan\text{-}hr4}$ (4) and CpBAC (5) genotype *Bam*HI specific restriction fragments. **(C)** *Bam*HI restriction profile of the isolated virus offspring DNA. The table shows the measured peaks (bands), *Bam*HI shared fragments (A-O) and their corresponding sizes (kb). The numbers in brackets represent the volume (Pixel) of the single restriction fragments making up the double or triple bands.

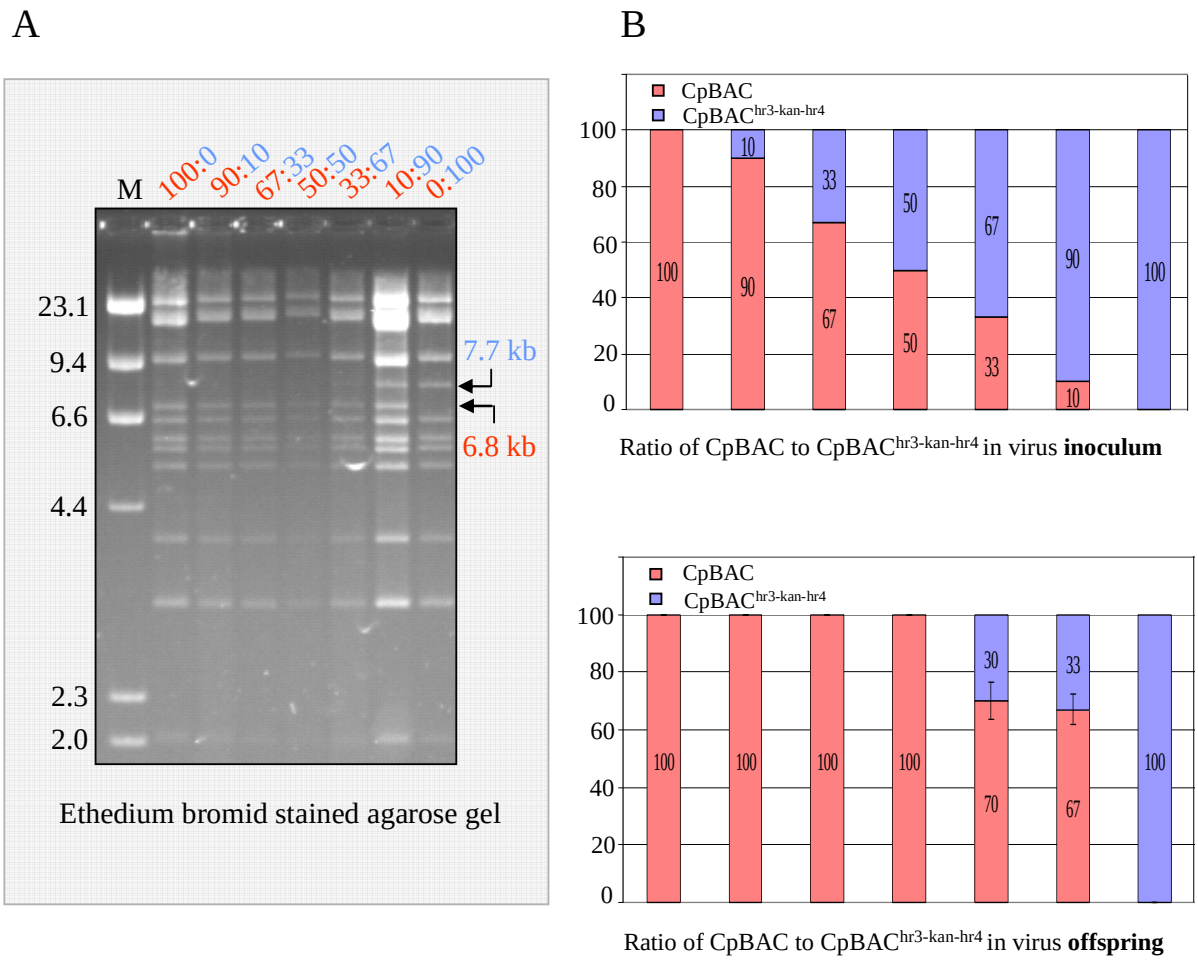

Fig. 28. Co-infection experiments between CpBAC and the mutant CpBAC$^{hr3\text{-}kan\text{-}hr4}$. **(A)** *Bam*HI restriction profile of CpBAC:CpBAC$^{hr3\text{-}kan\text{-}hr4}$ shared DNA of virus offspring using different ratios of CpBAC:CpBAC$^{hr3\text{-}kan\text{-}hr4}$ virus inoculums. The numbers above the gel represent the percentage of CpBAC (red) to CpBAC$^{hr3\text{-}kan\text{-}hr4}$ (blue) in the inoculums. Arrows indicate the 6.8 kb and 7.7 kb specific fragments for CpBAC and CpBAC$^{hr3\text{-}kan\text{-}hr4}$ on the right, respectively. M: Lambda *Hin*dIII standard marker. **(B)** The bar graphs show the ratios of CpBAC: CpBAC$^{hr3\text{-}kan\text{-}hr4}$ that applied in the virus inoculums and the obtained ratios of each genotype in virus offspring. The bars indicate the standard deviation. Each experiment was 5 times repeated.

In this example, the final calculated ratio for each genotype would be 0.67 (0.83/1.23) and 0.33 (0.40/1.23) for CpBAC and CpBAC$^{hr3\text{-}kan\text{-}hr4}$, respectively. And thus, the final sum ration of CpBAC and CpBAC$^{hr3\text{-}kan\text{-}hr4}$ in this example would be 0.67 + 0.33 = 1.0.

For each co-infection, the CpBAC:CpBAC$^{hr3\text{-}kan\text{-}hr4}$ ratio in the virus offspring was determined as described above. As shown in Fig. 28A, the absence of the CpBAC$^{hr3\text{-}kan\text{-}hr4}$ (7.7 kb) specific *Bam*HI-G1 fragment in the virus offspring could be observed with increasing CpBAC percentage in the virus inoculum. In all experiments, a lower CpBAC$^{hr3\text{-}kan\text{-}hr4}$

proportion was found in virus offspring than was introduced as inoculum (Fig. 28B). For example, by using an infection ratio of 90% CpBAC$^{hr3\text{-}kan\text{-}hr4}$ and 10% CpBAC, only 33% of the virus offspring was CpBAC$^{hr3\text{-}kan\text{-}hr4}$ but 67% was CpBAC. This shift towards CpBAC continued with increasing proportions of CpBAC in the inoculum. In all other co-infections experiment, where the proportions of CpBAC$^{hr3\text{-}kan\text{-}hr4}$ were 50% or less, no CpBAC$^{hr3\text{-}kan\text{-}hr4}$ was detected in the virus offspring. Only infections using 100% of either CpBAC or CpBAC$^{hr3\text{-}kan\text{-}hr4}$ genotype resulted in a pure corresponding virus offspring (Fig. 28). These results showed that the parental CpGV-M bacmid (CpBAC) virus has a selection advantage over the mutant CpBAC$^{hr3\text{-}kan\text{-}hr4}$ in all co-infection experiments that were applied using different ratios of both viruses. The mimic constructed CpBAC$^{hr3\text{-}kan\text{-}hr4}$ virus to the MCp5 (mutant virus carrying TCl4.7 transposon) showed a similar replication disadvantage in the presence of CpBAC as previous competition experiment between CpGV-M and MCp5 had demonstrated (Arends et al., 2005).

V. DISCUSSION

In this study, the influence of transposon TCl4.7 insertion on the function of the genome of *Cydia pomonella* granulovirus CpGV-M (Mexican) was studied in detail. The TCl4.7 transposon was found in the spontaneous mutant CpGV-MCp5 and is stably integrated into the genome of CpGV-M (Jehle et al., 1995). The TCl4.7 transposon is located between ORFs Cp15 and Cp16 and separates two palindrome sequences hr3 and hr4, which have been recently identified to be CpGV-M origins of replication (ori) (Hilton and Winstanley, 2007). As shown by Arends et al. (2005), MCp5 had very similar biological parameters (LC_{50}, ST_{50}, OB production) as the parental CpGV-M. However, in mixed infection experiments performed with both viruses, MCp5 was efficiently outcompeted by CpGV-M. Therefore this thesis focused on two aims,

(1) Functional studies of the adjacent Cp15 and Cp16 ORFs.

(2) Functional studies of the adjacent hr3 and hr4 palindromes.

A prerequiste for this study was the generation of a bacmid construct of CpGV-M that can replicate in *E. coli* as a plasmid and can infect CM larvae in order to allow easy manipulation of the CpGV-M genome, such as the knockout of Cp15, Cp16 and hr3/hr4 and thus determining their role in the context of CpGV-M life-cycle. For this, the CpGV-M bacmid (CpBAC) was constructed by direct cloning of the CpGV-M genomic DNA that was linearized at a unique non protein coding *Pac*I locus (nt 101956) into the cloned *Pac*I locus of the recombinant plasmid pCC1-hr5-ie1-GFP harboring the backbone of the Copy Control pCC1BAC vector. The enhanced green florescent protein (*egfp*) was introduced also in the bacmid construct as a marker gene in order to monitor the infection spreading of the bacmid in CM larvae. After verifying the correct construction of CpBAC by *Pac*I and *Bam*HI restriction analysis, CpBAC DNA was subjected for injection into CM larval (L4) hemocoel in order to investigate its infectivity. The productive infection of injected larvae showed that CpBAC was able to infect CM larvae and to produce virus OB. This suggested that the generated CpBAC is biologically active against CM larvae. It was noticed, however that infected CM larvae did not show EGFP expression as it would have been expected from the CpBAC construct. The lack of EGFP expression was most likely due to a point mutation located in ATG start codon of *egfp* ORF as was observed by nucleotide sequencing of *egfp* ORF. Thus, GFP florescence could not be used as a marker to monitor the infection spreading of the CpBAC virus. Therefore, virus infection symptoms and OB production were used to investigate the CpBAC virus infectivity. By performing per oral infection of CM larvae using

the obtained CpBAC OBs, all larvae orally inoculated with CpBAC OBs died from virus infection suggesting that the produced CpBAC OBs were also orally infective. The LC_{50} values of CpBAC (1698 OB/ml) and the parental virus CpGV-M (1740 OB/ml) did not significantly differ, indicating that the CpBAC has similar infectivity to CM as CpGV-M. Thus, the generation of a viable CpGV-M bacmid construct (CpBAC) was succeeded and could be used for gene manipulation of the CpGV-M genome in *E. coli*.

Recently, bacmid technology has been extensively used for genetic studies of NPVs in cell culture. It permits rapid mutagenesis, modification, and analysis of many genes and proteins that were previously intractable. The bacterial artificial chromosomes (BACs) from baculovirus have been widely used since the first AcMNPV bacmid (a baculovirus shuttle vector) was constructed (Luckow et al., 1993). They can not only simplify the construction of recombinant baculoviruses for heterologous gene expression, but can autonomously replicate in *E. coli*, and thus can be handled easily (Yan-Hong et al., 2007). Expansion of this system to other baculoviruses is severely restricted by the limited number of permissive cell lines (Hajos et al., 1998). This constraint not only limited the exploration for other potent baculoviruses as expression vectors, but it also hampered genetic studies of GVs for which no cell line is available (Obregon-Barboza et al., 2007). Only a very limited number of insect cell lines permissive for baculovirus exist, the majority has serious drawbacks. For example, the replication of SeMNPV in cultured cells results in the rapid generation of deletion mutants (Heldens et al., 1996). In the case of CpGV the replication in cultures cells is slow and not very efficient (Winstanley and Crook, 1993).

Recently, Hilton et al. (2008) succeeded to construct a CpGV bacmid by transfecting a *C. pomonella* cell line to generate viable viruses from the bacmid DNA that was constructed in a similar way using the unique *Pac*I site in the CpGV genome for introducing the 8.6 kb BAC cassette originated from Bac-to-Bac Baculovirus Expression System (Invitrogen). In this study, the CpBAC virus was generated by transfecting CM larvae with a CpBAC/lipofectin complex through injection into larval hemocoel and subsequently isolation of virus OBs. This method is an alternative strategy for baculoviruses to generate bacmid based pseudovirus, when no cell line is available. The produced CpBAC was stably maintained as single-copy bacterial artificial chromosome in *E. coli* and was used as a starting material to knockout Cp15, Cp16 and hr3/hr4.

1. Analysis of CpGV Cp15

The role of Cp15 in the context of CpGV-M infection cycle was investigated by studing Cp15 transcription and expression and by the generation of a Cp15 knockout bacmid. Using bacmid technology and the Red/ET-Recombination system the ORF Cp15 was deleted from the CpBAC resulting in the mutant bacmid CpBAC^{Cp15KO} (Luckow et al., 1993; Stewart et al., 1998). By using the Red/ET-Recombination system, also referred to as λ-mediated recombination, target DNA molecules are precisely altered by homologous recombination in *E. coli* in the presence of pRed/ET expression plasmid.

For the deletion of Cp15 from CpBAC DNA, a PCR product of the Kan^R gene was generated using two long arms oligonucleotides carrying in their ends a homologous region of the Cp15 flanking sequences. The Kan^R gene was used to replace the Cp15 ORF in CpBAC through lambda Red/ET mediated recombination. After verification of the CpBAC^{Cp15KO} construct using PCR and REN, it was transfected into CM larvae hemocoel in order to investigate its infectivity. The CpBAC^{Cp15KO} virus was not able to propagate in CM larvae (L4) after injection into larval hemocoel suggesting that the Cp15 was required to continue the virus infection cycle.

In order to demonstrate unequivocally that indeed Cp15 knockout was the only reason for the replication failure of CpBAC^{Cp15KO}, the same methodology using Red/ET recombination was applied to rescue the CpBAC^{Cp15KO} infectivity by restoration of Cp15. The Cp15 gene under control of its own putative promoter region (nt 10382-11914) was cloned into pUC19 vector fused with the Amp^R gene as a selectable marker. The generated Cp15-Amp^R PCR fragment (3147 bp) flanked by *egfp* homology regions was used in order to replace the inactive *egfp* cassette in CpBAC^{Cp15KO}. The restoration of Cp15 in CpBAC^{Cp15KO} using Red/ET-recombination did not succeed, although the Cp15-Amp^R PCR product was generated with the predicted size. A possible reason preventing the homologous recombination to occur is a low purity of the long arms oligonucleotides, which were used to generate the Cp15-Amp^R PCR product, and/or presence of a wrong nucleotide in one of the homologous regions, which hindered the recombination. A different strategy to rescue the mutant CpBAC^{Cp15KO} infectivity as well as other knockout CpBAC mutants could be achived based on the utilization of a Tn7 attachment site, which is used in the Bac-to-Bac system (Luckow et al., 1993). Introducing of mini-*att*Tn7 site in the CpBAC construct would facilitate the site specific transposition recombination, by applying the commercial Bac-to-

Bac system. Moreover, a fusion construct consisting of the Cp15 fused with the green florescent protein (*gfp*) might be useful for rescue of the CpBAC^{Cp15KO} infectivity in order to monitor the infection spreading of the rescued virus in CM larvae. With a combination of these strategies, the generation of rescued CpBAC^{Cp15KO} would be more straight forward. Until the restoration of Cp15 in CpBAC^{Cp15KO} construct is not achieved, it can not unequivocally concluded that Cp15 is an essential gene, although this is rather likely (see below the discussion of ac142).

In order to investigate the potential influence of TCl4.7 transposon insertion in MCp5, the Cp15 gene transcription was compared in MCp5 and wt CpGV-M. Temporal transcriptional analyses of cDNAs of Cp15 transcripts were performed using RT-PCR and quantified by qRT-PCR in a time course experiment. Since the midgut epithelial cells are the first tissue to be infected by the CpGV ODV, a synchronous infection of this tissue was expected to be more likely than in any other tissue. The total RNA was isolated from pooled midguts and cDNAs were synthesized and subsequently used as a template for Cp15 RT-PCR analysis. The results showed that Cp15 transcripts were first detected at 12 hpi until 96 hpi in larvae infected with CpGV-M. In MCp5 infected larvae, Cp15 transcripts detected at 6 hpi and remained until 96 hpi with a very low of RT-PCR product intensity. These observations suggested that Cp15 may transcribe at the early and late phases of viral infection. This is consistent with the presence of an early promoter motif (ATCATTT) and late promoter motif (GTAAG) which are located within 120 nt upstream from the first ATG start codon. The RT-PCR also showed a strong band at 6 hpi in MCp5 infected CM larvae. Since this band was not observed in CpGV-M infected CM larvae at the same time point, this observation may be attributed to a possible presence of virus genomic DNA residues in this sample. Hence, RT-PCR results suggested a reduction of Cp15 gene transcription in MCp5 infected midguts compared to CpGV-M.

The qRT-PCR showed a steady increase in the transcription amount of Cp15 by the time going from 6 to 96 hpi in CpGV-M samples resulted in 4.5 fold increase at 48 hpi up to 10.2 x 10^3 fold at 96 hpi. In contrast, the Cp15 transcription revealed 2.8 fold increases at 48 hpi and only 2 fold at 96 hpi in MCp5. The qRT-PCR analyses were in agreement with the RT-PCR results which showed a clear reduction of RT-PCR products of Cp15 cDNAs. An increase of cDNA of 6 hpi of MCp5 infected miguts could not be verified by qRT-PCR. Taken together, the qRT-PCR analysis confirmed that the Cp15 gene transcription in MCp5 was altered or reduced compared to CpGV-M over the time course.

In order to investigate whether the observed difference in MCp5 had any effect on the temporal protein expression of Cp15, Western blotting detection of Cp15 was performed on infected larvae either with MCp5 or CpGV-M viruses in a time course infection. A group of 5 larval midguts or fat bodies were applied to total protein extraction and SDS-PAGE followed by Western blot analysis using polyclonal antibody (pAB) that were generated against Cp15 protein expressed in *E. coli*. Neither extracts of MCp5 nor CpGV-M infected larvae midgut samples showed immuno-reactive protein response when using its specific antiserum against Cp15. In order to exclude the possibility that midgut samples may have had a low amount of Cp15 protein, samples of larval fat bodies which were expected to have a higher concentration of viral proteins were sampled and subjected for Western blot analysis. Furthermore, the antiserum produced against Cp15 protein was specifically concentrated by producing the mono-specific anti-Cp15 pAB against the bacterial expressed protein of Cp15. Similar to the results observed with the midguts, the Cp15-monospecific pAB did not detect any specific immune response to a predicted 53-kDa protein (Cp15) when protein extracts from fat bodies of CpGV-M and MCp5 infected larvae were used. Only a protein with a molecular mass of ~29 kDa was detected at 48 hpi until 120 hpi in infected CM larvae either with MCp5 or CpGV-M. Since the same 29 kDa protein band was detected using extracts of a purified CpGV-M OB, and since the granulin is overexpressed at these time points, a non-specific binding of the Cp15 mono-specific pAB to the granulin protein is the most plausible explanation for this observation. These results suggested that the Cp15 temporal protein expression in CM larvae infected either with CpGV-M or MCp5 was probably too low to exceed the detection level of the generated antibody and/or the affinity of the antiserum to the Cp15 protein was too low. Hence, the Western blot analysis did not clearly elucidate whether the Cp15 temporal protein expression of MCp5 was different to that of CpGV-M and could not corroborate the results obtained by Cp15 transcription analysis. However, as suggested by the deletion of Cp15 from CpBAC, the Cp15 gene was required for virus infection cycle.

The CpGV-M Cp15 (*p49*) gene is one of the 30 core genes found in all sequenced baculovirus genomes suggesting that they perform key functions in the baculovirus life cycle (Herniou et al., 2003; van Oers and Vlak, 2007). Within the family *Baculoviridae*, the Cp15 ORF is highly conserved among GVs with overall amino acids identities of 60 to 74% (Table 11). However, the conservation of Cp15 ORF within NPVs group I and II is moderate with 31 to 35% overall identity (Table 11). Recently, AcMNPV ac142, a homologue of Cp15, was functionally studied (McCarthy et al., 2008). Ac142 encodes a protein previously shown to be associated with AcMNPV ODV. A similar observation to the results presented here was

detected by the deletion of ac142 from the AcMNPV bacmid generating an ac142 knockout virus; the mutant virus was not able to produce budded virus (BV) and to produce viable offspring virus. These results revealed that ac142 is essential for BV and ODV production. Comparison of the initiation and levels of viral DNA replication via quantitative real-time PCR between the ac142 knockout bacmid and the wt AcMNPV bacmid transfected cells, showed that the onset and level of genome replication in individual infected cells were unaffected by deletion of ac142. Western blot analysis of ac142 in purified BV and ODV and fractionated BV indicated that ac142 is a structural component of nucleocapsids of both BV and ODV, and the deletion of ac142 also results in the dramatic effect of producing occlusion bodies that were completely devoid of ODV. This was in agreement with previous proteomic analysis which identified ac142 or its homologues as a component of ODVs of AcMNPV, HearSNPV, and CuniNPV (Braunagel et al., 2003; Deng et al., 2007; Perera et al., 2007).

Similar results were demonstrated by Vanarsdall et al. (2007) who reported that the ac142 deletion exhibited a single cell phenotype and did not produce any BV. However, unlike the results of McCarthy et al. (2008), Vanarsdall et al. (2007) did not detect mature nucleocapsids but instead found aberrant looking empty capsid structures and concluded that ac142 is required for normal nucleocapsid production. In addition, McCarthy and Theilmann (2008), showed that the entire ac143 promoter, which includes three late promoter motifs, is located within the ORF ac142. They reported that ac143 was an unrecognized core gene and that it is an essential gene for mediating BV production. Different deletion mutants of this region showed that the integrity of the ac142-ac143 core gene cluster was required for the bacmids to display wild-type patterns of viral replication, BV production and RNA transcription. And thus it was not clear whether the phenotype resulting from the deletion of ac142 is due to the lack of ac142 as a structural protein or because of the disruption of the ac143 promoter region, which is located within ac142 ORF.

Here, the generation of pseudovirus with a deletion of Cp15 ORF revealed that it was required in the context of CpGV infection cycle. In order to elucidate whether the deletion of Cp15 ORF may influenced virus DNA replication or only the production of viable OB as a possibly structure protein, further studies on Cp15 will be required possibly by the virus genomic DNA replication quantification of the mutant CpBAC^{Cp15KO} compared to the parental CpBAC using qPCR.

2. Analysis of CpGV Cp16

The second ORF located adjacent to the TCl4.7 insertion site is Cp16. The RT-PCR analysis of Cp16 revealed that transcription of Cp16 started at 12 hpi and remained until 96 hpi in CpGV-M infected larvae. In MCp5, Cp16 cDNAs were detected at 6 hpi and remained until 48 hpi at low concentration. Then they disappeared below the PCR detection level after this time point. The detection of Cp16 transcripts at early phase of infection (12 hpi) in CM larvae infected with CpGV-M suggests that it is possibly an early gene since a consensus TATA box and a consensus early gene motif CAGT located within 120 nt upstream from the first ATG start codon (Luque et al., 2001). However Cp16 cDNAs were also observed at late stage of virus infection (96 hpi), though no putative late promoter motive was identified within 120 nt upstream of the first ATG start codon. The quantification of Cp16 transcripts showed a steady increase in Cp16 transcripts by the time going from 12 to 96 hpi in CpGV-M samples resulted in 6.25 fold increase at 48 hpi up to 12.1 x 10^3 fold at 96 hpi. In contrast, no increase of Cp16 transcription could be detected in MCp5 during 96 hpi. Thus, Cp16 gene transcription in MCp5 was altered or dramatically reduced compared to CpGV-M.

The Western blotting analysis of Cp16 proteins could not detect any immuno-reactive response with midgut or fat body protein extracts of MCp5 or CpGV-M infected larvae using mono-specific anti-Cp16 pAB. Cp16 temporal protein expression in CM larvae infected either with CpGV-M or MCp5 was probably too low to exceed the detection level of the generated antibody and/or the affinity of the antiserum to the Cp16 protein was not specific enough. Similar to results obtained for Cp15, the Western blot analysis did not elucidate whether the Cp16 temporal protein expression in MCp5 is different from that in CpGV-M. Cp16 temporal protein expression analysis using more specific antibodies e.g. monoclonal antibodies are required in order to investigate whether the insertion of TCl4.7 transposon had influenced the Cp16 temporal protein expression in MCp5 compared to the CpGV-M. This may confirm the gene transcription alteration that was observed by the RT-PCR and qRT-PCR analysis, and can give a more insight in the possible influence of TCl4.7 transposon on gene transcription and translation in the mutant MCp5.

The role of Cp16 in CpGV-M life cycle was further investigated by deletion of Cp16 ORF from the generated CpGV-M bacmid (CpBAC) as described before. In contrast to the Cp15 knock-out, the $CpBAC^{Cp16KO}$ lacking Cp16 caused larval virus infection and released infective OB after injection of $CpBAC^{Cp16KO}$ DNA into CM larval hemocoel. The isolated

OBs of CpBAC^{Cp16KO} were orally infective to CM larvae. So it can be concluded that Cp16 is not a required gene for virus *in vivo* infection of CpGV. The median lethal concentration (LC_{50}) was determined for CpBAC^{Cp16KO} in CM larvae in order to investigate whether the deletion of Cp16 from CpBAC had an influence on the virulence against neonates CM larvae. No significant difference was observed between the LC_{50} for CpBAC^{Cp16KO} (1151 OB/ml) and the CpGV-M (1297 OB/ml) demonstrating that the Cp16 is not an essential gene for larval *in vivo* infection. Apparently, the deletion of Cp16 from CpBAC did not affect virus replication cycle or virus efficacy against CM larvae.

Compared to other baculoviruses, the Cp16 ORF is moderately conserved among a number of GVs with amino acids identities of 30 to 67% (Table 11). However, the conservation of Cp16 ORF within NPVs group I and II is only 13 to 36% overall identity (Table 11). Previously, it was demonstrated that Cp16 is homologous to the N-terminal part of *Orgyia pseudotsugata* MNPV (OpMNPV) (Op31), LdMNPV (Ld138) and SeMNPV (Se54). Op31 appears to be a fusion of two ORFs, as it has an N-terminus of unknown function and a C-terminus encoding dUTPase (Fig. 29). DUTPase is involved in nucleotide metabolism and may facilitate virus replication in non-dividing cells, in which dNTP pathways are inactive. Previous analysis of dUTPase genes in baculoviruses has shown that dUTPase has been gained several times during baculovirus evolution (Herniou et al., 2003). However, no dUTPase homologue is present in CpGV (Luque et al., 2001). van Oers et al. (2005) demonstrated the presence of a Cp16 homologue in *Chrysodeixis chalcites* NPV (ChchNPV) in a full complement of genes potentially involved in preventing DNA mutations. These include in ChchNPV, Chch106 (Cp16, Ld138), Chch151 (rr1) and Chch122 (rr2), respectively.

Preventing of virus DNA mutations through the homologous Ld138, Chch106 and Op31 suggest that this gene might play an important role in the protection of CpGV virus genome with a predicted role in UV-damage repair. The knockout of Cp16 indicated that the Cp16 gene is not an essential gene for CpGV virus infection cycle as it is typical for many auxiliary baculoviruses genes. These genes may be important for specific environmental conditions or in certain tissues only.

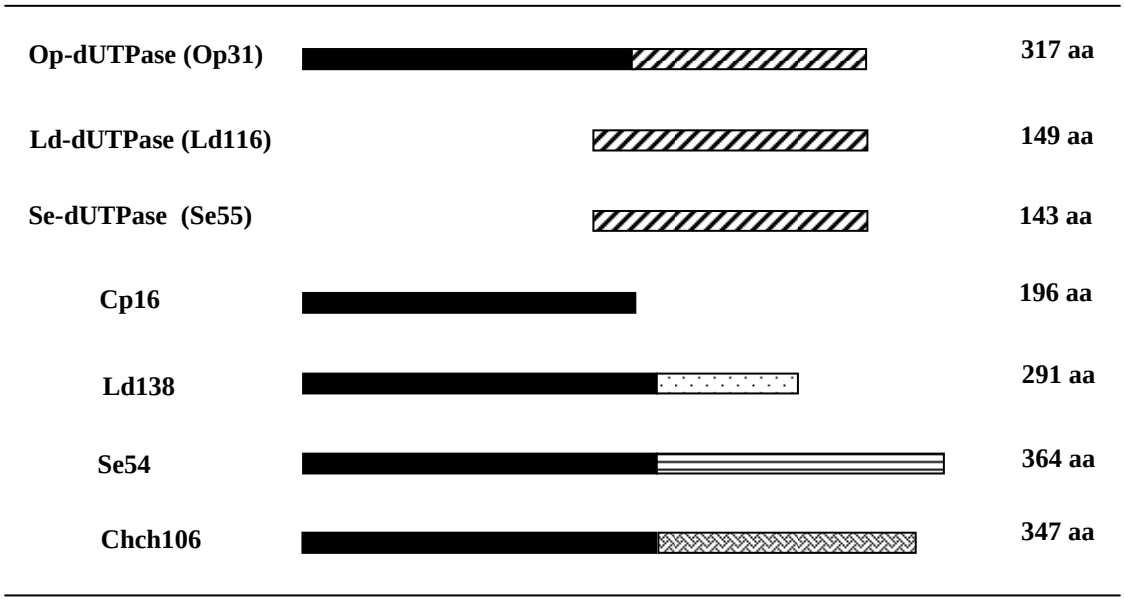

Fig. 29. Relationships of *dutpase* genes and associated ORFs from several baculoviruses. The solid black box indicates the 5´ region of Op31 and ist homologous ORFs. The diagonally striped box represents *dutpase*. The 3´ portion of Ld138 (not related to other ORFs) is denoted by the stippled box. Comparisons were based on gap analysis. The length of each ORF is indicated on the right-hand side (modified from Luque et al., 2001).

Transcription analysis of Cp31 (F protein)

The observation of a reduced transcriptional activity of Cp15 and Cp16 in the midgut of MCp5 infected larvae left the question whether this was a direct effect of transposon TCl4.7 insertion or whether there was a general delay/reduction of MCp5 gene transcription. In order to get an answer to this question, temporal transcription of a gene not adjacent to Cp15 and Cp16 and which was known to be essential for virus replication was studied. Hence, for this control experiment, Cp31 encoding the F protein was chosen. By the transcription analysis of F protein in a time course infection it was shown that F protein transcription initiation was started at 24 hpi in CpGV-M CM infected larvae and accumulated until 96 hpi. In contrast, a low transcription level of F protein was detected in MCp5 infected CM larvae only from 6 to 24 hpi. These observations suggested also a delay or reduction of F protein transcription in MCp5. This corresponded to qRT-PCR of F protein transcription, which was only slightly increased in MCp5. Whereas with CpGV-M an increase of F protein transcription up to 24.7 x 10^3 at 96 hpi was observed, similar to the results of Cp15 and Cp16. Thus, the delay and reduction of gene transcription in midguts was not only restricted to Cp15 and Cp16 but also for F protein gene and most likely to other genes of MCp5, suggesting an overall reduction/delay of gene transcription of MCp5 midgut infection.

The F protein is the major envelope fusion protein of group II NPVs and GVs and it is thus a functional analogue of gp64, the fusion protein of group I NPVs, such as AcMNPV (Monsma and Blissard, 1995; Oomens and Blissard, 1999). This protein is involved in BVs attachment to host cells and is required for efficient budding from the cell surface (Hefferon et al., 1999). Complete sequencing of CpGV did not identify a putative early or late promoter within 120 nt upstream of the first ATG start codon of F protein (Luque et al., 2001). In other NPVs it is transcribed from early and late promoter as in NPVs group II e.g. ChchNPV (ORF11), *Trichoplusia ni* SNPV (TnSNPV) (ORF11), LdMNPV (ORF20) and SeMNPV (ORF137) (Table 11). Early promoters were identified in some GVs e.g. *Choristoneura occidentalis* GV (ChocGV) (ORF13) and *Adoxophyes orana* GV (AdorGV) (ORF11) (Table 11). Although, no putative early or late promoter motives was found for F protein gene of CpGV, conventional RT-PCR revealed that F protein may transcribe at early and late phases of virus infection cycle since its transcription was detected at 24 hpi and continued until 96 hpi in CM larvae infected with CpGV-M.

Due to the lack of *C. pomonella* cell line, transcriptional analysis of Cp15, Cp16 and F was performed *in vivo* using infected CM larvae midgut tissues. Since the RT-PCR could not clearly distinguished between early or late gene transcription initiation, repetition of the RT-PCR analysis using single larvae will be required in order to confirm the obtained results. Moreover, using of *C. pomonella* cell line for virus infection is also suggested in order to obtain highly synchronized infections. Using the 3' and 5' RACE (Rapid amplification of cDNA end by PCR) may also facilitate the detection of the regulatory regions and transcription factor binding sites which allow the identification of the potential promoter region of the target gene by PCR and nucleotide sequencing of the PCR fragments. Using these approaches the identification of Cp15, Cp16 and F protein gene transcriptional regulation might be more reliable in order to figure out the possible influence of the transposon TCl4.7 insertion in MCp5 gene transcription regulation compared to wt CpGV-M.

Table 11. Homologues of Cp15, Cp16 and F protein in selected completely sequenced baculoviruses. The homologous ORFs are shown with the percentage amino acid sequence identity (ID%). The presence of baculovirus early (E) and late (L) promoter elements, located within 120 nt of the ATG, is indicated. Pairwise amino acids sequences alignments were carried out using the Basic Local Alignment Search Tool (BLAST) (Stephen et al., 1997).

Group	Virus name	Cp15				Cp16				Cp31 (F protein)				References
		ORF	ID%	Size (a.a)	Prom	ORF	ID%	Size (a.a)	Prom	ORF	ID%	Size (a.a)	Prom	
GVs	CpGV	15	100	457	E,L	16	100	196	E	31	100	601	-	Luque et al., 2001
	CrleGV	14	74	451	L	15	67	197	-	30	70	592	-	Lange and Jehle, 2003
	ChocGV	13	55	455	L	-	-	-	-	23	60	585	E	Escasa et al., 2006
	AdorGV	11	47	459	L	-	-	-	-	23	43	574	E	Wormleaton et al., 2003
	AgseGV	12	46	446	-	14	44	211	-	25	54	598	-	NC_ 005839
	SpliGV	11	43	456	-	100	30	321	-	24	39	585	-	NC_009503
	PlxyGV	14	42	446	L	-	-	-	-	26	44	544	-	Hashimoto et al., 2000
	XecnGV	13	44	453	L	-	-	-	-	27	32	599	-	Hayakawa et al., 1999
	PhopGV	13	61	426	-	14	53	205	-	27	59	595	-	NC_ 004062
Group II NPVs	ChchNPV	11	35	475	E,L	106	31	347	E	150	27	661	E,L	van Oers et al., 2005
	TnSNPV	11	34	475	L	101	30	347	E	143	28	661	E,L	Willis et al., 2005
	MacoNPV-A	167	33	461	L	72	36	359	E	9	25	680	E,L	Li et al., 2002
	LdMNPV	20	34	483	L	138	35	291	-	130	25	676	E,L	Kuzio et al., 1999
	EcobNPV	11	33	482	E	-	-	-	-	118	25	676	E,L	Ma et al., 2007
	SeMNPV	137	34	460	L	54	30	364	E	8	25	667	E,L	Ijkel et al., 1999
	AgseNPV	151	33	460	L	60	32	362	E	8	24	670	E,L	Jakubowska et al., 2006
	HearNPV-G4	9	33	468	L,L,L	-	-	-	-	133	-	677	E,L	Chen et al., 2001
Group I NPVs	AcMNPV	142	32	477	L	-	-	-	-	23	25	690	L	Ayres et al., 1994
	CfMNPV	135	31	479	-	-	-	-	-	21	-	655	-	De Jong et al., 2005
	BmNPV	118	31	476	L	-	-	-	-	14	-	673	E,L	Gomi et al., 1999
	OpMNPV	139	32	484	L	31	29	317	E	21	24	627	E	Ahrens et al., 1997
	EppoNPV	124	29	487	L	-	-	-	-	19	23	649	E	Hyink et al., 2002
Hymenopteran NPVs	NeleNPV	60	24	442	-	-	-	-	-	-	-	-	-	Lauzon et al., 2004
	NeabNPV	63	25	442	E,L	-	-	-	-	-	-	-	-	Duffy et al., 2006
	NeseNPV	63	24	441	E,L	-	-	-	-	-	-	-	-	Garcia-Maruniak et al., 2004
Depteran NPVs	CuniNPV	30	13	474	L	-	-	-	-	-	-	-	-	Afonso et al., 2001

3. Determining the function of hr3 and hr4 palindromes

Since the TCl4.7 transposon insertion had disrupted the intergenic region between hr3 and hr4 palindromes, the function of hr3 and hr4 as origin of replication or their auxiliary sequences might be influenced in the mutant MCp5. To investigate this possibility, two mutant bacmids were generated by using Red/ET-Recombination system. The first bacmid was constructed by replacing hr3 and hr4 in CpBAC with the Kan^R cassette resulting in the mutant virus $CpBAC^{hr3/hr4KO}$. The second bacmid was generated by replacing the intergenic region (90 bp) between hr3 and hr4 in CpBAC with the Kan^R cassette of about 1 kb resulting in the mutant virus $CpBAC^{hr3\text{-}kan\text{-}hr4}$. $CpBAC^{hr3\text{-}kan\text{-}hr4}$ was generated to mimic the interruption of hr3 and hr4 as it was observed in MCp5 carrying the TCl4.7 transposon at the same locus between hr3 and hr4. After cloning of the two bacmid DNAs and injecting them into the hemocoel of CM larvae (L4), both mutant bacmids infected CM larvae and produced viral OBs. The oral inoculation of CM larvae (L4) using OBs isolated from infected larvae revealed that the isolated OBs from both mutant viruses were biological active against CM larvae *per os*. Thus the disruption of hr3 and hr4 or even their complete deletion did not impair their capacity to replicate in CM. In order to investigate the potential consequences of deletion or interruption of hr3 and hr4 on the biological fitness of the mutant viruses, their median lethal concentrations (LC_{50}) and the median survival times (ST_{50}) were determined.

The LC_{50} of $CpBAC^{hr3/hr4KO}$ (5044 OB/ml) and the $CpBAC^{hr3\text{-}kan\text{-}hr4}$ (2837 OB/ml) did not statistically differ from CpBAC (2439 OB/ml). These findings are in agreement with the earlier results from Jehle et al. (1995) who demonstrated that LC_{50} determination of the mutant virus MCp5 carrying the TCl4.7 transposon in the intergenic region between hr3 and hr4 was not significant different from the parental CpGV-M. Thus, deletion or interruption of hr3 and hr4 did not influence concentration mortality response of CM larvae. The ST_{50} value for CpBAC (150 hour), $CpBAC^{hr3\text{-}kan\text{-}hr4}$ (142 hour) and $CpBAC^{hr3/hr4KO}$ (150 hour) was similar if not identical and thus was not statistically different. In contrast to these observations, the ST_{50} values of MCp5 was about 10 hours less than that of the wt CpGV-M (Arends et al., 2005). From the LC_{50} and ST_{50} analysis it was concluded that neither the deletion nor the interruption of hr3 and hr4 of CpGV had affected the virus infectivity or the biological efficacy based on the LC_{50} and ST_{50} parameters.

Recently it was demonstrated that the mutant MCp5 had a replication disadvantage when CM larvae were co-infected with MCp5 and the CpGV-M using different virus ratios

concentration (Arends et al., 2005). In order to prove this finding with CpBAC$^{hr3\text{-}kan\text{-}hr4}$, co-infection experiments were performed with CM larvae using CpBAC$^{hr3\text{-}kan\text{-}hr4}$ virus and the parental CpBAC virus. Fourth instar of CM larvae were co-infected with the mutant virus CpBAC$^{hr3\text{-}kan\text{-}hr4}$ and CpBAC in a competition experiments using different virus ratios in order to exclude possible dose effects by the infection. By comparing the CpBAC: CpBAC$^{hr3\text{-}kan\text{-}hr4}$ ratio in the virus inoculumn with the ratio in the virus progeny it was shown that CpBAC$^{hr3\text{-}kan\text{-}hr4}$ replication was efficiently out-competed by CpBAC replication. Quantification of genotype specific *Bam*HI restriction fragments revealed that no CpBAC$^{hr3\text{-}kan\text{-}hr4}$ was observed in the virus offspring, when its proportions in the inoculums were 50% or less. Only 100% of CpBAC$^{hr3\text{-}kan\text{-}hr4}$ proportion in virus inoculums showed also 100% CpBAC$^{hr3\text{-}kan\text{-}hr4}$ in virus offspring. Apparently, the replication of CpBAC$^{hr3\text{-}kan\text{-}hr4}$ is significantly disadvantaged in the presence of CpBAC. These results were in agreement with Arends et al. (2005), who demonstrated that the mutant MCp5 genotype carrying the TCl4.7 tranposon between hr3 and hr4 had a replication disadvantage in direct competition experiments with wt CpGV-M. Although CpBAC$^{hr3\text{-}kan\text{-}hr4}$ and CpBAC did not significantly differ in their LC_{50} and ST_{50} values, the mutant CpBAC$^{hr3\text{-}kan\text{-}hr4}$ was effectively out-competed by the parental CpBAC when CM larvae were co-infected with OBs of both CpBAC and the mutant CpBAC$^{hr3\text{-}kan\text{-}hr4}$. It is striking that a similar out-competition of CpBAC$^{hr3\text{-}kan\text{-}hr4}$ can be observed as for MCp5.

The out-competition of MCp5 or its mimic CpBAC$^{hr3\text{-}kan\text{-}hr4}$ was observed after oral infection of CM larvae. By performing serial passaging experiments between MCp5 and the wt CpGV-M in which OBs were inoculated *per os* and BV were inoculated by injection into larval hemolymph, a quick out-competition of the mutant BV was also detected after injection into larval hemolymph in the presence of the CpGV-M BV (Arends et al., 2005). The quick out competition of MCp5 BV suggested that it is probably related to parameters later in the infection process, e.g. the speed of BV replication or to the virus spread. A similar situation may be expected for CpBAC$^{hr3\text{-}kan\text{-}hr4}$. It is not yet clear, which molecular mechanisms cause the lack of competitiveness of CpBAC$^{hr3\text{-}kan\text{-}hr4}$ in the presence of the parental genotype CpBAC. This result suggests that the distance between hr3 and hr4 crucial and that there may be an unknown functional co-operation of these two hrs.

There was no obvious difference in the infection process of either CpBAC OBs or CpBAC$^{hr3\text{-}kan\text{-}hr4}$ OBs. The hr3 and hr4 are even not needed for CpGV replication as demonstrated by CpBAC$^{hr3/hr4KO}$. On the other hand, the replication rate of the mutants in this situation might be affected by the insertion of the transpson TCl4.7 or Kan^{R} in MCp5 and

CpBAC$^{hr3\text{-}kan\text{-}hr4}$ between palindromes hr3 and hr4, respectively, which could be attributed to the interruption of hrs flanking sequences.

Recently, by using an infection-dependent DNA replication assay where plasmids carrying hrs replicated in the presence of virus DNA, Hilton and Winstanley (2007) demonstrated that the entire 76 bp palindrome of hrs is the required region for replication with flanking regions enhancing replication, and the amount of replication increasing with the size of the fragment containing hrs. Although there is no homology between the CpGV sequences flanking the palindromes, specific flanking regions are obviously required for optimal replication. There was no increase in the amount of replication of the plasmid containing two palindromes (hr3 and hr4) compared to plasmids containing one palindrome, however a direct comparison to either palindrome hr3 or hr4 had not been made (Hilton and Winstanley, 2007). Here, a functional co-operation might be expected between hr3 and hr4. It would be worthy to analyze the replication capability of hr3 or hr4 independently. This could be achieved by separation of hr3 and hr4 and testing them in an infection-dependent DNA replication assay.

Typically, baculoviruses have many hrs interspersed throughout their genomes. These regions may act as enhancers of RNA transcription, as origin of DNA replication and as sites of recombination (For review see Hayakawa et al., 2000). In GVs, e.g. XecnGV contains nine hrs each with three to six direct repeats lacking a palindromic core (Hayakawa et al., 1999). PlxyGV has four large repeat regions centered on a palindrome that more closely resemble NPV hrs (Hashimoto et al., 2000), while AdorGV has nine repeat regions unlike NPV hrs (Wormleaton et al., 2003). ChocGV contains five hrs repeat regions varying in size and number of direct repeats (Escasa et al., 2006). Despite the differences between GV and NPV hrs, and between GV hrs themselves, the relative locations of hrs in ChocGV were found to be similar to the locations of three of the hrs in CrleGV, and to eight of 13 repeats in CpGV (Escasa et al., 2006). This reveals the possible specificity of hrs with their distribution throughout the virus genome. The consensus of the 13 CpGV palindromes shows dyad symmetry throughout the palindrome but are mainly conserved at the ends in the first and last 7 nt, and they all have a 20 bp AT-rich core (Hilton and Winstanley, 2007). In comparison to NPVs, e.g. AcMNPV, hrs comprise eight A/T-rich regions that contain between two and eight highly conserved repeated sequences of about 72 bp (Carstens and Wu, 2007). Previously, investigations using plasmid constructs of AcMNPV hr1a indicated that the central four nucleotides of the core of the palindrome are essential for ori function (Leisy et al., 1995). The CpGV hr regions differ to NPV hrs in that they consist of a single palindrome and do not

contain direct repeats. Deletion mutagenesis of AcMNPV hr5, which contains six palindromes, indicated that the efficiency of replication of an individual hr was dependent on the number of palindromes present (Pearson et al., 1992). The relative efficiency of replication of particular hr-containing plasmid was found to increase by increasing the number of palindromes located in hr (Leisy et al., 1995; Pearson et al., 1992).

The presence of multiple hrs throughout the genome may have evolved to provide redundancy in the initiation of viral DNA replication to ensure that DNA replication (and early gene expression) occurs efficiently in the event that a single hr is deleted. This hypothesis is supported by the results of studies demonstrating that deletion of a single hr element from the genome of AcMNPV and *Bombyx mori* MNPV (BmMNPV) does not affect the phenotype of the virus *in vitro* or *in vivo* (Majima et al., 1993; Rodems and Friesen, 1993). Elements flanking hr sequences have been also shown to be necessary for optimal infection-dependent plasmid replication (Leisy et al., 1995; Pearson and Rohrmann, 1995; Xie et al., 1995). Two of these elements have been characterized in LdMNPV and *Choristoneura fumiferana* MNPV (CfMNPV) and are composed of multiple repeats that are relatively A/T-rich (Pearson and Rohrmann, 1995; Xie et al., 1995). These elements can enhance replication independent of their orientation relative to the hr sequence (Pearson and Rohrmann, 1995). These observations evidenced the essential role of hrs and its flanking sequences in sustaining of the replication rate of the virus genome through out the infection process.

In addition to the function of hrs as origin of replication, hrs have been demonstrated to be cis-acting enhancers of transcription of baculovirus early genes including 39K, ie-2, p35 and helicase (Carson et al., 1991; Guarino and Summers, 1986; Lu and Carstens, 1993; Nissen and Friesen, 1989). The AcMNPV hr1 was also found to function as an enhancer, both when placed in *cis* as well as in *trans*, in heterologous mammlian cells (Viswanathan et al., 2003). However, it was not functional as an ori sequence in these cells. A host cell protein has been identified from *Spodoptera frugiperda* Cells (Sf9), hr1-BP, which binds very specifically to the AcMNPV hr1 palindromes plus the flanking sequences This protein was found to be required for the enhancer function of hr1 (Habib and Hasnain, 1996). Putative CpGV early genes have been identified based on their putative promoters and homology to NPV genes. The possible enhancing activity of CpGV hrs for early genes transcription is still unknown. The hypothesis that CpGV hrs might have the enhancing activity toward virus early gene transcription could be a useful line to investigate the possible influence of TCl4.7 transposon insertion between hr3 and hr4 on the function of hrs and thus the transcriptional

regulation of virus early genes which is responsible for virus replication initiation. Further characterization and studies of CpGV early genes and their transcription regulation in the presence or absence of hrs are required to establish if CpGV hrs act as enhancers of virus gene transcription.

The forces that foster and sustain genotypic diversity in virus populations are complex and appear to arise from processes acting on parasite reproduction within a host, that favor certain genotypes, and processes acting on between host transmission, that may favor other variants (Ebert and Hamilton, 1996). Co-infection by different genotypes resulting in a high prevalence of mixed genotypes appears to be common characteristics of many host-parasite systems, particularly viruses (Ennos, 1992; Hodgson et al., 2002). For example, defective viruses lacking genes essential for survival restore replication capacity by co-infection with complete genotypes and use gene products from the complete genotypes for their replication and transmission. This was proven by injection of *S. frugiperda* larvae (Lepidoptera) using the wild type *Spodoptera frugiperda* MNPV (SfMNPV) in a mixture with two variants of SfMNPV lacking about 15 kb. These mutants were not able to infect *S. frugiperda* larvae but retained the ability to replicate in cell culture or by injection into larvae after injection in presence of wt SfMNPV (Lopez-Ferber et al., 2003). In addition, the presence of a defective genotype in mixtures with a complete genotype results in a phenotype with increased pathogencity compared with that of the complete genotype alone (Lopez-Ferber et al., 2003). The complete genotype in this situation appears to act as a helper that facilitates transmission of the defective genotype. Interestingly, in a co-infection experiments whereas mixtures of ODVs of the mutant lack 15 kb and the complete genome were injected into hosts, the progeny OBs contained approximately the same proportion of genotypes as the original mixture, indicating that each genotype had a similar rate of replication on a single passage (Lopez-Ferber et al., 2003). In contrast to these observations, the generated mutant CpBAC$^{hr3\text{-}kan\text{-}hr4}$ showed similar biological parameters against CM larvae as CpBAC, but the CpBAC showed a replication advantage over the mutant CpBAC$^{hr3\text{-}kan\text{-}hr4}$. Apparently, the mutant CpBAC$^{hr3\text{-}kan\text{-}hr4}$ could not sustain in virus population in the presence of the CpBAC.

4. Conclusion

Natural occurring transposon mutagenesis substantially promotes genetic heterogeneity of baculoviruses. In this study, the possible influence of TCl4.7 transposons found in CpGV genetic variants such as CpGV-MCp5 on virus replication and gene transcription regulation was examined. A general dramatically delay and reduction of MCp5

gene transcription was observed compared to the wt CpGV-M. The generated CpGV bacmid (CpBAC) added a new tool for CpGV gene manipulation and further investigation of gene function. The interruption or deletion of hr3 and hr4 palindromes had no effect on virus virulence or efficacy against CM larvae. However, the mutant CpBAC$^{hr3\text{-}kan\text{-}hr4}$ generated as a mimic in the interruption of hr3 and hr4 as it was observed in MCp5 was out-competed in a virus population in the presence of the parental pseudovirus CpBAC similar to MCp5 in the presence of the wt CpGV-M. These results led to the hypothesis that there is unknown functional co-operation between hr3 and hr4 which was interrupted by the Kan^{R} insertion in CpBAC$^{hr3\text{-}kan\text{-}hr4}$ and possibly by TCl4.7 transposon insertion in MCp5 and thus affected the replication rate of the mutants MCp5 and CpBAC$^{hr3\text{-}kan\text{-}hr4}$ in the presence of the parental viruses CpGV-M and CpBAC, respectivily. Using bacmid constructs lacking only hr3 or hr4 might facilitate the function analysis of each palindrome independently. Also *in vitro* co-infection of *C. pomonella* cell line using the parental pseudovirus CpBAC with the variants CpBAC$^{hr3/hr4KO}$ lacking hr3 and hr4 and the CpBAC$^{hr3\text{-}kan\text{-}hr4}$ as a mimic for MCp5 can prove this hypothesis by determining the replication rate of each genotype in virus population offspring and may elucidate the functional co-operation of hr3 and hr4. Whatever the mechanism responsible for the observed effects, it is evident that variants carrying such transposons can affect the virus genetic structure, the virus replication efficacy and fitness which may influence their competitivity and persistence in the ecological system.

VI. REFERENCES

Afonso, C. L., Tulman, E. R., Lu, Z., Balinsky, C. A., Moser, B. A., Becnel, J. J., Rock, D. L., and Kutish, G. F. (2001). Genome sequence of a baculovirus pathogenic for *Culex nigripalpus*. *Journal of Virology* **75,** 11157-11165.

Ahrens, C. H., Russell, R., Funk, C. J., Evans, J. T., Harwood, S. H., and Rohrmann, G. F. (1997). The sequence of *Orgyia pseudotsugata* multinucleocapsid nuclear polyhedrosis virus genome. *Virology* **229,** 381-399.

Arends, H. M. (2003). Molecular and biological analysis on the horizontal transfer of insect transposons in Baculoviruses. PhD thesis. Mainz University, Mainz.

Arends, H. M., and Jehle, J. A. (2002). Homologous recombination between the inverted terminal repeats of defective transposon TCp3.2 causes an inversion in the genome of *Cydia pomonella* granulovirus. *Journal of General Virology* **83,** 1573-1578.

Arends, H. M., Winstanley, D., and Jehle, J. A. (2005). Virulence and competitiveness of *Cydia pomonella* granulovirus mutants: parameters that do not match. *Journal of General Virology* **86,** 2731-2738.

Asser-Kaiser, S., Fritsch, E., Undorf-Spahn, K., Kienzle, J., Eberle, K. E., Gund, N. A., Reineke, A., Zebitz, C. P. W., Heckel, D. G., Huber, J., and Jehle, J. A. (2007). Rapid emergence of baculovirus resistance in codling moth due to dominant, sex-linked inheritance. *Science* **317,** 1916-1918.

Ayres, M. D., Howard, S. C., Kuzio, J., Lopez-Ferber, M., and Possee, R. D. (1994). The complete DNA sequence of *Autographa californica* nuclear polyhedrosis virus. *Virology* **202,** 586-605.

Baudry, O., Corroyer, N., and Orts, R. (1996). Carpovirusine and the control of codling moth. *Phytoma* **482,** 22-24.

Beames, B., and Summers, M. D. (1988). Comparisons of host cell DNA insertions and altered transcription at the site of insertions in few polyhedra baculovirus mutants. *Virology* **162,** 208-220.

Bender, W., Akam, M., Karch, F., Beachy, P. A., Peifer, M., (1983). Molecular genetics of the bithorax complex in *Drosophila melanogaster*. *Science* **221,** 23-29.

Bertin, J., Mendrysa, S. M., LaCount, D. J., Gaur, S., Krebs, J. F., Armstrong, R. C., Tomaselli, K. J., and Friesen, P. D. (1996). Apoptotic suppression by baculovirus P35 involves cleavage by and inhibition of a virus-induced CED-3/ICE-like protease. *Journal of Virology* **70,** 6251-6259.

Bilimoria, S. L. (1991). The biology of nuclear polyhedrosis viruses. *In* "Viruses of Invertebrates" (E. Kurstak, Ed.), pp. 1-72. Marcel Dekker Inc., New York.

Blissard, G. W., Kogan, P. H., Wei, R., and Rohrmann, G. F. (1992). A synthetic early promoter from a baculovirus: roles of the TATA box and conserved start site CAGT sequence in basal levels of transcription. *Virology* **190,** 783-793.

Blissard, G. W., and Rohrmann, G. F. (1990). Baculovirus diversity and molecular biology. *Annual Review of Entomology* **35,** 127-155.

Blissard, G. W., and Wenz, J. R. (1992). Baculovirus gp64 envelope glycoprotein is sufficient to mediate pH- dependent membrane fusion. *Journal of Virology* **66,** 6829-6835.

Braunagel, S. C., Russell, W. K., Rosas-Acosta, G., Russell, D. H., and Summers, M. D. (2003). Determination of the protein composition of the occlusion-derived virus of *Autographa californica* nucleopolyhedrovirus. *The Proceedings of the National Academy of Sciences U S A* **100,** 9797-9802.

Britten, R. J. (1997). Mobile elements inserted in the distant past have taken on important functions. *Gene* **205,** 177-182.

Broer, R., Heldens, J. G. M., van Strien, E. A., Zuidema, D., and Vlak, J. M. (1998). Specificity of multiple homologous genomic regions in *Spodoptera exigua* nucleopolyhedrovirus DNA replication. *Journal of General Virology* **79,** 1563-1572.

Bulach, D. M., Kumar, C. A., Zaia, A., Liang, B. F., and Tribe, D. E. (1999). Group II nucleopolyhedrovirus subgroups revealed by phylogenetic analysis of polyhedrin and DNA polymerase gene sequences. *Journal of Invertebrate Pathology* **73,** 59-73.

Bull, J. C., Godfray, H. C., and O'Reilly, D. R. (2003). A few-polyhedra mutant and wild-type nucleopolyhedrovirus remain as a stable polymorphism during serial coinfection in *Trichoplusia ni*. *Applied and Environmental Microbiology* **69,** 2052-2057.

Capy, P., Gasperi, G., Biemont, C., and Bazin (2000). Stress and transposable elements: co-evolution or useful parasites? *Heredity* **85,** 101-106.

Carbonare, B. D., and Gehring, W. J. (1985). Excision of copia element in a revertant of the white-apricot mutation of *Drosophila melanogaster* leaves behind one long-terminal repeat. *Molecular and General Genetics* **199,** 1-6.

Carson, D. D., Summers, M. D., and Guarino, L. A. (1991). Transient expression of the *Autographa californica* nuclear polyhedrosis virus immediate-early gene, IE-N, is regulated by three viral elements. *Journal of Virology* **65,** 945-951.

Carstens, E. B., and Wu, Y. T. (2007). No single homologous repeat region is essential for DNA replication of the baculovirus *Autographa californica* multiple nucleopolyhedrovirus. *Journal of General Virology* **88,** 114-122.

Cartier, J. L., Hershberger, P. A., and Friesen, P. D. (1994). Suppression of apoptosis in insect cells stably transfected with baculovirus p35: dominant interference by N-terminal sequences p35 (1-76). *Journal of Virology* **68,** 7728-7737.

Chen, X. W., Ijkel, W. F. J., Tarchini, R., Sun, X. L., Sandbrink, H., Wang, H. L., Peters, S., Zuidema, D., Lankhorst, R. K., Vlak, J. M., and Hu, Z. H. (2001). The sequence of the *Helicoverpa armigera* single nucleocapsid nucleopolyhedrovirus genome. *Journal of General Virology* **82,** 241-257.

Chisholm, G. E., and Henner, D. J. (1988). Multiple early transcripts and splicing of the *Autographa californica* nuclear polyhedrosis virus IE-1 gene. *Journal of Virology* **62,** 3193-3200.

Clem, R. J. (2001). Baculoviruses and apoptosis: the good, the bad, and the ugly. *Cell Death & Differentiation* **8,** 137-143.

Clem, R. J. (2005). The role of apoptosis in defense against baculovirus infection in insects. *In* "Role of Apoptosis in Infection", Vol. 289, pp. 113-129. Springer-Verlag Berlin, Berlin.

Clem, R. J., and Miller, L. K. (1994). Induction and inhibition of apoptosis by insect viruses. *In* "Apoptosis II: The Molecular Basis of Apoptosis in Disease", pp. 89-110. Cold Spring Harbor Laboratory Press.

Cochran, M. A., Carstens, E. B., Eaton, B. T., and Faulkner, P. (1982). Molecular cloning and physical mapping of restriction endonuclease fragments of *Autographa californica* nuclear polyhedrosis virus DNA. *Journal of Virology* **41,** 940-946.

Coen, E. S., Carpenter, R., and Martin, C. (1986). Transposable elements generate novel spatial patterns of gene expression in *Antirrhinum majus*. *Cell* **47,** 285-296.

Corsaro, B. G., Gljzen, M.R., Wang, P. and Granados, R.R. (1993). "Baculovirus enhancing proteins as determinants of viral pathogenesis. In *"Parasites and Pathogens of Insects"* (N. E. Beckage, S. N. Thompson & B. A. Federici, Eds.), Vol. 2, pp. 125-145 Academic Press, San Diego.

Crook, N. E. (1991). Baculoviridae: subgroup B. Comparative aspects of granulosis viruses. *In* "Viruses of Invertebrates" (E. Kurstak, Ed.), pp. 73-110. Marcel Dekker Inc., New York.

Crook, N. E., Clem, R. J., and Miller, L. K. (1993). An apoptosis-inhibiting baculovirus gene with a zinc finger-like motif. *Journal of Virology* **67,** 2168-2174.

Crook, N. E., James, J. D., Smith, I. R. L., and Winstanley, D. (1997). Comprehensive physical map of the *Cydia pomonella* granulovirus genome and sequence analysis of the granulin gene region. *Journal of General Virology* **78,** 965-974.

Crook, N. E., Spencer, R. A., Payne, C. C., and Leisy, D. J. (1985). Variation in *Cydia pomonella* granulosis virus isolates and physical maps of the DNA from three variants. *Journal of General Virology* **66,** 2423-2430.

Cross, J. V., Solomon, M. G., Chandler, D., Jarrett, P., Richardson, P. N., Winstanley, D., Bathon, H., Huber, J., Keller, B., Langenbruch, G. A., and Zimmerman, G. (1999). Biocontrol of pests of apples and pears in northern and central Europe: Microbial agents and nematodes. *Biocontrol Science & Technology* **9,** 125-149.

Crouch, E. A., and Passarelli, A. L. (2002). Genetic requirements for homologous recombination in *Autographa californica* nucleopolyhedrovirus. *Journal of Virology* **76,** 9323-9334.

Dai, X. J., Willis, L. G., Huijskens, I., Palli, S. R., and Theilmann, D. A. (2004). The acidic activation domains of the baculovirus transactivators IE1 and IE0 are functional for transcriptional activation in both insect and mammalian cells. *Journal of General Virology* **85,** 573-582.

de Jong, J. G., Lauzon, H. A. M., Dominy, C., Poloumienko, A., Carstens, E. B., Arif, B. M., and Krell, P. J. (2005). Analysis of the *Choristoneura fumiferana* nucleopolyhedrovirus genome. *Journal of General Virology* **86,** 929-943.

Deng, F., Wang, R. R., Fang, M. G., Jiang, Y., Xu, X. S., Wang, H. Z., Chen, X. W., Arif, B. M., Guo, L., Wang, H. L., and Hu, Z. H. (2007). Proteomics analysis of *Helicoverpa armigera* single nucleocapsid nucleopolyhedrovirus identified two new occlusion-derived virus-associated proteins, HA44 and HA100. *Journal of Virology* **81,** 9377-9385.

Derksen, A. C. G., and Granados, R. R. (1988). Alteration of a lepidopteran peritrophic membrane by baculoviruses and enhancement of viral infectivity. *Virology* **167,** 242-250.

Doolittle, W. F., and Sapienza, C. (1980). Selfish genes, the phenotype paradigm and genome evolution. *Nature* **284,** 601-603.

Duffy, S. P., Young, A. M., Morin, B., Lucarotti, C. J., Koop, B. F., and Levin, D. B. (2006). Sequence analysis and organization of the *Neodiprion abietis* nucleopolyhedrovirus genome. *Journal of Virology* **80,** 6952-6963.

Eberle, K. E., and Jehle, J. A. (2006). Field resistance of codling moth against *Cydia pomonella* granulovirus (CpGV) is autosomal and incompletely dominant inherited. *Journal of Invertebrate Pathology* **93,** 201-206.

Ebert, D., and Hamilton, W. D. (1996). Sex against virulence: the coevolution of parasitic diseases. *Trends in Ecology and Evolution* **11,** 79–82.

Engelhard, E. K., and Volkman, L. E. (1995). Developmental resistance in fourth instar *Trichoplusia ni* orally inoculated with *Autographa californica* M nuclear polyhedrosis virus. *Virology* **209,** 384-389.

Ennos, R. (1992). "Ecological genetics of parasitism." In *Genes in ecology* (R. J. Berry, T. J. Crawford, and G. M. Hewitt, Eds.), pp. 255-279, Oxford: Blackwell.

Errede, B. T., Cardillo, T. S., Sherman, F., Dubois, E., Deschamps, J. M., and Waime, J. (1980). Mating signals control expression of mutations resulting from insertion of a transposable repetitive element adjacent to diverse yeast genes. *Cell* **25,** 427-36.

Escasa, S. R., Lauzon, H. A. M., Mathur, A. C., Krell, P. J., and Arif, B. M. (2006). Sequence analysis of the *Choristoneura occidentalis* granulovirus genome. *Journal of General Virology* **87,** 1917-1933.

Evans, H. F. (1986). Ecology and epizootiology of baculoviruses. *In* "The Biology of Baculoviruses, Vol.II, Practical Application for Insect Control" (R.R.Granados, B.A. Federici, Ed.), pp. 89-132. CRC Press, Inc., Boca Raton, Florida, US.

Fraser, M. J. (1986). Transposon-mediated mutagenesis of baculoviruses: transposon shuttling and implications for speciation. *Annals of the Entomological Society of America* **79,** 773-783.

Friesen, P. D. (1993). Invertebrate transposable elements in the baculovirus genome: characterization and significance. *In* "Parasites and Pathogens of Insects, Vol. 2: Parasites", pp. 147-178. Academic Press, London.

Friesen, P. D. (1997). Regulation of baculovirus early gene expression. *In* "The Baculoviruses" (L. K. Miller, Ed.), pp. 141-170. Plenum Press, New York.

Friesen, P. D. (2007). "Insect viruses." 5th ed. Fields virology (D. M. Knipe, P. M. Howley, D. E. Griffin, R. A. Lamb, M. A. Martin, B. Roizman, and S. E. Straus, Eds.), pp. 725-727, Lippincott Williams & Wilkins, Philadelphia, PA.

Friesen, P. D., and Nissen, M. S. (1990). Gene organization and transcription of TED, a lepidopteran retrotransposon integrated within the baculovirus genome. *Molecular and Cellular Biology* **10,** 3067-3077.

Friesen, P. D., Rice, W. C., Miller, D. W., and Miller, L. K. (1986). Bidirectional transcription from a solo long terminal repeat of the retrotransposon TED: symmetrical RNA start sites. *Molecular and Cellular Biology* **6,** 1599-1607.

Fritsch, E., Undorf-Spahn, K., Kienzle, J., Zebitz, C. P. W., and Huber, J. (2005). Apfelwickler-Granulovirus: Erste Hinweise auf Unterschiede in der Empfindlichkeit lokaler Apfelwickler-Population. *Nachrichtenblatt des Deutschen Pflanzenschutzdienstes* **57,** 29-34.

Garcia-Maruniak, A., Maruniak, J. E., Zanotto, P. M. A., Doumbouya, A. E., Liu, J. C., Merritt, T. A., and Lanoie, J. S. (2004). Sequence analysis of the genome of the *Neodiprion sertifer* nucleopolyhedrovirus. *Journal of Virology* **78,** 7036-7051.

Glaser, R. W. (1927). Studies of the polyhedral diseases of insects due to filterable viruses. *Annual Meeting of the Entomological Society of America* **20,** 319-343.

Gomi, S., Majima, K., and Maeda, S. (1999). Sequence analysis of the genome of *Bombyx mori* nucleopolyhedrovirus. *Journal of General Virology* **80,** 1323-1337.

Granados, R. R., and Williams, K. A. (1986). In vivo infection and replication of baculoviruses. *In* "The Biology of Baculoviruses, Vol. I, Biological Properties and Molecular Biology" (R. R. Granados, and B. A. Federici, Eds.), pp. 89-108. CRC Press, Boca Raton.

Gröner, A. (1990). "Safety to nontarget invertebrates of baculoviruses. In "Safety of Microbial Insecticides". (M. Laird, Lacey, L.A., Davidson, E.W. , Ed.), CRC Press, Boca Raton.

Guarino, L. A., Gonzalez, M. A., and Summers, M. D. (1986). Complete sequence and enhancer function of the homologous DNA regions of *Autographa californica* nuclear polyhedrosis virus. *Journal of Virology* **60,** 224-229.

Guarino, L. A., and Smith, M. (1992). Regulation of delayed-early gene transcription by dual TATA boxes. *Journal of Virology* **66,** 3733-3739.

Guarino, L. A., and Summers, M. D. (1986). Interspersed homologous DNA of *Autographa californica* nuclear polyhedrosis virus enhances delayed-early gene expression. *Journal of Virology* **60,** 215-223.

Guarino, L. A., Xu, B., Jin, J. P., and Dong, W. (1998). A virus-encoded RNA polymerase purified from baculovirus-infected cells. *Journal of Virology* **72,** 7985-7991.

Guillon, M., and Biache, G. (1995). IPM strategies for control of codling moth (*Cydia pomonella* L.) (Lepidoptera: Olethreutidae). Interest of CmGV for long term biological control of pest complex in orchards. *Mededelingen Faculteit Landbouwkundige en Toegepaste Biologische Wetenschappen, Universiteit Gent, Belgium* **60,** 695-705.

Guzman L.M., Belin D., Carson M.J., and J., B. (1995). Tight regulation, modulation, and high-level expression by vectors containing the arabinose pBAD promoter. *Journal of Bacteriology* **177,** 4121-4130

Habib, S., and Hasnain, S. E. (1996). A 38-kDa host factor interacts with functionally important motifs within the *Autographa californica* multinucleocapsid nuclear polyhedrosis virus homologous region (hr1) DNA sequence. *Journal of Biological Chemistry* **271,** 28250–28258.

Hajek, K., and Friesen, P. D. (1998). Proteolytic processing and assembly of gag and gag-pol proteins of TED, a baculovirus-associated retrotransposon of the gypsy family. *Journal of Virology* **72,** 8718-8724.

Hajos, J. P., Zuidema, D., Kulcsar, P., Heldens, J. G. M., Zavodszky, P., and Vlak, J. M. (1998). Recombination of baculovirus DNA following lipofection of insect larvae. *Archives of Virology* **143,** 2045-2050.

Harvey, J. P., and Volkman, L. E. (1983). Biochemical and biological variation of *Cydia pomonella* (codling moth) granulosis virus. *Virology* **124,** 21-34.

Hashimoto, Y., Corsaro, B. G., and Granados, R. R. (1991). Location and nucleotide sequence of the gene encoding the viral enhancing factor of the *Trichoplusia ni* granulosis virus. *Journal of General Virology* **72,** 2645-2651.

Hashimoto, Y., Hayakawa, T., Ueno, Y., Fujita, T., Sano, Y., and Matsumoto, T. (2000). Sequence analysis of the *Plutella xylostella* granulovirus genome. *Virology* **275,** 358-372.

Hayakawa, T., Ko, R., Okano, K., Seong, S. I., Goto, C., and Maeda, S. (1999). Sequence analysis of the *Xestia c-nigrum* granulovirus genome. *Virology* **262,** 277-297.

Hayakawa, T., Rohrmann, G. F., and Hashimoto, Y. (2000). Patterns of genome organization and content in lepidopteran baculoviruses. *Virology* **278,** 1-12.

Hefferon, K. L., Oomens, A. G. P., Monsma, S. A., Finnerty, C. M., and Blissard, G. W. (1999). Host cell receptor binding by baculovirus GP64 and kinetics of virion entry. *Virology* **258,** 455-468.

Heldens, J. G., van Strien, E. A., Feldmann, A. M., Kulcsar, P., Munoz, D., Leisy, D. J., Zuidema, D., Goldbach, R. W., and Vlak, J. M. (1996). *Spodoptera exigua* multicapsid nucleopolyhedrovirus deletion mutants generated in cell culture lack virulence in vivo. *Journal of General Virology* **77,** 3127-3134.

Herniou, E. A., Luque, T., Chen, X., Vlak, J. M., Winstanley, D., Cory, J. S., and O'Reilly, D. (2001). Use of whole genome sequence data to infer Baculovirus phylogeny. *Journal of Virology* **75,** 8117-8126.

Herniou, E. A., Olszewski, J. A., Cory, J. S., and O'Reilly, D. R. (2003). The genome sequence and evolution of baculoviruses. *Annual Review of Entomology* **48,** 211–234.

Herniou, E. A., Olszewski, J. A., O'Reilly, D. R., and Cory, J. S. (2004). Ancient coevolution of baculoviruses and their insect hosts. *Journal of Virology* **78,** 3244-3251.

Hilton, S., and Winstanley, D. (2007). Identification and functional analysis of the origins of DNA replication in the *Cydia pomonella* granulovirus genome. *Journal of General Virology* **88,** 1496-1504.

Hodgson, D. J., Vanbergen, A. J., Hartley, S. E., Hails, R. S., and Cory, J. S. (2002). Differential selection of baculovirus genotyps mediated by different species of host food plant. *Ecology Letters* **5,** 512-518.

Huang, Y., Deng, F., Hu, Z. H., Vlak, J. M., and Wang, H. Z. (2007). Baculovirus-mediated gene silencing in insect cells using intracellularly produced long double-stranded RNA. *Journal of Biotechnology* **128,** 226-236.

Huber, J. (1998). Western Europe. *In* "Insect viruses and pest management". (F. R. Hunter-Fujita, P. F. Entwistle, H. F. Evans, and N. E. Crook Eds.), pp.201-215. John Wiley & Sons Ltd., Chichester, England.

Hunter-Fujita, F. R., Entwistle, P. F., Evans, H. F., and Crook, N. E. (Eds.) (1998). Characteristics of insect pathogenic viruses. *In* "Insect Viruses and Pest Management". pp. 7-26. John Wiley & Sons Ltd., Chichester, England.

Hyink, O., Dellow, R. A., Olsen, M. J., Caradoc-Davies, K. M. B., Drake, K., Herniou, E. A., Cory, J. S., O'Reilly, D. R., and Ward, V. K. (2002). Whole genome analysis of the *Epiphyas postvittana* nucleopolyhedrovirus. *Journal of General Virology* **83,** 957-971.

Ijkel, W. F. J., van Strien, E. A., Heldens, J. G. M., Broer, R., Zuidema, D., Goldbach, R. W., and Vlak, J. M. (1999). Sequence and organization of the *Spodoptera exigua*

multicapsid nucleopolyhedrovirus genome. *Journal of General Virology* **80,** 3289-3304.

Ijkel, W. F. J., Westenberg, M., Goldbach, R. W., Blissard, G. W., Vlak, J. M., and Zuidema, D. (2000). A novel baculovirus envelope fusion protein with a proprotein convertase cleavage site. *Virology* **275,** 30-41.

Ivaldi-Sender, C. (1974). Techniques simples pour elevage permanent de la tordeuse orientale, *Grapholita molesta* (Lep., Tortricdae), sur milieu artificiel. *Annual Zoology and Ecology of Animal* **6,** 337-343.

Jakubowska, A. K., Peters, S. A., Ziemnicka, J., Vlak, J. M., and van Oers, M. M. (2006). Genome sequence of an enhancin gene-rich nucleopolyhedrovirus (NPV) from *Agrotis segetum*: collinearity with *Spodoptera exigua* multiple NPV. *Journal of General Virology* **87,** 537-551.

Jaques, R. P., Hardman, J. M., Laing, J. E., Smith, R. F., and Bent, E. (1994). Orchard trials in Canada on control of *Cydia pomonella* (Lep: Tortricidae) by granulosis virus. *Entomophaga* **39,** 281-292.

Jehle, J. A. (1996). Transmission of insect transposons into baculovirus genomes: An unusual host-pathogen interaction. *In* "Transgenic Organsims: Biological and Social Implications" (K. Wöhrmann, J. Tomiuk, and A. Sentker, Eds.), pp. 81-97. Birkhäuser Verlag, Basel.

Jehle, J. A., Backhaus, H., Fritsch, E., and Huber, J. (1992). Physical map of the *Cryptophlebia leucotreta* granulosis virus genome and its relationship to the genome of *Cydia pomonella* granulosis virus. *Journal of General Virology* **73,** 1621-1626.

Jehle, J. A., Blissard, G. W., Bonning, B. C., Cory, J. S., Herniou, E. A., Rohrmann, G. F., Theilmann, D. A., Thiem, S. M., and Vlak, J. M. (2006a). On the classification and nomenclature of baculoviruses: A proposal for revision. *Archives of Virology* **151,** 1257-1266.

Jehle, J. A., Lange, M., Wang, H. L., Hu, Z. H., Wang, Y. J., and Hauschild, R. (2006b). Molecular identification and phylogenetic analysis of baculoviruses from Lepidoptera. *Virology* **346,** 180-193.

Jehle, J. A., Fritsch, E., Nickel, A., Huber, J., and Backhaus, H. (1995). TCl4.7: a novel lepidopteran transposon found in *Cydia pomonella* granulosis virus. *Virology* **207,** 369-379.

Jehle, J. A., Nickel, A., Vlak, J. M., and Backhaus, H. (1998). Horizontal escape of the novel Tc1-like lepidopteran transposon TCp3.2 into *Cydia pomonella* granulovirus. *Journal of Molecular Evolution* **46,** 215-224.

Kaplan-Meier (1958). Nonparametric estimation from incomplete observations. *Journal of the American Statistical Association* **53,** 457– 481.

Keddie, B. A., Aponte, G. W., and Volkman, L. E. (1989). The pathway of infection of *Autographa californica* nuclear polyhedrosis virus in an insect host. *Science* **243,** 1728-1730.

Kogan, P. H., Chen, X., and Blissard, G. W. (1995). Overlapping TATA-dependent and TATA-independent early promoter activities in the baculovirus gp64 envelope fusion protein gene. *Journal of Virology* **69,** 1452-1461.

Kool, M., van den Berg, P. M., Tramper, J., Goldbach, R. W., and Vlak, J. M. (1993). Location of two putative origins of DNA replication of *Autographa californica* nuclear polyhedrosis virus. *Virology* **192,** 94-101.

Kuzio, J., Pearson, M. N., Harwood, S. H., Funk, C. J., Evans, J. T., Slavicek, J. M., and Rohrmann, G. F. (1999). Sequence and analysis of the genome of a Baculovirus pathogenic for *Lymantria dispar*. *Virology* **253,** 17-34.

Lacey, L. A., Knight, A., Huber, J., (2000). "Microbial control of lepidopterous pests of apple orchards." Field Manual of Techniques for the Evaluation of Entomopathogens. (L. A. Lacey, Kaya, H.K, Eds.), pp. 557–576 Kluwer Academic Publishers, Dordrecht, Netherlands.

Lacey, L. A., Vail, P. V., and Hoffman, D. F. (2002). Comparative activity of baculoviruses against the codling moth *Cydia pomonella* and three other tortricid pests of tree fruit. *Journal of Invertebrate Pathology* **80,** 64-68.

LaCount, D. J., and Friesen, P. D. (1997). Role of early and late replication events in induction of apoptosis by baculoviruses. *Journal of Virology* **71,** 1530-1537.

LaCount, D. J., Hanson, S. F., Schneider, C. L., and Friesen, P. D. (2000). Caspase inhibitor P35 and inhibitor of apoptosis Op-IAP block in vivo proteolytic activation of an effector caspase at different steps. *Journal of Biological Chemistry* **275,** 15657-15664.

Lange, M., and Jehle, J. A. (2003). The genome of the *Cryptophlebia leucotreta* granulovirus. *Virology* **317,** 220-236.

Lange, M., Wang, H. L., Zhihong, H., and Jehle, J. A. (2004). Towards a molecular identification and classification system of lepidopteran-specific baculoviruses. *Virology* **325,** 36-47.

Lannan, E., Vandergaast, R., and Friesen, P. D. (2007). Baculovirus caspase inhibitors P49 and P35 block virus-induced apoptosis downstream of effector caspase DrICE activation in *Drosophila melanogaster* cells. *Journal of Virology* **81,** 9319-9330.

Lauzon, H. A. M., Lucarotti, C. J., Krell, P. J., Feng, Q. L., Retnakaran, A., and Arif, B. M. (2004). Sequence and organization of the *Neodiprion lecontei* nucleopolyhedrovirus genome. *Journal of Virology* **78,** 7023-7035.

Leisy, D. J., Rasmussen, C., Kim, H. T., and Rohrmann, G. F. (1995). The *Autographa californica* nuclear polyhedrosis virus homologous region 1a: identical sequences are

essential for DNA replication activity and transcriptional enhancer function. *Virology* **208,** 742-752.

Lenz, C. J., McIntosh, A. H., Mazzacano, C., and Monderloh, U. (1991). Replication of *Heliothis zea* nuclear polyhedrosis virus in cloned cell lines. *Journal of Invertebrate Pathology* **57,** 227-233.

Li, Q., Donly, C., Li, L., Willis, L. G., Theilmann, D. A., and Erlandson, M. (2002). Sequence and organization of the *Mamestra configurata* nucleopolyhedrovirus genome. *Virology* **294,** 106-121.

Lin, G. Y., and Blissard, G. W. (2002). Analysis of an *Autographa californica* nucleopolyhedrovirus lef-11 knockout: LEF-11 is essential for viral DNA replication. *Journal of Virology* **76,** 2770-2779.

Lodish, H., Berk, A., Zipursky, l., Matsudaira, P., Baltimore, D., and Darnell, J., (Eds.) (2000). Molecular Cell Biology. 4th ed. New York: Elsevier.

Long, G., Pan, X. Y., Kormelink, R., and Vlak, J. M. (2006a). Functional entry of baculovirus into insect and mammalian cells is dependent on clathrin-mediated endocytosis. *Journal of Virology* **80,** 8830-8833.

Long, G., Pan, X. Y., Westenberg, M., and Vlak, J. M. (2006b). Functional role of the cytoplasmic tail domain of the major envelope fusion protein of group II baculoviruses. *Journal of Virology* **80,** 11226-11234.

Lopez-Ferber, M., Simon, O., Williams, T., and Caballero, P. (2003). Defective or effective? Mutualistic interactions between virus genotypes. *Proceedings of the Royal Society B-Biological Sciences* **270,** 2249-2255.

Lu, A., and Carstens, E. B. (1993). Immediate-early baculovirus genes transactivate the p143 gene promoter of *Autographa californica* nuclear polyhedrosis virus. *Virology* **195,** 710-718.

Lu A. and Miller L. K. (1997). Regulation of Baculovirus Late and Very Late Gene Expression, *In "The Baculoviruses"* (Lois K. Miller Ed.), pp. 193-216 Plenum Press, New York.

Lu, A., Krell, P. J., Vlak, J. M., and Rohrmann, G. F. (1997). Baculovirus DNA replication. *In* "The Baculoviruses" (L. K. Miller, Ed.), pp. 171-191. Plenum Press, New York.

Luckow, V. A., Lee, S. C., Barry, G. F., and Olins, P. O. (1993). Efficient generation of infectious recombinant baculoviruses by site-specific transposon-mediated insertion of foreign genes into a baculovirus genome propagated in *Escherichia coli*. *Journal of Virology* **67,** 4566-4579.

Lung, O., Westenberg, M., Vlak, J. M., Zuidema, D., and Blissard, G. W. (2002). Pseudotyping *Autographa californica* multicapsid nucleopolyhedrovirus (AcMNPV): F proteins from group II NPVs are functionally analogous to AcMNPV GP64. *Journal of Virology* **76,** 5729-5736.

Lung, O. Y., Cruz-Alvarez, M., and Blissard, G. W. (2003). Ac23, an envelope fusion protein homolog in the baculovirus *Autographa californica* multicapsid nucleopolyhedrovirus, is a viral pathogenicity factor. *Journal of Virology* **77,** 328-339.

Luque, T., Finch, R., Crook, N., O'Reilly, D. R., and Winstanley, D. (2001). The complete sequence of the *Cydia pomonella* granulovirus genome. *Journal of General Virology* **82,** 2531-2547.

Ma, X. C., Shang, J. Y., Yang, Z. N., Bao, Y. Y., Xiao, Q., and Zhang, C. X. (2007). Genome sequence and organization of a nucleopolyhedrovirus that infects the tea looper caterpillar, *Ectropis obliqua*. *Virology* **360,** 235-246.

Majima, K., Kobara, R., and Maeda, S. (1993). Divergence and evolution of homologous regions of *Bombyx mori* nuclear polyhedrosis virus. *Journal of Virology* **67,** 7513-7521.

Manji, G. A., Hozak, R. R., LaCount, D. J., and Friesen, P. D. (1997). Baculovirus inhibitor of apoptosis functions at or upstream of the apoptotic suppressor P35 to prevent programmed cell death. *Journal of Virology* **71,** 4509-4516.

McCarthy, C., and Theilmann, D. (2008). AcMNPV ac143 (odv-e18) is essential for mediating budded virus production and is the 30th baculovirus core gene. *Virology* **375,** 277-291.

McCarthy, C. B., Dai, X., Donly, C., and Theilmann, D. A. (2008). *Autographa californica* multiple nucleopolyhedrovirus ac142, a core gene that is essential for BV production and ODV envelopment. *Virology* **372,** 325-339.

McGinnis, W., Shermoen, A. W., Beckendorf, S. K. (1983). A transposable element inserted just 5' to a Drosophila glue protein gene alters gene expression and chromatin structure. *Cell* **34,** 75-84.

Miller, C. A., Ingmer, H., and Cohen, S. (1995). Boundaries of the pSC101 Minimal Replicon are Conditional. *Journal of Bacteriology* **177,** 4865-4871

Miller, D. W., and Miller, L. K. (1982). A virus mutant with an insertion of a copia-like transposable element. *Nature* **299,** 562-564.

Miller, L. K. (1988). Baculoviruses as gene expression vectors. *Annual Review of Microbiology* **42,** 177-199.

Miller, L. K. (1997). "The Baculoviruses." The Viruses (H. Fraenkel-Conrat, and R.R. Wagner, Eds.), Plenum Press, New York.

Monsma, S. A., and Blissard, G. W. (1995). Expression of wild type and mutant baculovirus envelope fusion protein GP64 EFP in stably-transfected insect cells. *Proceedings of 28th Annual Meeting of the Society for Invertebrate Pathology, Ithaka, USA.*

Monsma, S. A., Oomens, A. G., and Blissard, G. W. (1996). The GP64 envelope fusion protein is an essential baculovirus protein required for cell-to-cell transmission of infection. *Journal of Virology* **70,** 4607-4616.

Moscardi, F. (1999). Assessment of the application of baculoviruses for control of Lepidoptera. *Annual Review of Entomology* **44,** 257-289.

Moser, B. A., Becnel, J. J., White, S. E., Afonso, C., Kutish, G., Shanker, S., and Almira, E. (2001). Morphological and molecular evidence that *Culex nigripalpus* baculovirus is an unusual member of the family Baculoviridae. *Journal of General Virology* **82,** 283-297.

Nakai, M., Goto, C., Kang, W., Shikata, M., Luque, T., and Kunimi, Y. (2003). Genome sequence and organization of a nucleopolyhedrovirus isolated from the smaller tea tortrix, *Adoxophyes honmai*. *Virology* **316,** 171-183.

NCSS statistical system for windows (2007). Published by: Dr. Jerry L. Hintze. Kaysville, Utah , USA.

Nissen, M. S., and Friesen, P. D. (1989). Molecular analysis of the transcriptional regulatory region of an early baculovirus gene. *Journal of Virology* **63,** 493-503.

Obregon-Barboza, V., Del Rincon-Castro, M. C., Cabrera-Ponce, J. L., and Ibarra, J. E. (2007). Infection, transfection, and co-transfection of baculoviruses by microprojectile bombardment of larvae. *Journal of Virological Methods* **140,** 124-131.

Oomens, A. G., Monsma, S. A., and Blissard, G. W. (1995). The baculovirus GP64 envelope fusion protein: synthesis, oligomerization, and processing. *Virology* **209,** 592-603.

Oomens, A. G. P., and Blissard, G. W. (1999). Requirement for GP64 to drive efficient budding of *Autographa californica* multicapsid nucleopolyhedrovirus. *Virology* **254,** 297-314.

Orgel, L. E., and Crick, F. H. (1980). Selfish DNA: The ultimate parasite. *Nature* **284,** 604-607.

Ozers, M. S., and Friesen, P. D. (1996). The Env-like open reading frame of the baculovirus-integrated retrotransposon TED encodes a retrovirus-like envelope protein. *Virology* **226,** 252-259.

Pearson, M. N., Bjornson, R. M., Pearson, G., and Rohrmann, G. F. (1992). The *Autographa californica* baculovirus genome: Evidence for multiple replication origins. *Science* **257,** 1382-1384.

Pearson, M. N., Groten, C., and Rohrmann, G. F. (2000). Identification of the *Lymantria dispar* nucleopolyhedrovirus envelope fusion protein provides evidence for a phylogenetic division of the Baculoviridae. *Journal of Virology* **74,** 6126-6131.

Pearson, M. N., and Rohrmann, G. F. (1995). *Lymantria dispar* nuclear polyhedrosis virus homologous regions: characterization of their ability to function as replication origins. *Journal of Virology* **69,** 213-221.

Perera, O., Green, T. B., Stevens, S. M., White, S., and Becnel, J. J. (2007). Proteins associated with *Culex nigripalpus* nucleopolyhedrovirus occluded virions. *Journal of Virology* **81,** 4585-4590.

Pijlman, G. P., de Vrij, J., van den End, F. J., Vlak, J. M., and Martens, D. E. (2004). Evaluation of baculovirus expression vectors with enhanced stability in continuous cascaded insect-cell bioreactors. *Biotechnology and Bioengineering* **87,** 743-753.

Reynolds, A., Felton, J., Wright, A. (1981). Insertion of DNA activates the cryptic bgl operon in *E. coli* KI2. *Nature* **293,** 625-629.

Robertson, J. L., and Preisler, H. K. (1992). "Pesticide Bioassay with Arthropods." CRC Press, Boca Raton, Florida.

Rodems, S. M., and Friesen, P. D. (1993). The *hr*5 transcriptional enhancer stimulates early expression from the *Autographa californica* nuclear polyhedrosis virus genome but is not required for virus replication. *Journal of Virology* **67,** 5776-5785.

Roelvink, P. W., Corsaro, B. G., and Granados, R. R. (1995). Characterization of the *Helicoverpa armigera* and *Pseudaletia unipuncta* granulovirus enhancin genes. *Journal of General Virology* **76,** 2693-2705.

Rohrmann, G. F. (1986). Evolution of occluded baculoviruses. *In* "The Biology of Baculoviruses, Vol.I, Biological Properties and Molecular Biology" (R.R. Granados, B.A. Federici, Eds.), Vol. 1, pp. 203-215. Vol. 2. CRC Press, Inc., Boca Raton, Florida, US.

Sait, S. M., Begon, M., and Thompson, D. J. (1994). The effects of a sublethal baculovirus infection in the Indian meal moth, *Plodia interpunctella*. *Journal of Animal Ecology* **63,** 541-550.

Sambrook, J., Fritsch, E. F., and Maniatis, T. (1989). "Molecular Cloning: A Laboratory Manual." 2 ed., Cold Spring Harbor Laboratory, New York.

Sauphanor, B., Berling, M., Toubon, J.-F., Reyes, M., Delnatte, J., and Allemoz, P. (2006). "Cas de résistance au virus de la granulose en vergers biologique". Phytoma-La Défense des Végétaux **590**, 24–27.

Shuler, M. L., Hammer, D. A., Granados, R. R., and Alan Wood, H. (1995). "Overview of Baculovirus insect culture system. *In* "Baculovirus Expression System and Bioinsecticides" (H. D. A. Shuler M.L., Granados R.R. and Alan Wood H, Eds.), pp. 1-11 Academic Press, New York.

Shure, M., Wessler, S., and Federoff, N. (1983). Molecular identification and isolation of the Waxy locus in maize. *Cell* **35,** 225-233.

Stephen, F., Altschul, T. L., Schäffer, A. A., Zhang, J., Zhang, Z., Miller, W., and Lipman, D. J. (1997). "Gapped BLAST and PSI-BLAST: a new generation of protein database search programs". *Nucleic Acids Research* **25,** 3389-3402.

Stewart, A. F., Zhang, Y., and Buchholz, F. (1998). Novel DNA cloning method. European Patent No.1034260 (issued on 12th of March, 2003), United States Patent No 6,509,156.

Summers, M. D. (2006). Milestones leading to the genetic engineering of baculoviruses as expression vector systems and viral pesticides. *Advances in virus research* **68**, 3-73.

Tanada, Y. (1964). A granulosis virus of the codling moth, *Carpocapsa pomonella* (L.) (Olethreutidae, Lepidoptera). *Journal of Insect Pathology* **6,** 378-380.

Theilmann, D. A., Blissard, G. W., Bonning, B., Jehle, J., O'Reilly, D. R., Rohrmann, G. F., Theim, S., and Vlak, J. M. (2005). "Baculoviridae" Eighth Report of the International Committee on Taxonomy of Viruses (H. V. Van Regenmortel, Bishop, D.H.L., Van Regenmortel, M.H., Fauquet, C.M., Eds.), pp.177-185 Elsevier Academic Press, New York.

Theilmann, D. A., and Stewart, S. (1992). Tandemly repeated sequence at the 3' end of the IE-2 gene of the baculovirus *Orgyia pseudotsugata* multicapsid nuclear polyhedrosis virus is an enhancer element. *Virology* **187,** 97-106.

Tsubota, S., and Schedl, P. (1986). Hybrid dysgenesis-induced revertants of insertions at the 5’ end of the rudimentary gene in *Drosophila melanogaster*: transposon- induced control mutations. *Genetics* **114,** 165-182.

van Oers, M. M., Abma-Henkens, M. H. C., Herniou, E. A., de Groot, J. C. W., Peters, S., and Vlak, J. M. (2005). Genome sequence of *Chrysodeixis chalcites* nucleopolyhedrovirus, a baculovirus with two DNA photolyase genes. *Journal of General Virology* **86,** 2069-2080.

van Oers, M. M., and Vlak, J. M. (2007). Baculovirus genomics. *Current Drug Targets* **8,** 1051-1068.

Vanarsdall, A. L., Pearson, M. N., and Rohrmann, G. F. (2007). Characterization of baculovirus constructs lacking either the Ac101, Ac142, or the Ac144 open reading frame. *Virology* **367,** 187-195.

Viswanathan, P., Venkaiah, B., Kumar, M. S., Rasheedi, S., Vrati, S., Bashyam, M. D., and Hasnain, S. E. (2003). The homologous region sequence (hr1) of *Autographa californica* multinucleocapsid polyhedrosis virus can enhance transcription from non-baculoviral promoters in mammalian cells. *Journal of Biological Chemistry* **278,** 52564-52571.

Volkman, L. E., Goldsmith, P. A., Hess, R. T., and Faulkner, P. (1984). Neutralization of budded *Autographa californica* NPV by a monoclonal antibody: identification of the target antigen. *Virology* **133,** 354-362.

Washburn, J. O., Kirkpatrick, B. A., and Volkman, L. E. (1996). Insect protection against viruses. *Nature* **383,** 767.

Willis, L. G., Siepp, R., Stewart, T. M., Erlandson, M. A., and Theilmann, D. A. (2005). Sequence analysis of the complete genome of *Trichoplusia ni* single

nucleopolyhedrovirus and the identification of a baculoviral photolyase gene. *Virology* **338,** 209-226.

Winstanley, D., and Crook, N. E. (1993). Replication of *Cydia pomonella* granulosis virus in cell cultures. *Journal of General Virology* **74,** 1599-1609.

Wormleaton, S., Kuzio, J., and Winstanley, D. (2003). The complete sequence of the *Adoxophyes orana* granulovirus genome. *Virology* **311,** 350-365.

Wyllie, A. H., Kerr, J. F., and Currie, A. R. (1980). Cell death: the significance of apoptosis. *International Review of Cytology* **68,** 251-306.

Xie, W. D., Arif, B., Dobos, P., and Krell, P. J. (1995). Identification and analysis of a putative origin of DNA replication in the *Choristoneura fumiferana* multinucleocapsid nuclear polyhedrosis virus genome. *Virology* **209,** 409-419.

Yamamoto, T., and Tanada, Y. (1978). Biochemical properties of viral envelopes of insect baculoviruses and their role in infectivity. *Journal of Invertebrate Pathology* **32,** 202-211.

Yan-Hong SI, M.-G. F., Yi Huang, Fang-Liang Zheng, Ting Li, Zhi-Hong Hu, and Han-Zhong Wang (2007). Construction and characterization of a *Heliocoverpa armigera* Nucleopolyhedrovirus Bacterial Artificial Chromosome with Deletion of Ecdysteroid UDP-Glucosyltransferase Gene. *Bioscience Biotechnology and Biochemistry* **71,** 2435-2441.

Yin, F., Wang, M., Tan Y, Deng, F., Vlak, J., Hu, Z., and Wang, H. (2008). A functional F analogue of *Autographa californica* nucleopolyhedrovirus GP64 from the *Agrotis segetum* granulovirus. *Journal of Virology* **82,** 8922-8926.

APPENDIX I (Media and Buffers)

A.1 Media

A.1.1 Insect semi-artificial diet (500 ml)

10 g Agar-Agar
32 g maize meal
33 g wheat germ
15 g brewer's yeast
2.85 g Ascorpic acid
1.15 g Nipagien (hydroxybenzoic acid methyl ester)
tap water up to 500 ml

A.1.2 LB Medium (Luria-Bertani Medium) (for 1 liter)

10 g Tryptone
5 g Yeast extract
10 g NaCl
(15 g Agar-Agar for solid medium)
- Dissolve in l liter bdH_2O and adjust to pH 7.2 – 7.5 using 5 N NaOH
- Sterilize by autoclaving for 20 min at 121°C

A.1.3 2X YT Medium (for 1 liter)

16 g Tryptone
10 g Yeast extract
5 g NaCl
- Dissolve in 1 liter bdH_2O and adjust to pH 7.2 – 7.5 using 5 N NaOH
- Sterilize by autoclaving for 20 min at 121°C

The following additives were added to the LB-agar plates depending on the experiments:

X-Gal 40 mM/ml (stock solution 20 mg/ml in Dimethylformamid)
IPTG 100 mM/ml (stock solution 2% IPTG in sterile bdH_2O)
Ampicillin 50 µg/ml (stock solution 50 mg/ml in sterile bdH_2O)
Kanamycin 15 µg/ml (stock solution 10 mg/ml in sterile bdH_2O)
Chloramphenicol 12.5 µg/ml (stock solution 25 mg/ml in EtOH)
Tetracyclin 3 µg/ml (stock solution 5 mg/ml in EtOH)

A.2 Buffers and solution used for DNA analysis

A.2.1 TE buffer

1 mM EDTA

10 mM Tris-HCl, pH 8.0

A.2.2 50X TAE (for 1 liter), working solution 1X TAE

242 g Tris-base

57.1 ml Acetic Acid

100 ml 0.5 M EDTA (pH 8.0)

add bdH_2O up to 1 liter

A.2.3 10X TBE (for 1 liter), working solution 0.5X TBE

54 g Tris-base

27.5 g Boric acid

20 ml 0.5 M EDTA (pH 8.0)

add bdH_2O up to 1 liter

A.2.4 6X DNA loading dye

0.25% bromophenol blue

40% sucrose (w/v) in sterile bdH_2O

A.2.5 1X PBS buffer (for 1 liter)

8 g NaCl

0.2 g KCl

1.44 g Na_2HPO4

0.24 g KH_2PO4

- Dissolve in 800 ml bdH_2O, adjust pH 7.4 with HCl and add bdH_2O up to 1 liter
- Sterilize by autoclaving for 20 min at 121°C

A.3 Buffers and solutions used for RNA analysis

A.3.1 DEPC-treated water

Add DEPC (diethylpyrocarbonate) 0.01% (v/v) to bdH_2O, let stand overnight and autoclave for 20 min at 121°C

A.3.2 0.1 M Sodium Phosphat Buffer (100 ml)

3.9 ml 1 M NaH_2PO_4

6.1 ml 1 M Na_2HPO_4

80 ml bdH_2O

Adjust pH 7.0 using NaH_2PO_4 or $NaHPO_4$ and add bdH_2O up to 100 ml

A.3.3 8 M Glyoxal

Deionize stock solution (~ 40% Glyoxal solution, Sigma 50649) through a mixed bed resin (Bio-Rad 501-X8) until pH 5.0

A.3.4 Glyoxal loading dye

50% glycerol (v/v)

10 mM sodium phosphate buffer

0.25% bromophenol blue

A.4 Buffers and solutions used for protein analysis

A.4.1 1X SDS-PAGE running buffer (for 1 liter)

3.2 g Tris-base

14.4 g Glycine

0.1 g SDS

add bdH_2O up to 1 liter

A.4.2 Protein lysis buffer

50 mM glucose

10 mM EDTA

25 mM Tris-HCl, pH 8.0

A.4.3 (4X) Protein loading dye

40 mM Tris-HCl, pH 8.0

0.4 mM EDTA

8% SDS (w/v)

40% glycerol (v/v)

0.004% bromophenol blue

A.4.4 Protein staining solution (500 ml)

325 ml bdH_2O

125 ml Isopropanol

50 ml Acetic acid

0.2 g coomassie brilliant blue

A.4.5 Protein destaining solution (500 ml)

37.5 ml Methanol

25 ml Acetic acid

add bdH_2O up to 500 ml

A.4.6 Protein transfer buffer (for protein transfer to PVDF membran)

0.025 M Tris-base

0.192 M Glycine

0.1% SDS

20% Methanol

A.4.7 Glycin-HCl buffer, pH 2.2

4.3 g Glycin

3.4 g NaCl

Adjust pH 2.2 with HCl conc.

A.4.8 10X Phosphate Buffer Salin (PBS) (0.1 M PBS, pH 7.2) (for 1 liter)

10.9 g Na_2HPO_4

3.2 g NaH_2PO_4

90 g NaCl

- Dissolve in bdH_2O, adjust pH to 7.2 and add H_2O to 1 liter

- Use 1X PBS as a working solution

A.4.9. PBS-Tween (PBS-T)

0.1 Tween-20 in PBS

A.4.10. Blocking buffer (5% skimmed milk) (for 500 ml)

50 g skimmed milk (> 0.5% fat)

Dissolve in PBS-T (0.1 Tween-20 in PBS) up to 500 ml

APPENDIX II (Plasmids Maps)

pGEM-T Easy Vector (*Promega*)

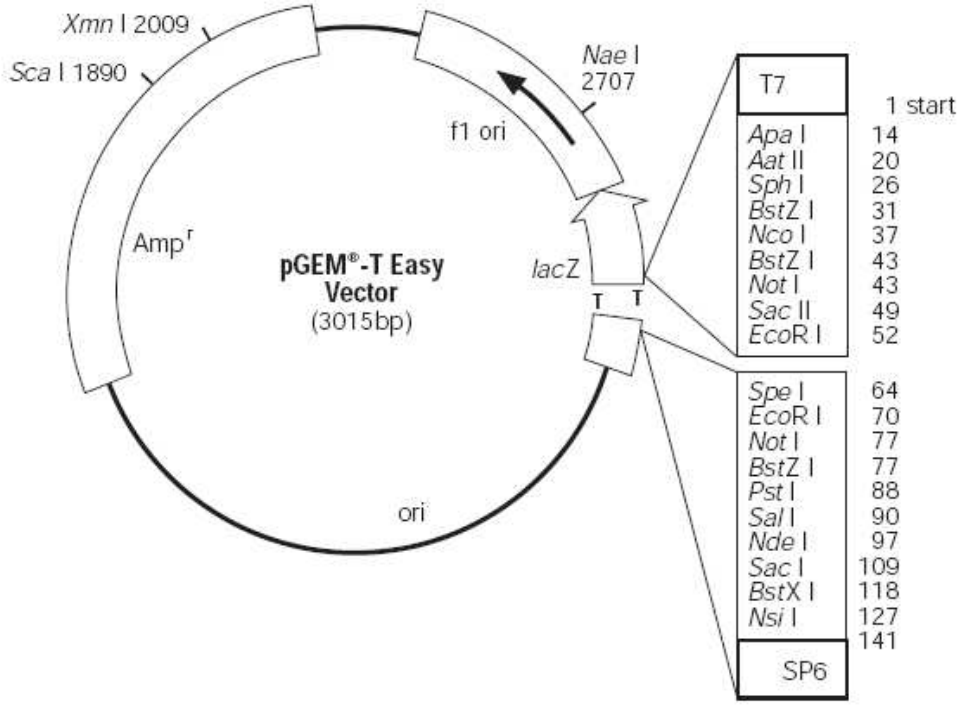

-Plasmid features and nucleotide sequence is available by *Promeg*.

pET-28a(+) expression vector (*Novagen*)

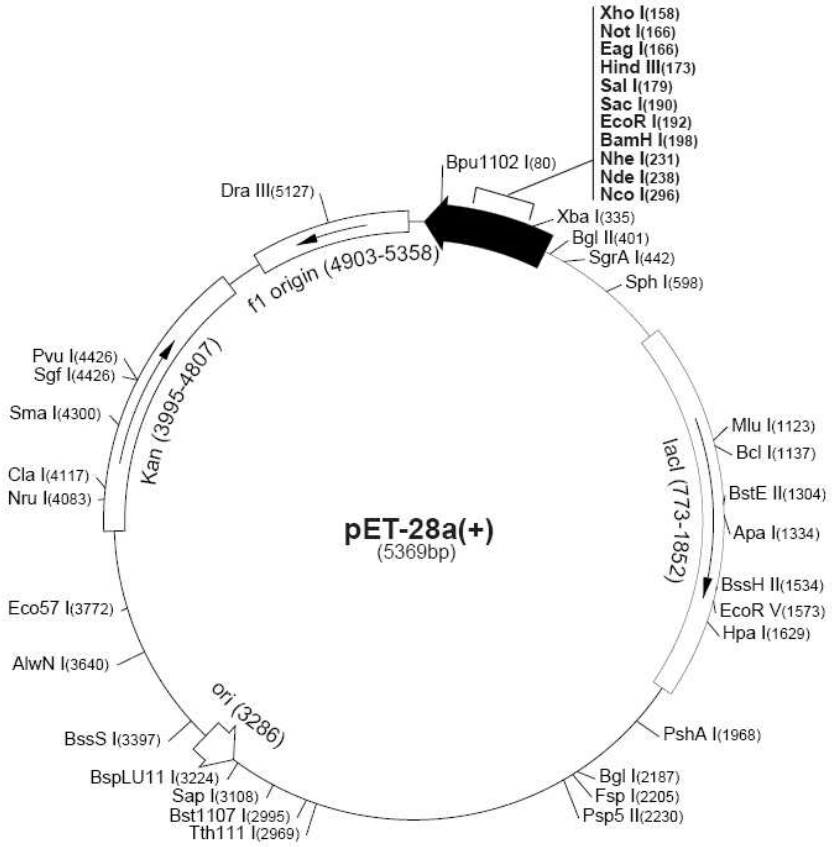

-The pET-28b(+) used in this study has the same features as pET-28a(+) with the following exception: pET-28b(+) is a 5368 bp plasmid; subtract 1 bp from each site beyond *Bam*HI at 198.

-Plasmid features and nucleotide sequence is available by *Novagen.*

Copy Control pCC1BAC vector (*EPICENTRE*)

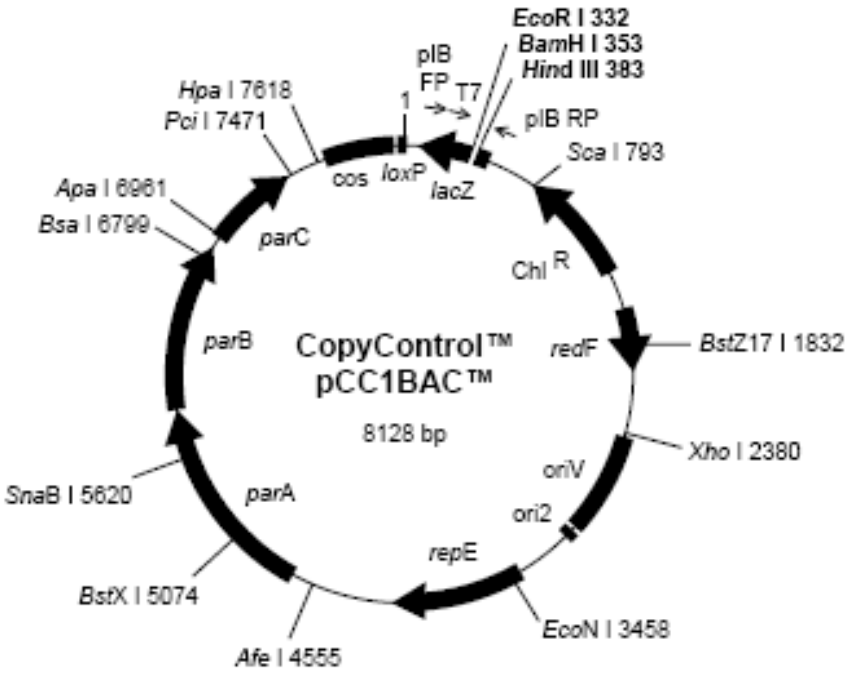

Copy Control pCC1BAC vector	
pUC19LacZ orf	56-435
pIB FP-1	230-256
M13F (Epicentre)	261-284
T7 Promoter 5'-3'	311-330
*Hin*d III	383-388
*Bam*H I	353-358
(del)non-SP6 promoter	396-413
M13R (Epicentre)	443-466
pIB RP-1	464-489
Chloramphenicol-R	765-1424
redF fragment	1643-1990
Xho I	2380-2385
oriV	2385-3002
Xho I	3002-3007
repE	3386-4141
sopA/parA	4729-5895
sopB/parB	5895-6866
sopC/parC	6939-7456
cos site	7671-8070
loxP	8084-8128

- Plasmid nucleotide sequence is available by *EPICENTRE.*

pIE1^{hr}/PA vector, Cartier et al. (1994)

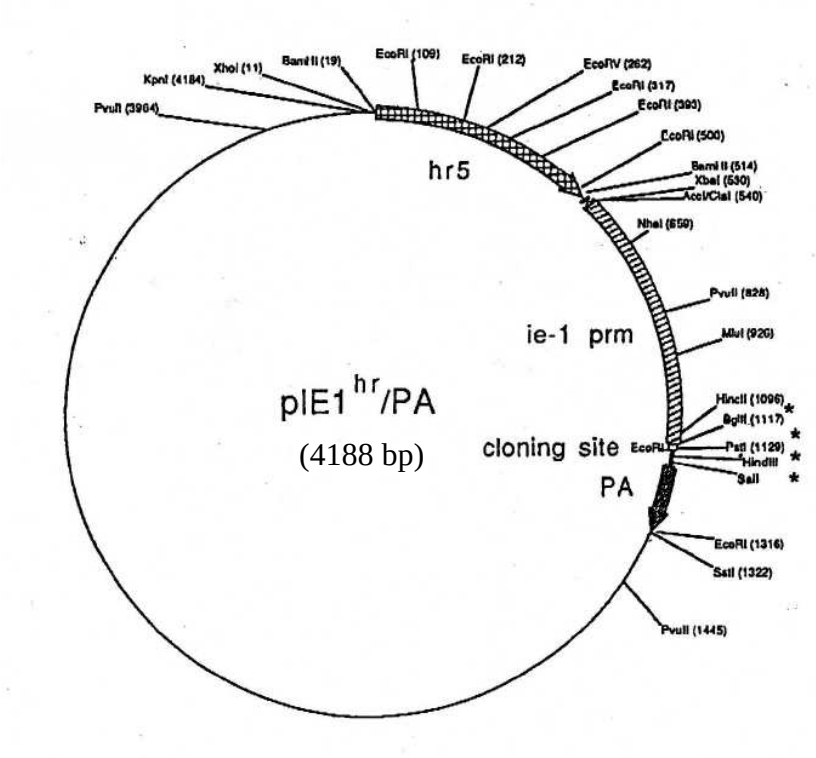

Plasmid features:

The pIE1^{hr}/PA consists of the AcMNPV hr5 transcription enhancer, the IE1 promoter (sequences -546 to +34), a cloning region (*Bgl*II, *Pst*I, *Hin*dIII and *Sal*I sites), followed by an AcMNPV polyadenylation signl (PA). This plasmid kindly provided by Dr. Friesen, U.W.-Madison, USA. Plasmid nucleotide sequence is available by the auther.

pRedET expression vector (*Gene Bridges*)

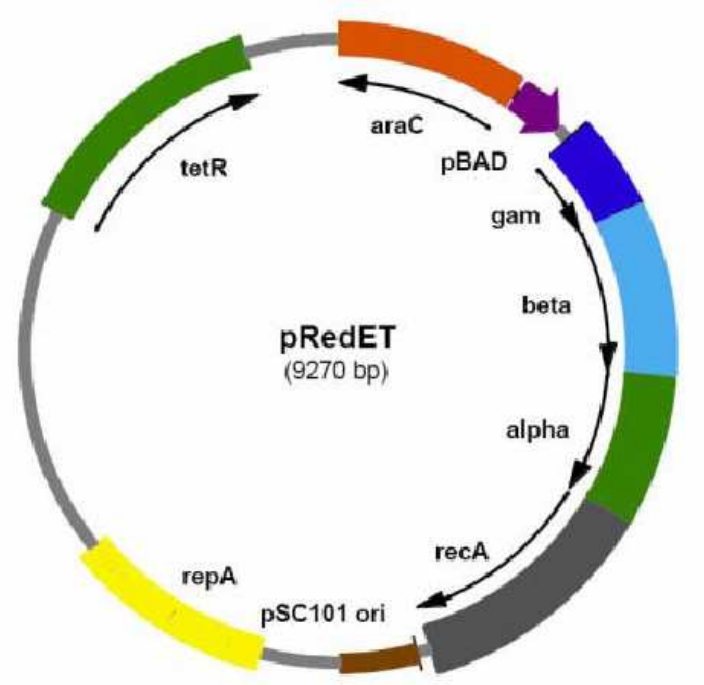

Map of the pRedET expression plasmid (pSC101-BAD-gbaA-tet) (*Gene Bridges*).

-The pRedET plasmid carries the red α, β, γ genes of the λ phage together with the recA gene in a polycistronic operon under the control of the arabinose-inducible pBAD promoter. Transformation of *E. coli* hosts with this plasmid is selected for by acquisition of tetracycline resistance at 30°C. Expression of the Red/ET recombination proteins is induced by L-arabinose activation of the BAD promoter at 37°C.

- Plasmid features and nucleotide sequence is available by *Gene Bridges*.

pUC19 cloning vector (*Novagen*)

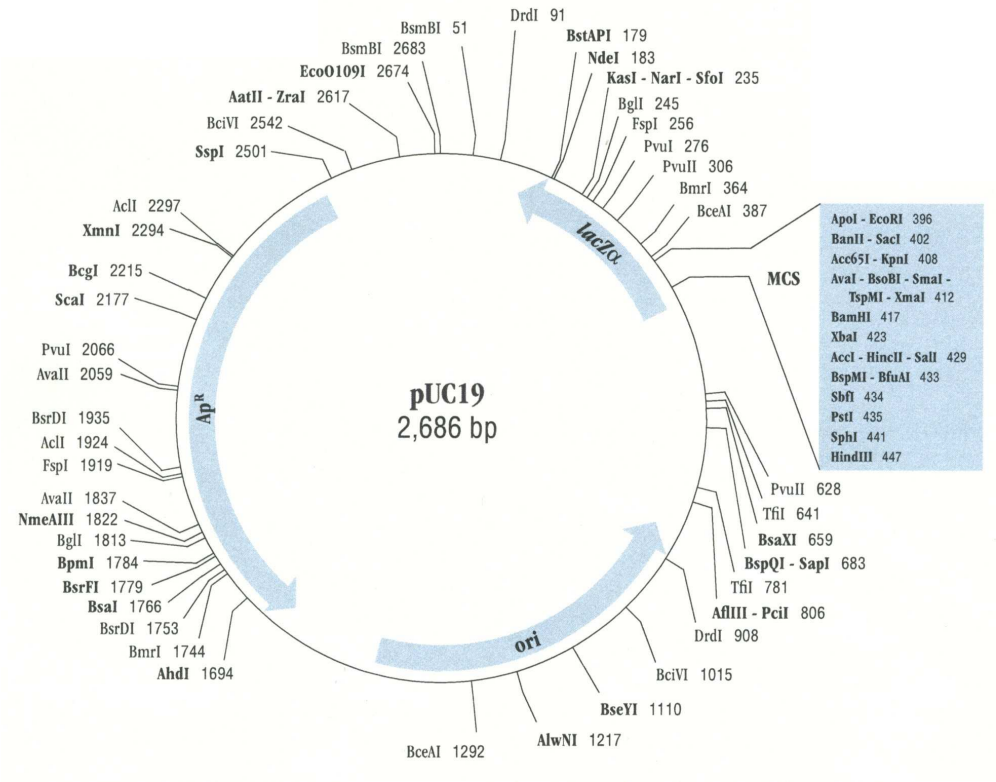

Feauture	Coordinate
lacZα	469-146
Origin (ori)	1455-867
Bla (Ap^R)	2486-1626

Ori = origin of replication

Ap^R = ampicillin

-Plasmid nucleotide sequence is available by *Novagen.*

CURRICULUM VITAE

Name:	Wael Hassan Ali Elmenofy
Date of birth:	24.03.1972
Place of birth:	Cairo, Egypt
Citizenship:	Egyptian
Marital status :	single

1978-1984:	Primary stage, Taha Husain School, Cairo, Egypt.
1984-1987:	Preparatory stage, Elmoneyra School, Cairo, Egypt.
1987-1990:	Secondary stage, Elibrahimeya Secondary School, Cairo, Egypt.
1990-1994:	Bachelor in Agricultural Sciences (B.Sc.), Cairo University, Egypt.
1995-1998:	Research Assistant, Molecular Entomology Laboratory, Agricultural Genetic Engineering Research Institute (AGERI), Giza, Egypt.
1998-2002:	Master of Science (M.Sc.) under the working title "Molecular and biological studies on baculoviruses and their bioinsecticides", Department of Genetics, Fac. of Agriculture, Cairo University, Egypt.
2004-2008:	Ph.D. programme undr the working title "Analysing the possible influence of transposon TCl4.7 insertion on the function of the genome of *Cydia pomonella* granulovirus". Biotechnological Crop Protection, Department of Plant Pathology, State Education and Research Center for Agriculture, Viticulure and Horticulture (SLFA), Neustadt an der Weinstrasse, Germany.

Address in Egypt

Home: 30 Elmawardy St., Qasr Elani, Cairo-Egypt

Work: Agricultural Genetic Engineering Research Institute (AGERI), Agricultural Reseach Centre (ARC), 9 Gamma Str., Giza-Egypt.

Address in Germany

Work: DLR-Rheinpfalz

Breitenweg 71,

67435 Neustadt an der Weintrasse

email: elmenofy10@hotmail.com